

Universidade do Minho

Escola de Ciências

Patrícia Dias Carvalho

**Exploring galectin-3/KRAS^{mut}/p16^{ink4a} interplay
in colorectal cancer**

Master's Thesis

Master's in Molecular Genetics

Supervisors

Professora Doutora Ana Arminda Lopes Preto Almeida

Professora Doutora Maria José Cardoso Oliveira

December 2014

DECLARAÇÃO

Nome: Patrícia Dias Carvalho

Endereço eletrónico: pat.dcarvalho@gmail.com

Telefone:967751409

Número do Bilhete de Identidade: 13926854

Título da dissertação:

Exploring galectin-3/KRAS^{mut}/p16^{INK4a} interplay in colorectal cancer

Orientadores:

Prof.^a Doutora Ana Arminda Lopes Preto Almeida

Prof.^a Doutora Maria José Cardoso Oliveira

Ano de conclusão: 2014

Designação do Mestrado: Mestrado em Genética Molecular

DE ACORDO COM A LEGISLAÇÃO EM VIGOR, NÃO É PERMITIDA A REPRODUÇÃO DE QUALQUER PARTE DESTA TESE

Universidade do Minho, 2 de Dezembro de 2014

Assinatura: _____

AGRADECIMENTOS

Terminada esta etapa não posso deixar de transmitir os meus sinceros agradecimentos a todos os que me apoiaram nesta caminhada e que, direta ou indiretamente, contribuíram para a realização deste trabalho.

Começo por agradecer à minha orientadora Dra. Ana Preto pela oportunidade de realização deste trabalho e pela confiança que depositou em mim ao longo deste ano. Não posso também deixar de mostrar a minha gratidão por todo o empenho e dedicação, por todos os conhecimentos que me transmitiu, pela presença e apoio incondicionais e acima de tudo pela amizade. Agradeço também o facto de ter posto no meu caminho a minha coorientadora, Dra. Maria José Oliveira. A ela agradeço tudo o que me ensinou e todo o tempo que dispensou para o fazer, todo o apoio, força e confiança que me transmitiu, todo o profissionalismo com que sempre me recebeu e por toda a amizade e carinho, um grande obrigada! Foi sem dúvida uma honra trabalhar com as duas e só posso agradecer toda a paciência que tiveram comigo e quanto me ajudaram a crescer!

Às pessoas que mais me aturaram durante estes anos de mestrado, todas as páginas desta tese não seriam suficientes para mostrar o quão grata estou por fazerem parte da minha vida. À Cátia, à Rita e à Tatiana, obrigada por todos os momentos que partilhamos durante estes anos, pela amizade que nutrimos, pelos sucessos que celebramos e pelas derrotas em que nos amparamos, por toda a preocupação, por estarem sempre dispostas para me ajudar, por independentemente de tudo estarem sempre lá com uma palavra de apoio e um abraço quentinho... obrigada por serem as melhores amigas do mundo!

Ao João e à Suellen por tudo o que ensinaram, pela ajuda sempre preciosa e apoio incondicional durante este ano, muito obrigada! À restante “grande família” LBA/LCCA, principalmente à Carla, à Ana Rita, à Cristina, à Cidália, à Dalila, à Cátia e à Lisandra (que continua a ter uma costela LBA), obrigada por terem tornado a minha integração tão simples, pelo companheirismo e amizade, pelo apoio, pelos momentos e confidências que partilhamos dentro e fora do laboratório, obrigada por tornarem todas as horas de trabalho mais leves e animadas! Um agradecimento também à Sara Alves pelos conhecimentos que me transmitiu.

Às meninas do laboratório do INEB no IPATIMUP, Ana, Cátia e Marta, obrigada por me terem recebido de braços de abertos, por tudo o que me ensinaram e por estarem sempre disponíveis para me ajudar. Um obrigada muito especial à Maria Lázaro por toda a paciência que

teve comigo, por tudo o que ensinou e por estar sempre disponível para me ajudar. Ao Hugo Osório e à Patrícia Castro, agradeço o facto de me terem ajudado em algumas experiências.

Por último, mas porque “os últimos são sempre os primeiros”, a eles devo tudo e por isso lhes dedico todo o meu esforço e trabalho: o maior agradecimento vai para os meus pais, o meu grande suporte. Obrigada por me darem a oportunidade de concretizar mais esta etapa, por estarem sempre presentes nos bons e maus momentos, por acreditarem em mim, por vezes mais do que eu própria, e por me darem sempre coragem para continuar. Um agradecimento especial também aos meus irmãos, à minha avó e restante família, por terem sempre uma palavra de incentivo.

Um agradecimento também ao projecto *European Marie Curie Initial Training Networks (ITN): FP7-PEOPLE-2012-ITN: “GLYCOPHARM: The sugar code: from (bio)chemical concept to clinics”* pelo financiamento e pela colaboração nas pessoas da Prof. Dra. Cândida Lucas e do Prof. Dr. Hans-Joachim Gabius; ao Centro de Biologia Molecular e Ambiental (CBMA) e ao Instituto Nacional de Engenharia Biomédica (INEB), ao programa FEDER através do POFC-COMPETE e COMPETE FCOMP-01-0124-FEDER-010915 e à Fundação para a Ciência e Tecnologia (FCT) através dos projectos PEst-OE/BIA/UI4050/2014 e PTDC-SAU-ONC/112511/2009.

Exploring galectin-3/KRAS^{mut}/p16^{INK4a} interplay in colorectal cancer

ABSTRACT

KRAS is the most frequently mutated RAS isoform in many cancers, including colorectal cancer (CRC; 30-50% of the cases), which is a leading cause of death worldwide. Hotspot mutations on this oncogene on codons 12, 13 and 61, mainly resulting in G12V, G12D or G13D substitutions, have an important impact on therapy-related decisions. KRAS signalling nanoclusters are stabilized by the scaffold protein galectin-3 (Gal-3). Gal-3, the only chimaera-type galectin within the galectin family, has numerous intra and extracellular ligands, playing central roles in many cellular functions. Alterations in Gal-3 expression profile are correlated to a variety of cancers, including CRC, being involved in cancer cell growth, transformation, apoptosis, angiogenesis, adhesion, invasion and metastasis. Gal-3 mediated transformation is partially attributed to its specific interaction with KRAS and consequent activation of its downstream signalling effectors. The phenotypic outcomes of this interaction are not well established and thus constitute an important subject of research, with possible therapeutic implications. On its turn, p16 is a well-known tumour suppressor, which plays several additional roles, including in the regulation of angiogenesis, apoptosis, anoikis, immortalization and senescence. p16 seems to be related with KRAS and Gal-3, exerting its tumour suppressor function by downregulating both proteins to achieve cancer cell anoikis resistance reversion.

It is possible to infer that KRAS and Gal-3 have a mutual and dual relationship, and that p16 downregulates both Gal-3 and KRAS, nevertheless, there is very limited knowledge about the Gal-3/KRAS/p16 interplay. In this project we aimed to understand if there is a direct interaction between these three proteins in CRC cell lines and to explore the effect of KRAS and/or Gal-3 silencing in their interplay and in cancer-associated phenotypic characteristics. For that purpose we used SW480 and HCT116 CRC-derived cell lines, the normal colon cell line NCM460 and four others NCM460-derived cell lines previously transfected with Flag-KRAS^{wt} and FLAG-KRAS harbouring hotspot mutations: Flag-KRAS^{G12V}, Flag-KRAS^{G12D} and Flag-KRAS^{G13D}.

In conclusion, this work provides, for the first time, evidences that support the existence of a biochemical interaction between Gal-3, KRAS and p16 in the CRC model, establishing a new research field that requires further exploration. Our data also suggest that KRAS can constitute a good target for new therapeutic strategies in CRC, as it impairs various cancer hallmarks.

Keywords: KRAS, Gal-3, p16, KRAS mutations, interaction, colorectal cancer

Caracterização da interação galectin-3/KRAS^{mut}/p16^{INK4a} no cancro colorretal

RESUMO

O KRAS é a isoforma RAS mais frequentemente mutada em vários cancros, incluindo no cancro colorretal (CCR; 30-50% dos casos), que é uma importante causa de morte em todo o mundo. As mutações mais frequentes neste oncogene, mutações pontuais nos codões 12, 13 e 61, que maioritariamente resultam em substituições G12V, G12D, ou G13D, têm um impacto importante nas decisões terapêuticas. As plataformas de sinalização KRAS na membrana são estabilizadas pela proteína galectina-3 (Gal-3). Gal-3, a única galectina tipo “quimera” dentro da família das galectinas, tem inúmeros ligandos intra e extracelulares, desempenhando papéis centrais em várias funções celulares. Alterações no perfil de expressão da Gal-3 estão correlacionadas com uma variedade de tumores, incluindo CCR, estando envolvidas no crescimento tumoral, transformação, apoptose, angiogénese, adesão, invasão e metastização. A transformação mediada pela Gal-3 é parcialmente atribuída à sua interação específica com KRAS e consequente ativação das suas vias de sinalização. Os resultados fenotípicos dessa interação não estão bem estabelecidos, constituindo assim um importante tema de investigação com possíveis implicações terapêuticas. Por sua vez, p16 é um conhecido supressor tumoral que desempenha vários papéis adicionais, inclusivamente na regulação da angiogénese, apoptose, *anoikis*, imortalização e senescência. A p16 parece estar relacionada com KRAS e Gal-3, exercendo a sua função de supressão tumoral por regulação negativa de ambas as proteínas para atingir reversão de resistência a *anoikis*.

Assim, é possível inferir que a KRAS e a Gal-3 têm uma relação mútua e dupla, e que a p16 regula negativamente tanto Gal-3 como KRAS, no entanto, o conhecimento sobre a interação p16/KRAS/Gal-3 é muito limitado. Neste projeto pretendíamos compreender se existe uma interação direta entre estas três proteínas em linhas celulares de CCR e explorar o resultado do silenciamento de KRAS e/ou Gal-3 nessa interação e em características fenotípicas tumorais. Com esse objetivo usamos as linhas celulares derivadas de CCR SW480 e HCT116, uma linha celular de cólon normal NCM460 e quatro outras linhas celulares derivadas da NCM460 anteriormente transfectadas com Flag-KRAS^{wt} e FLAG-KRAS com as mutações mais frequentes: Flag-KRAS^{G12V}, Flag-KRAS^{G12D} and Flag-KRAS^{G13D}.

Este trabalho fornece pela primeira vez, evidências a favor da existência de uma interação bioquímica entre Gal-3, KRAS e p16 no modelo CRC, estabelecendo um novo conceito que definitivamente deve constituir objeto de investigação futura. Sugerimos também que o

KRAS pode constituir um bom alvo para novas estratégias terapêuticas no CCR, na medida em que pode afetar vários *hallmarks* tumorais.

Palavras-chave: KRAS, Gal-3, p16, mutações KRAS, interação, cancro colorretal

LIST OF CONTENTS

Agradecimientos	iii
Abstract	v
Resumo	vi
List of contents	viii
List of figures	ix
List of tables	xi
List of abbreviations	xi

I. Introduction **15**

1.1. Cancer: the global burden.....	17
1.1.1. Colorectal carcinogenesis	18
1.2. The RAS family: small proteins, high significance	20
1.2.1. RAS signalling output: localization matters	22
1.2.2. <i>RAS</i> mutations and cancer.....	24
1.2.2.1. <i>KRAS</i> mutations in colorectal cancer: role and significance.....	25
1.3. The galectin family.....	26
1.3.1. Galectin-3: a pleiotropic lectin	27
1.3.1.1. Galectin-3 in cancer: roles and <i>KRAS</i> interaction	30
1.3.1.1.1. Galectin-3 in colorectal cancer	33
1.4. <i>p16^{INK4a}</i> : more than a tumour suppressor gene	34
1.4.1. <i>p16</i> connection with galectin-3 and <i>KRAS</i>	36
1.5. Rationale and aims.....	38

II. Materials and Methods **41**

2.1. Cell lines and culture conditions.....	43
2.2. Western Blotting analysis	43
2.2.1. Total protein extraction	43
2.2.2. Protein Quantification	44
2.2.3. Western Blotting	44
2.3. Immunofluorescence Assay	46
2.3.1. Cells fixation in methanol.....	46
2.3.2. Cells fixation in 4% paraformaldehyde	47

2.4.	Co-immunoprecipitation.....	48
2.5.	RNA Interference: silencing of KRAS and galectin-3	49
2.6.	Gelatin Zymography.....	50
2.7.	Trypan Blue exclusion assay	51
2.8.	Time-lapse microscopy	51
2.9.	Statistical analysis	52
III.	Results.....	53
3.1.	Basal expression levels of galectin-3, p16 and KRAS in colorectal cancer cells.....	55
3.2.	Galectin-3, KRAS and p16 localization patterns in normal colon and colorectal cancer cells	56
3.2.1.	Galectin-3, KRAS and p16 immunostaining in colorectal cancer cells.....	56
3.2.2.	Galectin-3 and p16 double immunostaining in colorectal cancer cells	61
3.2.3.	Galectin-3, KRAS and p16 immunostaining in NCM460-transfected cells	66
3.3.	Study of galectin-3, KRAS and p16 interaction by co-immunoprecipitation in SW480 cells.....	71
3.4.	Optimization of galectin-3 silencing conditions by RNA interference.....	73
3.5.	Phenotypic alterations induced by galectin-3 and/or KRAS silencing in SW480 cells.....	73
3.5.1.	Effect of galectin-3 and/or KRAS silencing on cell morphology.....	74
3.5.2.	Effect of galectin-3 and/or KRAS silencing on cell viability.....	76
3.5.3.	Effect of galectin-3 and/or KRAS silencing on galectin-3, KRAS and p16 expression levels.....	77
3.5.4.	Effect of galectin-3 and/or KRAS silencing on MMPs production/activity	78
3.5.5.	Effect of galectin-3 and/or KRAS silencing on cell migration	79
IV.	Discussion.....	83
V.	Concluding remarks and Future perspectives	93
VI.	References.....	99
VII.	Supplementary data	111

LIST OF FIGURES

Fig. 1.1.	The hallmarks and emerging characteristics of cancer.....	18
Fig. 1.2.	A genetic model for colorectal carcinogenesis.....	19
Fig. 1.3.	RAS mediated intracellular signal transduction pathways.....	21

Fig.1.4. <i>RAS</i> isoform-specific codon mutations.....	24
Fig. 1.5. Galectin family division into 3 groups.....	26
Fig. 1.6. Intracellular ligands and functions of Gal-3.....	29
Fig. 1.7. Gal-3 contributes to tumourigenesis and tumour progression through several different mechanisms.....	32
Fig. 1.8. Cell cycle regulation by p16.....	35
Fig. 1.9. Rationale of the project.....	39
Fig.3.1. Expression pattern of Gal-3, KRAS and p16 levels in CRC-derived cells HCT116 and SW480.....	55
Fig. 3.2. Confocal fluorescence microscopy analysis of KRAS localization shows no positive staining.....	57
Fig. 3.3. Confocal fluorescence microscopy analysis of Gal-3 staining in SW480 cells evidences differences between Gal-3 localization in low and high confluent cells.....	58
Fig. 3.4. Confocal fluorescence microscopy analysis of Gal-3 staining in HCT116 cells evidences a similar Gal-3 localization pattern in low and high confluent cells.....	59
Fig. 3.5. Confocal fluorescence microscopy analysis of p16 staining in SW480 cells evidences differences between Gal-3 localization in low and high confluent cells.....	60
Fig. 3.6. Confocal fluorescence microscopy analysis of p16 staining in HCT116 cells evidences a similar p16 localization pattern in low and high confluent cells.....	61
Fig. 3.7. Confocal fluorescence microscopy analysis of Gal3+p16 double immunostaining secondary antibodies control conditions in SW480 (A) and HCT116 cells (B).....	63
Fig. 3.8. Confocal fluorescence microscopy analysis of Gal-3+p16 double immunostaining in low and high confluent SW480 cells reveals the presence of some discreet yellow dots indicative of close proximity and co-localization of these proteins	64
Fig. 3.9. Confocal fluorescence microscopy analysis of Gal-3+p16 double immunostaining in low and high confluent HCT116 cells reveals the presence of some discreet yellow dots mainly localized at the cells nuclei and suggestive of co-localization.....	65
Fig. 3.10. Representative western blot analysis of Gal-3, endogenous KRAS, Flag-KRAS and p16 basal expression levels in NCM460 parental (P) cell line and NCM460 transfected with Flag-KRAS ^{wt} , Flag-KRAS ^{G12V} , Flag-KRAS ^{G12D} and Flag-KRAS ^{G13D}	66
Fig. 3.11. Confocal fluorescence microscopy analysis of Flag-KRAS and Gal-3 double immunostaining control conditions in NCM460 Flag-KRAS wt (A) and staining positive conditions in NCM460 Flag-KRAS wt, G12V, G12D and G13D (B).....	67
Fig. 3.12. Confocal fluorescence microscopy analysis of Gal-3 and p16 double immunostaining control conditions in NCM460 Flag-KRAS wt (A) and staining positive conditions in NCM460 Flag-KRAS wt, G12V, G12D and G13D (B).....	68
Fig. 3.13. Confocal fluorescence microscopy analysis of Flag-KRAS and p16 double immunostaining control conditions in NCM460 Flag-KRAS wt (A) and staining positive conditions in NCM460 Flag-KRAS wt, G12V, G12D and G13D (B).....	69
Fig. 3.14. Gal-3, KRAS and p16 co-immunoprecipitate	72

Fig. 3.15. A concentration of 50nM of Gal-3 siRNA is enough to obtain a silencing percentage of 81.2%	73
Fig. 3.16. Gal-3 and/or KRAS silencing induce morphology changes in SW480 cells.....	75
Fig. 3.17. Gal-3 and/or KRAS silencing decrease cell viability of SW480 cells.....	76
Fig. 3.18. Gal-3 silencing induces an increase in KRAS expression levels whereas KRAS silencing slightly decrease Gal-3 expression.....	77
Fig. 3.19. KRAS silencing and Gal-3/KRAS double silencing led to a decrease in Pro-MMP-9, MMP-9 and Pro-MMP-2 levels	79
Fig. 3.20. Gal-3 and/or KRAS silencing have no effect on colon cancer SW480 cells migration.	81
Fig. 4.1. Results outline of this project.	91
Fig. S1. Confocal fluorescence analysis of Gal-3 and p16 negative staining controls in high confluent SW480 and HCT116 cells.....	113
Fig. S2. Representative western blot showing similar Gal-3 expression independently of the cells confluence and nutritional availability	114
Fig. S3. Analysis of Gal-3 content in conditioned media (CM) from HCT116 and SW480 cells.....	114

LIST OF TABLES

Table. 1.1. Evidences of Gal-3-KRAS interaction in cancer cell models.....	33
Table. 2.1. Primary and secondary antibodies used in this study and their respective dilutions.....	45
Table. 2.2. Primary and secondary-conjugated antibodies and the respective dilutions used in immunofluorescence, with reference to cell lines and fixation methods.....	48
Table. 3.1. Localization patterns of Gal-3 and p16 in SW480 and HCT116 cells and Gal-3, p16 and (Flag-)KRAS in NCM460 cells transfected with KRAS ^{wt} and the three KRAS hotspot mutations.....	71

LIST OF ABBREVIATIONS

AKT	V-AKT murine thymoma viral oncogene
APC	Adenomatous polyposis coli
BRAF	V-RAF murine sarcoma viral oncogene homolog B
BSA	Bovine serum albumin
CDK	Cyclin dependent kinase
CIMP	CpG island methylator phenotype

CIN	Chromosomal instability
CKI	Cyclin dependent kinase inhibitor
Co-IP	Co-immunoprecipitation
COX-2	Cyclooxygenase 2
CRC	Colorectal cancer
DCC	Deleted in colorectal carcinoma
EGF	Epidermal growth factor
EGRF	Epidermal growth factor receptor
ERK	Extracellular regulated MAP kinase
FAP	Familial adenomatous polyposis
FBS	Fetal bovine serum
Gal-1	Galectin-1
Gal-3	Galectin-3
GAPs	GTPase activating proteins
GDP	Guanosine diphosphate
GEFs	Guanine nucleotide exchange factors
GTP	Guanosine triphosphate
GTPase	Guanosine triphosphatase
HBSS	Hank ´ s balanced salt solution
HNPCC	Hereditary non polyposis colorectal cancer
HRAS	Harvey rat sarcoma virus oncogene
IF	Immunofluorescence
IgG	Immunoglobulin G
IP	Immunoprecipitation
KRAS	Kirsten rat sarcoma viral oncogene
MAPK	Mitogen activated protein kinase
MEK	Mitogen associated extracellular signal-regulated kinase
MGMT	O ⁶ -methylguanine-methyltransferase
MLH1	MutL homolog 1
MMP	Matrix metalloproteinase
MRR	Mismatch repair
MSI	Microsatellite unstable
MSS	Microsatellite stable
MUC1	Mucin-1

NRAS	Neuroblastome rat sarcoma virus oncogene
OIS	Oncogenic stimuli-induced senescence
PBS	Phosphate buffered saline
PFA	Paraformaldehyde
PI	Propidium iodide
pRB	Retinoblastoma protein
PVDF	Polyvinylidene difluoride
RAF	Rapidly accelerated fibrosarcoma kinase
RAS	Rat sarcoma
RIPA Buffer	Radioimmunoprecipitation assay buffer
RNA	Ribonucleic acid
RNAi	RNA interference
Rpm	Revolutions per minute
RPMI	Roswell Park Memorial Institute medium
RT	Room temperature
RTK	Receptor tyrosine Kinase
SDS	Sodium dodecyl sulfate
shRNA	Short hairpin RNA
siRNA	Small interference RNA
VEGF	Vascular endothelial growth factor

I.

INTRODUCTION

1.1. Cancer: the global burden

According to the World Health Organization (WHO), cancer is defined as “the uncontrolled growth and spread of cells. It can affect almost any part of the body. The growths often invade surrounding tissue and can metastasize to distant sites” (WHO 2014). In 2012 cancer accounted for 14.1 million new cases and 8.2 million deaths worldwide. Predictions point to an increase of 19.3 million new cancer cases by 2025, due to growth and ageing of the global world population (GLOBOCAN, 2012).

Carcinogenesis is a multistep process with each step displaying dynamic changes in the genome. Such changes are translated by mutations in oncogenes with dominant gain of function, and tumour suppressor genes with recessive loss of function, which progressively transform normal cells into malignant derivatives. Through those steps, cells acquire a succession of capabilities that were initially referred as the “hallmarks of cancer” and were defined by the authors as “six essential alterations in cell physiology that collectively dictate malignant growth” (Hanahan & Weinberg 2000). Those six hallmarks were proposed as: self-sufficiency in growth signals, insensitivity to growth-inhibitory signals, evasion of programmed cell death, limitless replicative potential, sustained angiogenesis, and tissue invasion and metastasis (Hanahan & Weinberg 2000). Meanwhile, the past decade witnessed remarkable progresses in cancer biology that led to the update of the hallmarks list (Fig.1.1), adding two more: the capability to modify or reprogram the cellular metabolism and the ability of cancer cells to evade the immunological destruction. Moreover, two consequential characteristics that facilitate acquisition of both core and emerging hallmarks were mentioned: the genomic instability and mutability and the inflammation by innate immune cells (Hanahan & Weinberg 2011). Moreover, Floor et al. 2012, referred to another important characteristic - the loss of differentiation.

Deregulation of signalling pathways is very important to acquire these hallmark capabilities, and the interconnections and crosstalk between the individual sub-circuits can make a certain oncogenic event to affect multiple capabilities (Hanahan & Weinberg 2011).

The reductionist view that a tumour is nothing more than a collection of relatively homogeneous cancer cells has been put aside and tumours have increasingly been recognized as complex organs with specialized cell types and a tumour microenvironment constructed during the tumourigenesis process (Hanahan & Weinberg 2011). Therefore, this dynamic, complex and intra/inter-tumour heterogeneity contribute to explain the difficulty of treatment and the need for multi-target therapies. Despite the increasing accumulation of knowledge about

carcinogenesis and the successful advances in treatment strategies, scientific research must continue (Duffy 2013).

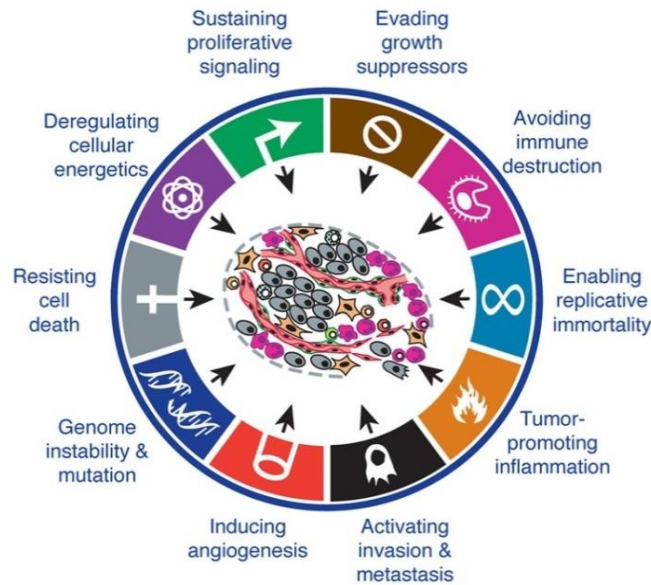


Fig. 1.1. The hallmarks and emerging characteristics of cancer (Adapted from Hanahan & Weinberg 2011).

1.1.1. Colorectal carcinogenesis

Colorectal cancer is the third most common cancer in men and the second in women, being the third most frequently diagnosed worldwide. About 694 000 deaths from CRC are estimated worldwide, making it the fourth most common cause of cancer mortality. In Portugal, this is the second most common type of cancer in men and women, being responsible for the highest number of cancer mortality (GLOBOCAN, 2012). Hereditary predisposition, age and lifestyle factors, namely fat and alcohol regular consumption, physical inactivity, obesity and tobacco smoking represent risk factors for CRC development (Haggard & Boushey 2009).

The first model of colorectal carcinogenesis was suggested in 1990 by Fearon and Vogelstein (Fearon & Vogelstein 1990) as a sequential pathway in which normal epithelium becomes hyperproliferative evolving to adenoma and ultimately to carcinoma. This pathway essentially requires mutational events in oncogenes, such as *KRAS*, and in tumour suppressor genes, such as *APC*, *DCC* and *p53*. Additional events may eventually lead to metastasis (Fig.1.2).

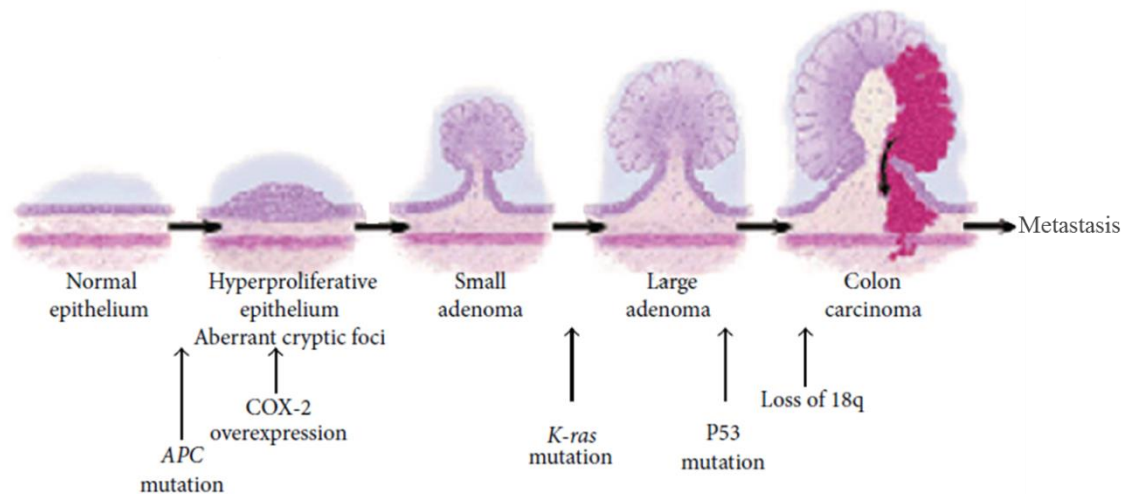


Fig. 1.2. A genetic model for colorectal carcinogenesis. Mutations in *APC*, activation of *KRAS* and inactivation of *p53* are essential events in this carcinogenic process (Adapted from Sandouk et al. 2013).

CRC can be subdivided in sporadic, which results from a stepwise accumulation of genetic and epigenetic alterations, or hereditary/familial, which arises from germline mutations in genes involved in colorectal carcinogenesis. Hereditary CRC accounts for less than 5% of all cases and among all the identified syndromes the most common are Familial Adenomatous Polyposis (FAP) and Lynch syndrome (also called Hereditary Non Polyposis Colorectal Cancer- HNPCC) (Al-Sohaily et al. 2012; Armaghany et al. 2012).

Currently, genomic instability is known to play an important role in colorectal carcinogenesis. Accordingly, three not mutually exclusive events are considered to cause this instability: (1) chromosomal instability (CIN), (2) microsatellite instability (MSI) and (3) CpG island methylator phenotype (CIMP) (Al-Sohaily et al. 2012; Armaghany et al. 2012). CIN, also called adenoma-carcinoma sequence, is the most common cause of genomic instability. It is characterized by karyotypic abnormalities and the accumulation of mutations that led to the activation of proto-oncogenes (e.g.: *KRAS*) and inactivation of tumour suppressor genes (e.g.: *APC* and *p53*). MSI results from a defective mismatch repair (MMR) system that leaves microsatellites either longer or shorter than usual. According to defined markers, MSI is classified as microsatellite high (MSI-H), microsatellite low (MSI-L) or microsatellite stable (MSS). Inactivation of MMR enzymes can result either from abnormal methylation of promoter CpG islands or from point mutations in MMR family members. Germline mutations in MMR genes are in the origin of HNPCC (Al-Sohaily et al. 2012; Armaghany et al. 2012). Aberrant epigenetic regulation via inappropriate methylation of gene promoter regions is common in CRC and is as

significant as DNA mutation in the inactivation of tumour suppressor genes. CIMP is a result of aberrant hypermethylation that takes place in repetitive CG dinucleotides or CpG-rich stretches of DNA in a given gene, such as *MLH1*, promoter region. As well as MSI, CIMP has also been classified in levels (e.g.: CIMP-low, CIMP-high) (Armaghany et al. 2012).

In addition to the traditional carcinogenesis adenoma-carcinoma sequence, some CRCs are believed to arise from lesions called serrated polyps, establishing the serrated pathway. Therefore, based on the molecular and pathological profile, Jass (2007) categorized 5 subtypes of CRC:

(1) CIMP-high, methylation of *MLH1*, *BRAF* mutation, chromosomally stable, MSI-H, origin in serrated polyps, known generally as sporadic MSI-H (accounts for 12% of CRCs);

(2) CIMP-high, partial methylation of *MLH1*, *BRAF* mutation, chromosomally stable, MSS or MSI-L, origin in serrated polyps (accounts for 8% of CRCs);

(3) CIMP-low, *KRAS* mutation, *MGMT* methylation, CIN, MSS or MSI-L, origin in adenomas or serrated polyps (accounts for 20% of CRCs);

(4) CIMP-negative, CIN, mainly MSS, origin in adenomas (sporadic or hereditary) (accounts for 57%).

(5) Lynch syndrome, CIMP-negative, *BRAF* mutation negative, chromosomally stable, MSI-H, origin in adenomas (accounts for 3%) (also referred as familial MSI-H CRC).

1.2. The RAS family: small proteins, high significance

RAS proteins belong to the RAS superfamily of small GTPases, which is divided into at least 5 subfamilies: the RAS, Rho/Rac, Rab, Arf and Ran (Castellano & Santos 2011). Mammalian RAS proteins have a molecular weight of approximately 21 kDa and are codified by 3 similar genes Harvey-RAS (*HRAS*), Neuroblastome-RAS (*NRAS*) and Kirsten-RAS (*KRAS*). *KRAS* gene originates two alternative spliced isoforms, A and B, being the latter an ubiquitously expressed form (Vögler et al. 2008) and hereafter designated as KRAS. As a result of their oncogenic role, these genes started to be identified more than 40 years ago and since then information has been accumulating, proving their relevance on signalling transduction and on molecular oncology (Malumbres & Barbacid 2003).

RAS proteins are regulated by guanine nucleotide exchange factors (GEFs) which activate the system by inducing GDP dissociation and GTP binding; and by GTPase activating proteins (GAPs) that inversely regulate the system (Fig.1.3). This binary behaviour enables RAS proteins to

function as molecular switches in a broad range of signalling transduction processes, from extracellular signals, for example soluble epidermal growth factor (EGF), to the interior of the cells. Importantly, the high number of RAS activators and effectors identified in mammalian cells, places these proteins at the crossroads of various cellular signalling networks, such as RAF/MEK/ERK, PI3K/AKT and RalGDS pathways. Consequently, they affect a wide range of cellular responses that influence cell fate, including proliferation, differentiation and apoptosis (Fig.1.3) (Normanno et al. 2009; Castellano & Santos 2011).

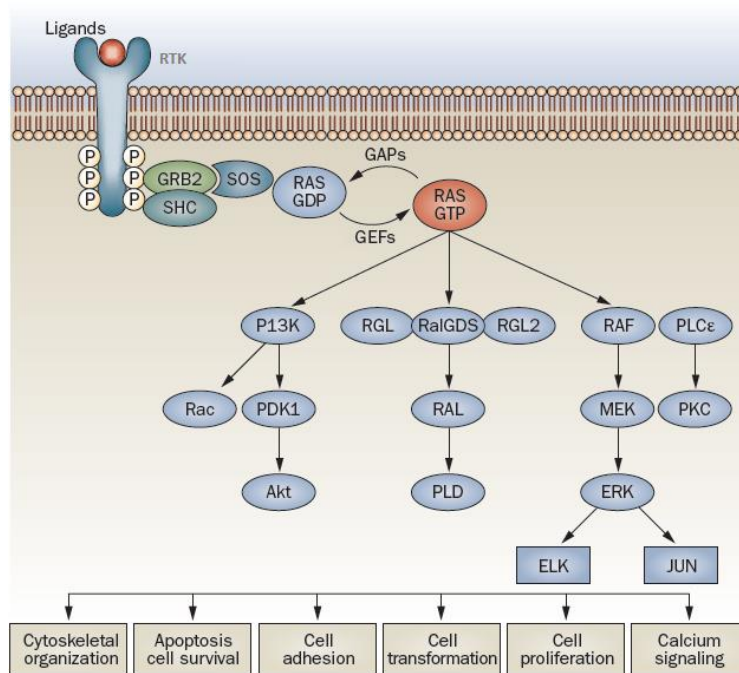


Fig. 1.3. RAS mediated intracellular signal transduction pathways. Ligand binding to the extracellular domain of receptor tyrosine kinases (RTKs) result in activation and initiation of signalling cascades. Activated receptor complexes contain adaptors such as SHC and GRB2 that recruit proteins like SOS1, increasing RAS–GTP levels by catalyzing nucleotide exchange on RAS. GTP-bound RAS activates different signalling pathways including: RAF/MEK/ERK cascade, that regulate cell proliferation and motility via the transcription factors JUN and ELK; PI3K, which via AKT controls a number of downstream effectors responsible for anti-apoptotic responses and via Rac, regulates the actin cytoskeleton dynamics, being important in RAS-mediated transformation; RalGDS, RGL and RGL2, which activate PLD, resulting in control of cell-cycle progression and in RAS-dependent transformation; and PLCε, which regulates calcium release and PKC activation. To terminate this signal transduction, GAPs (eg. neurofibromin- NF1) bind to RAS–GTP and accelerate its conversion to RAS–GDP (Adapted from Normanno et al. 2009).

The structure of these small monomeric G proteins can be divided into three domains (Vögler et al. 2008):

(1) The G domain that is approximately 95% conserved among the different isoforms. This region of the protein binds guanine nucleotides, contains the switch 1 and 2 loops, which undergo major conformational changes on GTP–GDP exchange and are also the binding surfaces for effectors, exchange factors, and GAPs;

(2) The poorly conserved C-terminal HVR (hypervariable region; less than 15% of sequence identity) domain that undergoes direct post-translational processing, being essential for plasma membrane anchoring as well as for the trafficking of newly synthesized and processed RAS, from the cytosolic surface of the endoplasmic reticulum to the inner surface of the plasma membrane. It also comprises the linker region that connects the anchor sequence with the N-terminal G-domain;

(3) The C-terminal CAAX (C=cysteine, A=aliphatic, X=amino acid) motif that is post-translationally processed to generate an S-farnesyl cysteine carboxymethyl ester. The membrane anchor is completed by one (NRAS) or two (HRAS) proximal S-palmitoylable cysteine residues or a polybasic domain of six lysine residues in KRAS.

1.2.1. RAS signalling output: localization matters

Besides being mainly found at the inner surface of the plasma membrane, these proteins can also be found in other intracellular membranes such as endosomes, endoplasmic reticulum/Golgi and mitochondria, where they can generate signal output as well (Omerovic & Prior 2009). RAS interaction with the plasma membrane is highly dynamic and is located in specific microdomains (sites within the plasma membrane that have a distinct lipid and/or protein composition) (Hancock 2003). One of the best characterized microdomains are the lipid rafts, which consist of dynamic assemblies of cholesterol and sphingolipids at the exoplasmic leaflet of the bilayer. Additionally, caveolae is one subset of lipid rafts found in cell surface invaginations, formed by polymerization of caveolins- hairpin-like palmitoylated integral membrane proteins- that tightly bind cholesterol (Simons & Toomre 2000). As there are different C-terminal lipid anchors on N, H and KRAS isoforms - a farnesyl group with one, two palmitate groups or a polybasic domain, respectively - it would therefore be expected that they sort or target RAS proteins to different membrane microdomains (Hancock 2003). In fact, the HRAS membrane anchor targets this protein to lipid rafts and caveolae but, in contrast, the membrane anchor of KRAS predominantly (85% of the proteins) targets it to non-raft plasma membrane. Notably, HRAS is in dynamic equilibrium between lipid rafts and non-rafts sites of the plasma membrane: when GDP-loaded, a percentage of HRAS localizes at lipid rafts, however, GTP-loading redistributes HRAS from rafts to non-raft sites. Although localization in the rafts is necessary for signalling, this release from rafts is essential for HRAS efficient activation of RAF (Prior et al. 2001). Additionally, many studies have demonstrated that activated HRAS and KRAS

operate in non-overlapping, non-raft microdomains of the plasma membrane (Hancock 2003). This differential lateral segregation of RAS proteins within the plasma membrane can be a plausible explanation for distinct signal outputs generated by these highly homologous proteins. Furthermore, the C-terminal membrane anchor was shown to regulate RAS signal output (Hancock 2003).

Additionally, at the plasma membrane, approximately 40% of activated RAS proteins form nanoclusters, whereas the remainder is distributed as monomers. These nanoclusters display some specific features: KRAS nanoclusters are actin-dependent and cholesterol-independent, and are stabilized by the scaffold protein galectin-3 (Gal-3), whereas HRAS-GDP nanoclusters are cholesterol and actin-dependent but, when activated (GTP loaded), are cholesterol and actin-independent and are stabilized by galectin-1 (Gal-1) (Abankwa et al. 2007; Omerovic & Prior 2009). Importantly, using KRAS^{G12V} it was shown that only nanoclustered proteins can recruit downstream signalling effectors and transduce signals with high-fidelity (Tian et al. 2007). In addition, RAF is recruited to and retained in KRAS nanoclusters but, in turn, it is not retained in HRAS nanoclusters. Similarly, upon epidermal growth factor receptor (EGFR) activation, RAF is preferentially recruited to KRAS and not to HRAS nanoclusters (Plowman et al. 2008).

RAS interactions with Gal-1 and Gal-3 act as regulators of signal duration and effector usage. Gal-1 binds active HRAS-GTP and active KRAS-GTP (preferentially and in a higher extent with the former) and Gal-3 only binds KRAS-GTP (Elad-Sfadia et al. 2002; Elad-Sfadia et al. 2004), all in a RAS farnesyl moiety-dependent manner (Paz et al. 2001; Elad-Sfadia et al. 2004). These interactions between RAS and galectins stabilize RAS in the active state (reducing the efficiency of GAP-mediated GTP hydrolysis) and promote its association with distinctive effectors (Elad-Sfadia et al. 2002; Elad-Sfadia et al. 2004). Thus, when HRAS-GTP interacts with Gal-1, it promotes activation of RAF but not of PI3K (Elad-Sfadia et al. 2002). In contrast, when KRAS-GTP interacts with Gal-3, it promotes activation of RAF and PI3K (Elad-Sfadia et al. 2004).

In summary, despite the similarity of RAS isoforms, they display some functional and biological specificity. This is most likely a result of their intrinsically different biological potency and of their different spatiotemporal and subcellular compartmentalization. The combination of these features with the different cellular contexts in which each isoform is expressed, dictates their distinct signalling and consequent output (Omerovic & Prior 2009; Castellano & Santos 2011).

1.2.2. *RAS* mutations and cancer

The central role of *RAS* gene products in normal cell signalling is consistent with the high frequency of oncogenic activation of *RAS* genes in human cancers (Castellano & Santos 2011). *RAS* genes exhibit a pattern of isoform-specific codon and point mutations, which display varying incidences in different cancers and presents a specific association with particular cancers types (Fig.1.4). Typically, single mutations occur at codons 12, 13 or 61 with different frequencies in each isoform (Prior et al. 2012). These mutations favour GTP binding, leading to constitutive activation of RAS, meaning that the protein no longer requires ligand for activation. This constitutive activation deregulates RAS target signalling pathways leading to malignant transformation (McCubrey et al. 2007).

KRAS is the most frequently mutated isoform in most cancers, having a higher occurrence in pancreatic cancer, where 90% of the tumours harbour *KRAS* mutations. Its patterns of mutation are dominated by G→A transitions at the second base of codons 12 or 13, resulting in G12D or G13D mutations; G→T transversions at the second base of codon 12, producing G12V, and a special case in lung cancer where G→T transversion at the first base of codon 12 produce G12C mutations (Prior et al. 2012).

Conclusively, one might speculate that this high frequency of *RAS* proto-oncogenes activation in human cancers makes RAS and their signalling pathways attractive targets for cancer therapy.

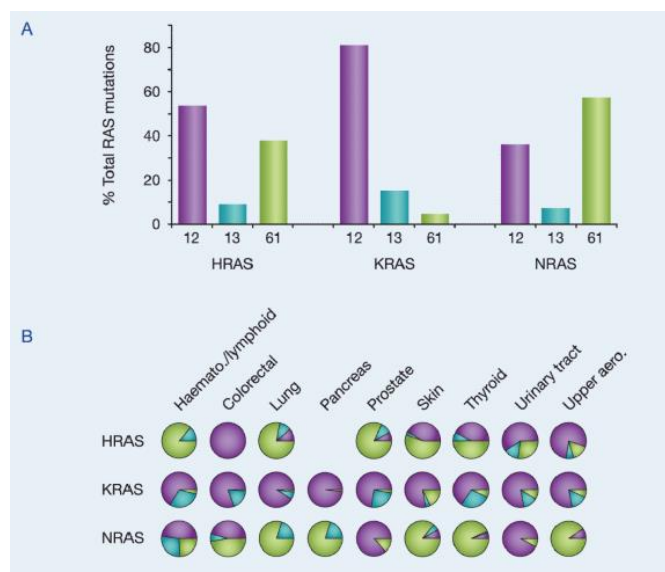


Fig.1.4. *RAS* isoform-specific codon mutations. (A) *RAS* oncogenes are frequently mutated at codons 12 (in purple), 13 (in blue) and 61 (in green) and the incidence of mutation differs between the isoforms. (B) Isoforms – specific mutation patterns are associated with particular cancer types (Adapted from Prior et al. 2012).

1.2.2.1. *KRAS* mutations in colorectal cancer: role and significance

Back in 1990, the significance of *KRAS* mutations in CRC had already been recognized as an initial event in colorectal carcinogenesis (Fearon & Vogelstein 1990). Indeed, *KRAS* mutations are very frequent in CRC, occurring in approximately 30-50% of the cases, being considered an important factor to be taken into account in therapy-related decisions (Arrington et al. 2012).

The RASCAL (Kirsten-RAS in colorectal cancer collaborative group) carried out the biggest studies about the impact of *KRAS* in CRC, reaching some important conclusions: *KRAS* mutations are associated with CRC development and progression, and their presence increase the risk of death; followed by codon 13, codon 12 is the most frequently mutated, being the change of glycine (G) to aspartate (D) the more frequent alteration. Additionally, also in codon 12, the mutation that results in the change of glycine (G) to valine (V) is associated with more aggressive and advanced cancers and represents an increased risk of tumour relapse and death (Andreyev et al. 1998; Andreyev et al. 2001). In sporadic MSS CRC, *KRAS* mutations have been related to more aggressive tumours and it has been suggested as a critical gene in the metastization process, increasing the ability to invade (Oliveira et al. 2007). In fact, primary CRC harbouring *KRAS* mutations is frequently associated with distant metastasis in liver and lungs, which are the main cause of death in CRC patients (Cejas et al. 2009; Nash et al. 2010). In MSI CRC, *KRAS* is less mutated than in MSS and mutations in this gene are inversely associated and mutually exclusive to the oncogenic *BRAF*^{V600E} mutation, more frequent in this type of cancer (Rajagopalan et al. 2002; Oliveira et al. 2003).

Additionally, the epidermal growth factor receptor (EGFR) is frequently overexpressed in CRC and its simultaneous presence with mutated *KRAS*, a downstream effector of EGFR-induced signalling cascade, has been identified as a potent predictor of anti-EGFR therapies resistance, namely to cetuximab and panitumumab (Vectibix) (Heinemann et al. 2009; Normanno et al. 2009). Recently, meta-analysis studies have suggested that among the patients with *KRAS* mutations, the ones that harbour the mutation on codon 13 are more sensitive and may benefit more from the anti-EGFR therapy with cetuximab (Chen et al. 2013a ; Mao et al. 2013). Hence, *KRAS* and EGFR mutation status should be evaluated before the therapeutic decisions are considered (Heinemann et al. 2009; Normanno et al. 2009).

In conclusion, the presence of *KRAS* mutations in CRC seems to be a bad prognostic biomarker with a relevant impact on therapy.

1.3. The galectin family

Galectins are members of a larger family of β -galactoside-binding lectins that before being named as galectins in 1994, were referred as S-type or S-lac lectins. The author that suggested the terminology defined that membership to galectin family requires the fulfilment of two essential criteria: (1) affinity for β -galactosides and (2) a significant sequence similarity in the carbohydrate-binding site (Barondes et al. 1994). These lectins are evolutionary ancient being expressed and conserved from vertebrates to invertebrates and protists. Their presence in so many species through evolution suggests that they may have evolved to play fundamental roles in cell biology (Cooper 2002).

The 15 identified mammalian galectins all contain conserved carbohydrate-recognition domains (CRDs) of about 130 amino acids, which served as a criteria for their classification into: prototypical galectins with one CRD (galectin-1, -2, -5, -7, -10, -11, -13, -14 and -15); the chimaera-type Gal-3 that contains a non-lectin N-terminal region (of about 120 amino acids) connected to a CRD; and the tandem-repeat-type galectins that contain two homologous CRDs in a single polypeptide chain, separated by a linker of up to 70 amino acids (galectin-4, -6, -8, -9 and -12) (Fig.1.5). Galectins have sugar-binding specificity and with regard to their binding activity, they are bivalent or multivalent having the ability to form lattice-like structures (Yang et al. 2008).

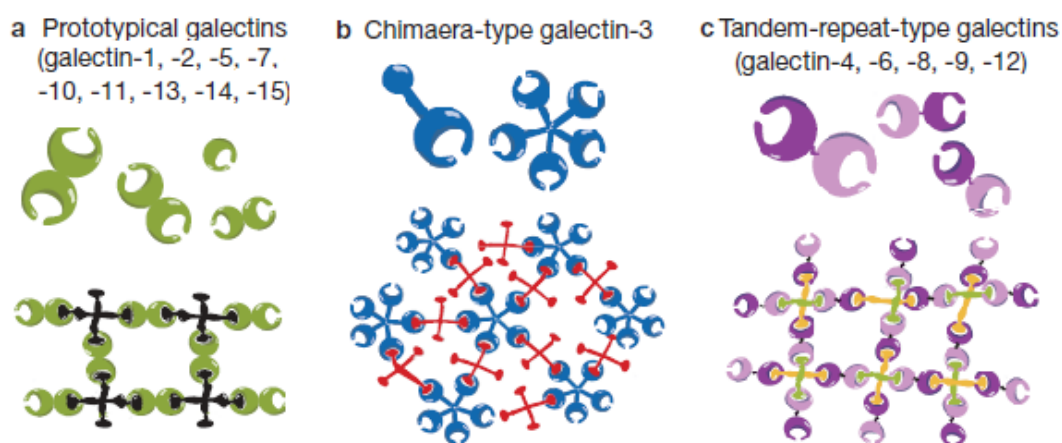


Fig. 1.5. Galectin family division into 3 groups: (a) prototypical galectins, (b) chimaera-type Gal-3 and (c) tandem-repeat-type galectins. As galectins are bivalent or multivalent, they can form lattices with multivalent glycoconjugates (Adapted from Yang et al. 2008).

In the extracellular space, galectins can modulate the interactions between matrix components and cell-surface integrins, regulating cell-cell and cell-matrix adhesion. These

interactions are extremely important in cellular motility, polarity and tissue formation, and their loss is associated with some diseases, such as inflammation and tumour progression (Hughes 2001). Also, due to their multivalency, they can crosslink cell-surface glycoconjugates and trigger signalling events that can modulate cell behaviour (Liu & Rabinovich 2005). Intracellularly, by interacting with some specific ligands, galectins play a role in the regulation of essential cell processes like growth, apoptosis and cell cycle regulation (Liu et al. 2002).

1.3.1. Galectin-3: a pleiotropic lectin

Firstly identified in 1982 as a 32kDa antigen (Muc-2) on the surface of mouse thioglycollate-elicited macrophages (Ho & Springer 1982), over the years Gal-3 was isolated from many other sources and received many designations, until the introduction of the “galectin” nomenclature. Among the galectins family, Gal-3 is the most studied member (Dumic et al. 2006).

Structurally Gal-3 is composed by two distinct conserved domains: the N-terminal domain (ND), responsible for multimerization, consists of a 110-130 amino acids sequence with 7-14 tandem repeats of Pro-Gly-Ala-Tyr-Pro-Gly followed by three additional amino acids, and the 130 amino acids C-terminal CDR, that accommodates the carbohydrate-binding site (Dumic et al. 2006). These two domains are necessary for Gal-3 functionality: the ND contributes to carbohydrate-binding (Barboni et al. 2000) and the C-terminal is involved in Gal-3 self-association (depending on whether it is bound to saccharides or not) (Yang et al. 1998). The ND is also necessary for Gal-3 subcellular localization (Gong et al. 1999) and is susceptible to cleavage by metalloproteinases (MMPs; particularly MMP-2 and MMP-9), which play an important function in several physiological processes such as extracellular matrix degradation and tissue remodeling (Ochieng et al. 1998). Its Ser⁶ residue phosphorylation was demonstrated to play key roles in Gal-3 ligand binding, acting like the “on/off” switch of some downstream biological effects, including its anti-apoptotic and anti-anoikis (apoptosis upon loss of anchorage) activities (Mazurek et al. 2000; Yoshii et al. 2002). The former has been attributed to the C-terminal NWGR (Asn-Trp-Gly-Arg) motif, which is similar to the BH1 domain of the Bcl-2 family proteins (Akahani et al. 1997).

Gal-3 is one of the members of the family that exhibits a dual localization, intra and extracellular, but lacks a transport signal sequence, thus its mechanism of externalization does not involve the classical endoplasmic reticulum-Golgi complex pathway (Hughes 1999). Meanwhile, Gal-3 was found in dendritic cells' secreted exosomes (Théry et al. 2001), and has

been shown to interact with membrane phospholipids and cholesterol, having the propensity to rapidly penetrate and traverse the lipid bilayer in either direction (Lukyanov et al. 2005). In the intracellular space, Gal-3 shuttles between the nucleus and the cytoplasm, being exclusively/mainly in one compartment or distributed by both, depending for example on cell type or specific *in vitro* experimental conditions, and many studies have been carried out in search for import and export signals (Haudek et al. 2010). Gal-3 can migrate into the nucleus by distinct pathways: passive diffusion, ND-dependent active transport system (Nakahara et al. 2006a), or it can be imported by the importin (karyopherin) α/β complex, as it has a nuclear localization signal (NLS)-like sequence in the C-terminal (Nakahara et al. 2006b). Recently, it was elucidated that nucleoporin Nup98 mediates Gal-3 nuclear export by interacting with its C-terminal domain (Funasaka et al. 2013).

Numerous intracellular molecules have been identified as Gal-3 ligands (Fig.1.6) and the interaction with most of them is established through protein-protein interactions instead of protein-carbohydrate recognitions (Haudek et al. 2010). In the nucleus, Gal-3 plays a part in spliceosome assembly by interacting with Gemin4 (Park et al. 2001), participates in the regulation of transcription by interacting with transcription factors like the thyroid transcription factor 1 (TTF-1) (Paron et al. 2003), or by enhancing/stabilizing transcription factor binding to CRE and possibly SP1 sites, which are often found at the promoter region of many genes, including cyclin D1 (Lin et al. 2002). In the cytoplasm Gal-3 interacts, among others, with Bcl-2, functioning in its pathway (Yang et al. 1996); with synexin, which mediates its translocation to the perinuclear mitochondrial membranes, where it regulates mitochondrial integrity (Yu et al. 2002); and with nucling, which downregulates Gal-3 and consequently mediates apoptosis (Liu et al. 2004). Furthermore, Gal-3 also can exert its anti-apoptotic activity by modulating mitochondrial homeostasis, in particular by reducing intracellular ROS generation and influencing the mitochondrial membrane potential (Matarrese et al. 2000). Hence, intracellular Gal-3 is an active participant and regulator of essential cell processes namely proliferation/cell cycle regulation, survival and death.

Gal-3 biological roles are also regulated by its subcellular localization, for example: in contrast with the intracellular anti-apoptotic activity, when extracellular, Gal-3 has an opposite effect, acting as a pro-apoptotic factor, what has been demonstrated in human thymocytes and T cells (Stillman et al. 2006). Extracellularly, Gal-3 is found on cell surfaces, in the extracellular

matrix, in biological fluids and sera, as well as in culture media of certain cell lines, exhibiting several autocrine and paracrine effects (Dumic et al. 2006).

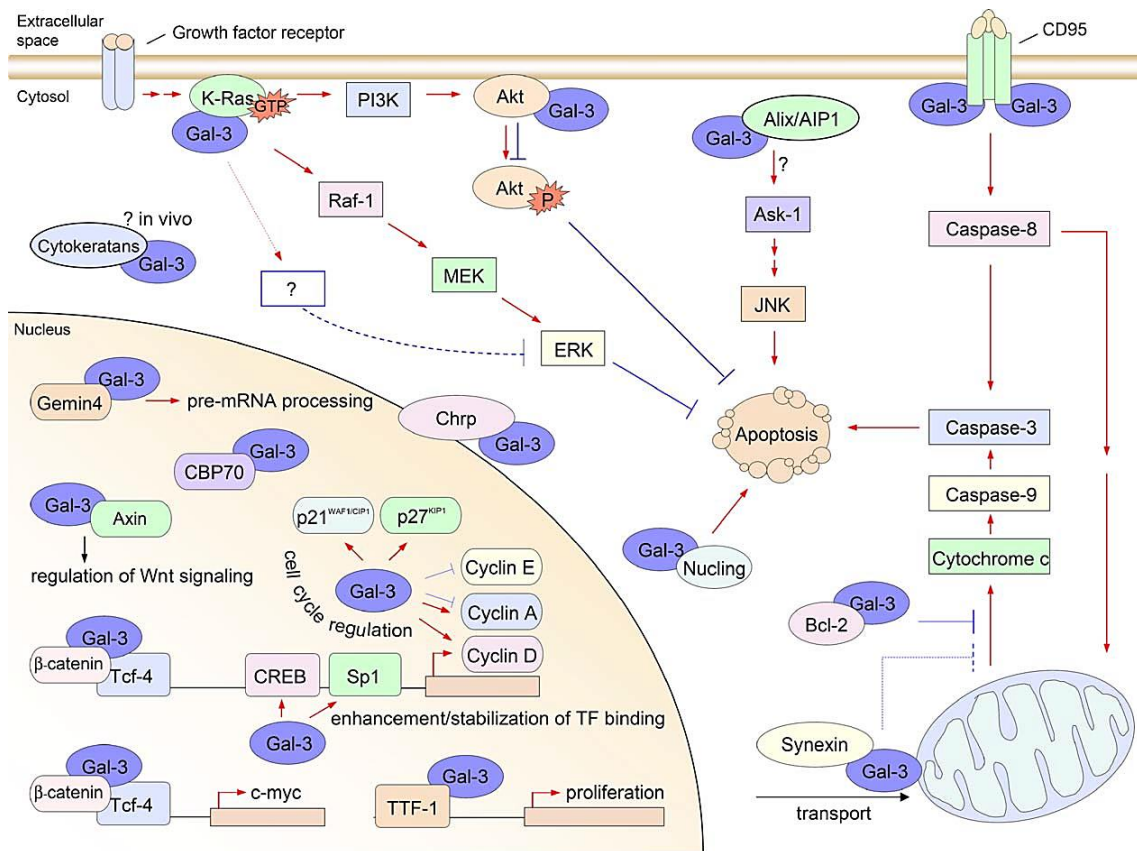


Fig. 1.6. Intracellular ligands and functions of Gal-3. Gal-3 plays important roles in cell biology, such as in: pre-mRNA splicing, transcription regulation, proliferation and regulation of cell cycle and apoptosis. (Red arrows indicate positive effects, blue lines indicate negative effects) (Adapted from Dumic et al. 2006).

As a result of its multivalent properties and the ability to bind cell surface glycoproteins and glycosylated components, like laminin, fibronectin, hensin, elastin, collagen IV and tenascin-C and -R, some integrins and lipopolysaccharides, Gal-3 participates in cell-cell, cell-matrix and also cell-pathogen interactions. These interactions translate into the modulation of cell adhesion, cell activation, receptor turnover and endocytosis, interfering with important biological processes, namely maintenance of cellular homeostasis, immune reactions, organogenesis and angiogenesis, tumour cell invasion and metastasis (Ochieng et al. 2004; Rabinovich et al. 2007). Regarding its membrane localization, in migrating dendritic cells, this lectin was found localized in membrane lipid rafts (in a lectin-carbohydrate interaction independent way), arising the suggestion that it is necessary for the formation of more complex ruffle structures, and possibly regulates cell migration at least in part by regulating the cell membrane architecture (Hsu et al. 2009).

As far as the immunoregulatory properties of this lectin are concerned, it acts as a chemoattractant for immune cells, namely monocytes, macrophages as well as neutrophils (Sano et al. 2000), participates in many T-cell mediated inflammatory processes, infections and autoimmune diseases (e.g.: diabetes mellitus and multiple sclerosis), acting in general as pro-inflammatory, and in innate anti-tumour immunity favouring tumour progression (Radosavljevic et al. 2012).

In summary, Gal-3 is a multifaceted protein: it displays pleiotropic effects that are dependent on its localization and interaction with its extensive list of ligands, being involved in normal cell function but also in pathological processes.

1.3.1.1. Galectin-3 in cancer: roles and KRAS interaction

Gal-3 altered expression has been connected to the progression of a variety of cancers, such as prostate (Knapp et al. 2013), thyroid (Chiu et al. 2010), breast (Zhang et al. 2014), colorectal (Endo et al. 2005; Povegliano et al. 2011), ovarian (Kim et al. 2011), hepatocellular (Jiang et al. 2014) and melanoma (Brown et al. 2012), being in some cases considered a potent diagnostic and prognostic biomarker and therefore a good therapeutic target.

Notably, Gal-3 is an active player in the carcinogenesis process from transformation to metastization (Fig. 1.7). Direct evidence has shown that Gal-3 plays a pivotal role in malignant transformation: inhibition of Gal-3 in breast cancer cells led to the reversion of the transformed phenotype both *in vivo* and *in vitro* (Honjo et al. 2001), and the introduction of Gal-3 cDNA into normal thyroid follicular cells conferred them a malignant phenotype (Takenaka et al. 2003). Additionally, Gal-3 participates in every step of the metastatic cascade including in angiogenesis, dissemination through the blood flow, tumour embolism formation and extravasation (Funasaka et al. 2014).

A list of evidences has been highlighting Gal-3 angiogenic role through different mechanisms (Funasaka et al. 2014). For example, Gal-3 seems to be connected to vascular endothelial factor (VEGF) and basic fibroblast growth factor-mediated angiogenesis by its carbohydrate-mediated interaction with $\alpha\beta 3$ integrin, which leads to subsequent activation of signalling pathways that promote the formation of new blood vessels (Markowska et al. 2010). Likewise, increased circulating Gal-3 is capable of induce secretion of metastasis promoting cytokines such as interleukin-6 and colony-stimulating factor from the blood vascular endothelial cells (*in vitro* and *in vivo*) that will enhance the expression of endothelial cell surface adhesion

molecules resulting in increased association between cancer and endothelial cells leading to increased migration and tubule formation (Chen et al. 2013b). Moreover, it has been recently demonstrated that Gal-3 produced by the tumour can induce M2-like macrophages migration and thereby, indirectly promoting angiogenesis and tumour growth (Jia et al. 2013). In addition, this lectin is required for stabilization of the epithelial-endothelial interactions, with proteolytically cleaved Gal-3 displaying a 20-fold higher affinity for endothelial cells when compared to the full-length protein (Shekhar et al. 2004). This ND-cleaved form occurs *in vivo* and has been demonstrated to play an important role in angiogenesis: tumour cells expressing non-cleavable Gal-3, showed reduced growth and angiogenesis (Nangia-Makker et al. 2007). In the same way, cells expressing an MMP-2/-9 cleavable-Gal-3 form showed increased endothelial cells chemotaxis, invasion and interaction with endothelial cells resulting in increased angiogenesis and 3D morphogenesis (Nangia-Makker et al. 2010).

Gal-3 subcellular localization also appears to be important and determinant for its roles in cancer. In prostate cancer, Gal-3 expression is generally decreased, but when detected it is only present in the cytoplasm, localization that is related to disease progression (Van Den Brùle et al. 2000). The same group proved that, in human prostate cancer, Gal-3 exerts opposite biological activities according to its localization: nuclear Gal-3 has anti-tumour functions whereas cytoplasmic Gal-3 promotes tumour progression (Califice et al. 2004). Also, in tongue cancer a translocation of Gal-3 from the nucleus to the cytoplasm during neoplastic progression was observed and was suggested to act as a prognostic factor (Honjo et al. 2000). On the other hand, in clear cell renal cell carcinoma, Gal-3 seems to be overexpressed and is significantly translocated into the nucleus (Straube et al. 2011).

Furthermore, by suppressing cancer cell drug-induced apoptosis, Gal-3 has been frequently implicated in drug resistance and its targeting could improve the efficacy of anticancer drug chemotherapy in several types of cancer (Fukumori et al. 2007). Fortunately, the investment on the design of therapeutic Gal-3 inhibitors is becoming a reality (Blanchard et al. 2014).

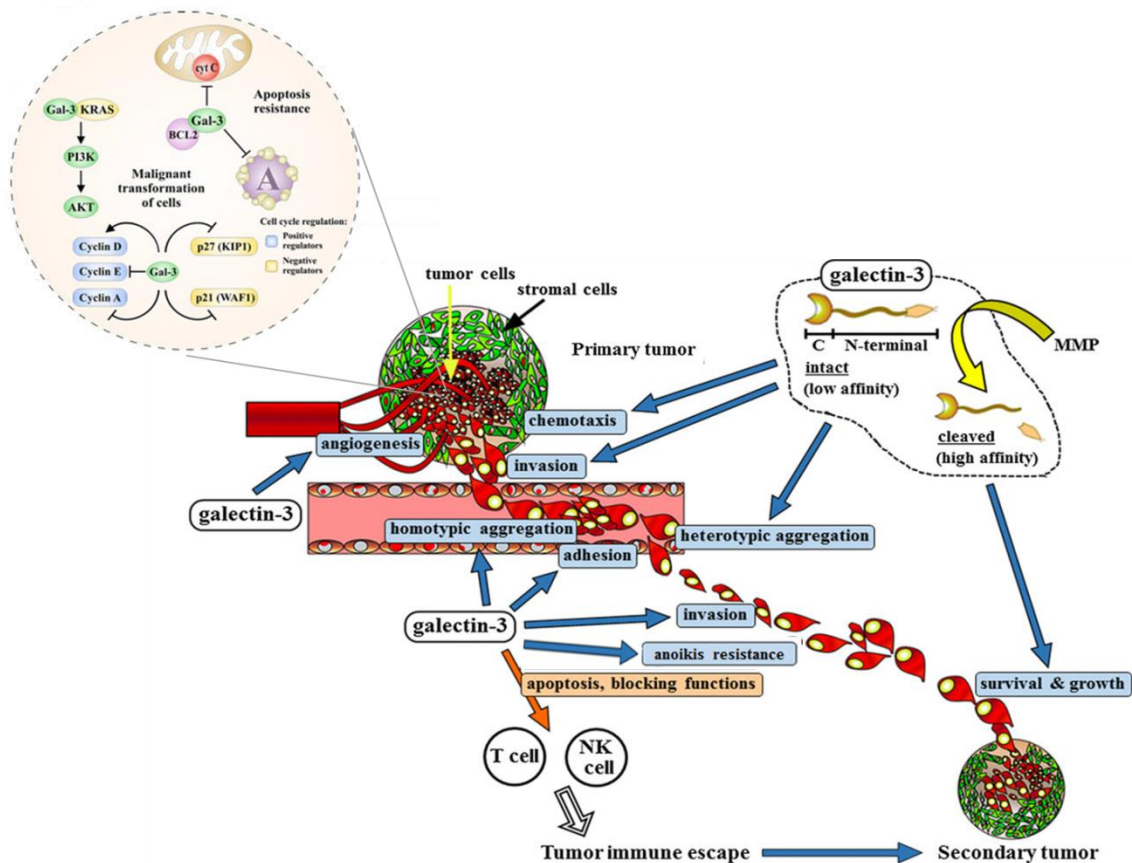


Fig. 1.7. Gal-3 contributes to tumorigenesis and tumour progression through several different mechanisms. Galectin-3 has an important role in the initiation of tumorigenesis especially through its interaction with KRAS triggering its downstream signalling pathways (not only PI3K/AKT pathway, represented in the image, but also the RAF/MEK/ERK pathway). Additionally, it has anti-apoptotic activity and maintains cell survival. Cell surface Gal-3 acts as an adhesion molecule in homotypic (cell–cell) and heterotypic (cell–matrix) interactions and is involved in the formation of tumour emboli and attachment of tumour cells to endothelium during metastasis. It is also able to protect cancer cells against anoikis allowing them to survive and spread through the blood flow, and to contribute to tumour immune escape by inducing apoptosis of immune cells. Gal-3 can also regulate tumour cell migration and invasion and sustains secondary tumour survival and growth. Particularly the ND-cleaved Gal-3 form has angiogenic activity promoting new capillaries formation (Adapted from Radosavljevic et al. 2012; Funasaka et al. 2014).

KRAS is one of the Gal-3 ligands (Fig. 1.6): they have been shown to interact in various cellular models and Gal-3 mediated transformation is partially attributed to this interaction (Fig. 1.7) (Elad-Sfadia et al. 2004; Shalom-Feuerstein et al. 2005; Levy et al. 2010; Song et al. 2012; Wu et al. 2013). Gal-3 specific interaction with KRAS-GTP promotes strong and prolonged KRAS activation of PI3K and RAF-1, but on the other hand, promotes attenuation of ERK activation by an unknown mechanism (Elad-Sfadia et al. 2004). Importantly, some results indicate that tumours can acquire KRAS-transforming characteristics without a *KRAS* activating mutation but by elevated expression of Gal-3 (Shalom-Feuerstein et al. 2005). Gal-3 is capable of directly bind KRAS and mediate the activation of its signalling pathways (Shalom-Feuerstein et al. 2005; Shalom-feuerstein et al. 2008; Song et al. 2012), but also indirectly increases KRAS expression

and improves its membrane stability and activity, by downregulating miRNA let-7, which is known for negatively regulating KRAS transcription (Levy et al. 2011). Data about this interaction using cancer cell models has been accumulating and proving its relevance in malignancy (Table 1.1).

Table. 1.1. Evidences of Gal-3-KRAS interaction in cancer cell models

Model	Gal-3-KRAS connection	Reference
Breast cancer cells	- Overexpression of Gal-3 coincide with a significant increase in KRAS ^{wt} -GTP coupled with loss of NRAS ^{wt} -GTP; - Gal-3 acquires several oncogenic properties by binding to KRAS ^{wt} with the consequent activation of RAF-MEK-ERK signalling.	Shalom-Feuerstein et al. 2005
	- Gal-3 is an integrant structural component of KRAS-GTP membrane nanoclusters and is determinant for nanoclusters formation and signal output.	Shalom-Feuerstein et al. 2008
Thyroid cancer cells	- Gal-3 overexpression positively correlates with high levels of KRAS ^{wt} -GTP, contributing to malignant phenotype.	Levy et al. 2010
Pancreatic cancers and cancer cells	- Gal-3 binds RAS, is responsible for its attachment to the membrane and mediates its downstream signalling activation.	Song et al. 2012
Colon cancer cells	- Through the activation KRAS/RAF/MEK/ERK pathway, Gal-3 mediates cancer cell migration and potential distal localization.	Wu et al. 2013

1.3.1.1.1. Galectin-3 in colorectal cancer

Gal-3 is expressed in the normal colonic mucosa both in the nucleus and cytoplasm, but more strongly in the nucleus (Lotz et al. 1993; Sanjuán et al. 1997). Despite some studies demonstrated a decreased Gal-3 expression in CRC (Lotz et al. 1993; Sanjuán et al. 1997) and that Gal-3 decrease is related with the malignant invasive behaviour (Tsuboi et al., 2007), the majority of the studies have confirmed an increased Gal-3 expression and a correlation with the degree of dysplasia and metastatic potential (Lotan et al. 1991; Irimura et al. 1991; Schoeppner et al. 1995; Legendre et al. 2003; Hittélet et al. 2003; Endo et al. 2005; Povegliano et al. 2011).

Emphasizing the relevance of Gal-3 in CRC, a CRC rat model was designed to study its expression and its ligands along carcinogenesis. The expression of Gal-3 demonstrated to be increased in primary lesions and diminished in tumours and metastasis (Hill et al. 2010), which is partially in agreement with the studies aforementioned. In one aspect seems to be consensus: along tumour progression, Gal-3 intracellular localization is cytoplasmic rather than nuclear. This localization seems to be related to a higher risk of recurrence and thereby can be considered a poor prognosis factor (Lotz et al. 1993; Sanjuán et al. 1997; Lotan et al. 1991; Irimura et al. 1991; Hittélet et al. 2003; Povegliano et al. 2011).

Overexpression of this lectin was also found at the cell surface of CRC cells (Lee et al. 1991; Greco et al. 2004) where it is suggested to facilitate metastization (Lee et al. 1991). In agreement with this author and the ones that described increased expression of Gal-3 correlated with metastatic potential, is the finding that reduction of Gal-3 mRNA and protein levels (both on cytoplasm and cell surface), through antisense inhibition, significantly reduced cells' ability to colonize the liver and conversely, elevation of the lectin levels resulted in a derivative cell line with a high liver-colonizing potential (Bresalier et al. 1998). This relation between Gal-3 and metastasis seems to be explained by its interaction with cancer-associated MUC1, via the oncofetal Thomsen-Friedenreich (TF) antigen, which induces polarization of MUC1 cell surface localization and thereby allows exposure of some underlying adhesion molecules, enhancing cancer-endothelial adhesion and promoting metastasis (Zhao et al. 2009). Gal-3 role in CRC cells adhesion, is also supported by its range of ligands that are involved in cell adhesion and metastasis, such as carcinoembryonic antigen (CEA; to which Gal-3 co-localizes on the cell membrane) and other members of the immunoglobulin superfamily, laminin, lamp-1 and lamp-2 (Ohannesian et al. 1995). Meanwhile, in the rat model, it was observed that Gal-3 ligands at the extracellular matrix are expressed in late phases of tumourigenesis (Hill et al. 2010), which is in agreement with the proposed role for Gal-3–ligand interactions in cancer invasion and metastasis.

Furthermore, serum levels of Gal-3 are greatly elevated in CRC patients, particularly those with metastasis (Barrow et al. 2011). Simultaneous detection of serum Gal-3/-4 levels can distinguish metastatic from non-metastatic patients with high specificity and sensitivity and can be a useful tool to detect CRC metastasis (Barrow et al. 2013).

Importantly, using human colon cancer cell lines (DLD-1 and Caco-2), it has been demonstrated that overexpression of Gal-3 is related to increased cell migration rate and to lamellipodia formation and distal lung localization in SCID mice, whereas its knockdown decreased the migration. Importantly, this Gal-3 effect on migration is mediated by KRAS and its subsequent activation of RAF/MEK/ERK pathway (Wu et al. 2013).

1.4. *p16^{INK4a}*: more than a tumour suppressor gene

p16^{INK4a} (abbreviated as p16) is part of the INK4 family of cyclin-dependent kinase (CDK) inhibitors, which includes three more members: *p15^{INK4b}*, *p18^{INK4c}*, *p19^{INK4d}* (Vermeulen et al. 2003). This protein was isolated in a yeast two-hybrid screening searching for proteins that interact with

the human CDK4 and it was suggested to be a negative regulator of proliferation in normal cells (Serrano et al. 1993). After its isolation, some authors established a direct connection between *p16* inactivation and tumour susceptibility and it was confirmed as a tumour suppressor gene (Liggett & Sidransky 1998).

The formation of CDK4/6-cyclin D active complexes is essential for entry in G1 phase, and during early G1 CDK4/6-cyclin D active complexes are responsible for retinoblastoma protein (pRb) phosphorylation. This, in turn, leads to the disruption of pRB complexes with the histone deacetylase protein and release of the transcription factors E2F-1 and DP-1, which positively regulate the transcription of genes whose products are required for S phase progression. As the CDK inhibitor (CKI) p16 inhibits the association of CDK4/6-cyclin D complexes, pRb is not phosphorylated and thereby the genes necessary for the progression to S phase are not transcribed, resulting in cell cycle arrest in G1 (Fig. 1.8). Therefore, cells that lose p16 will indiscriminately progress through the cell cycle (Liggett & Sidransky 1998; Vermeulen et al. 2003).

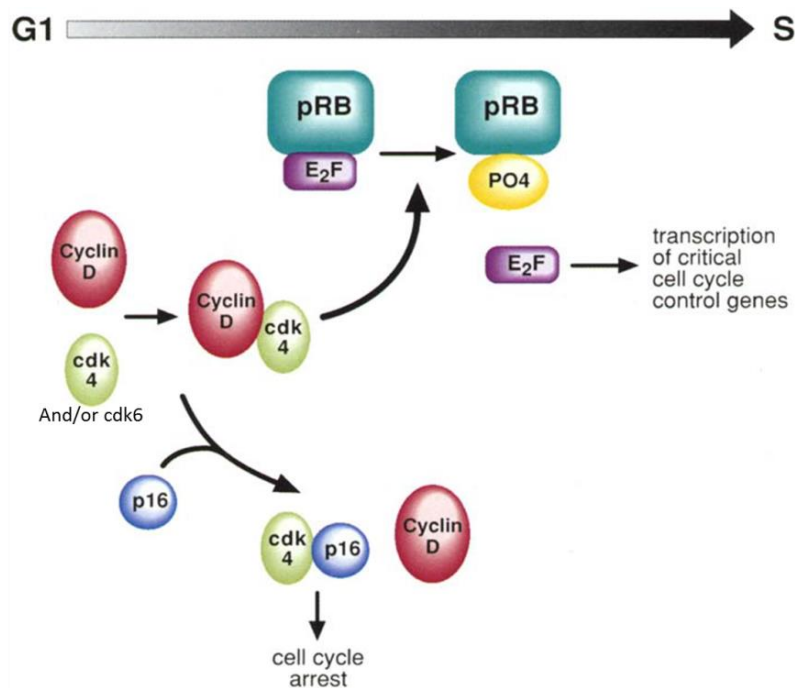


Fig. 1.8. Cell cycle regulation by p16. Cyclin D1 regulate the function of CDK4 and/or CDK6, which phosphorylates pRB. Phosphorylation inactivates pRB and allows E2F release followed by the transcription of critical cell-cycle proteins for the progression through the restriction point. p16 has a negative effect in this regulation and acting as a CKI, prevents cyclin D-CDK4 and/or CDK6 complex formation rendering cells to cell cycle arrest (Adapted from Liggett & Sidransky 1998)

The mechanisms behind *p16* inactivation involve point mutations, promoter methylation or deletions (Rocco & Sidransky 2001). The ubiquitous and frequent inactivation of *p16* in human tumours led to the hypothesis that loss of p16 must provide a selective cellular growth advantage to many tumours (Liggett & Sidransky 1998). Importantly, in CRC cell lines, inactivation of *p16* seems to be common and promoter methylation-dependent (Herman et al. 1995; Tominaga et al. 1997; Kim et al. 2005). Conversely, in CRC tissues, the methylation status had been demonstrated to be variable and p16 expression has been repeatedly detected, overexpressed in some cases (Ohhara et al. 1996; Dai et al. 2000; Palmqvist et al. 2000; Norrie et al. 2003; Kim et al. 2005). Decreased or no p16 expression as a result of promoter methylation is associated with a more aggressive phenotype and poor prognosis (Liang et al. 1999; Yi et al. 2001; Kim et al. 2005; Bihl et al. 2012). Moreover, the variable density of methylation (high, low or non-methylated) appears to be important since it correlates with p16 mRNA expression (Kim et al. 2005) and yet it might not result in transcriptional silencing (Norrie et al. 2003; Kim et al. 2005).

Aside from its tumour suppressor CKI status, p16 has been proving to exert a function in other cell biology aspects, including in the regulation of angiogenesis (Alhaja et al. 2004; Lu et al. 2012), apoptosis (Al-Mohanna et al. 2004; Lu et al. 2012), anoikis (Plath et al. 2000; André et al. 2007; Sanchez-Ruderisch et al. 2010; Amano et al. 2012) and, immortalization and senescence (Hara et al. 1996; Serrano et al. 1997; Lin et al. 1998; Jacobs & Lange 2004; Lu et al. 2012).

1.4.1. p16 connection with galectin-3 and KRAS

From the point of view of p16 connection with Gal-3 and KRAS, some of p16 roles in anoikis and senescence need to be addressed.

In a variety of cell lines, reconstitution of p16 expression confers the lost capability to undergo anoikis, what seems to be related to a p16-reconstitution induced upregulation of the fibronectin receptor ($\alpha 5\beta 1$ integrin) (Plath et al. 2000). Beyond the transcriptional upregulation of the $\alpha 5\beta 1$ integrin, p16 might have significant biological influences in other aspects. In fact, in Capan-1 pancreatic carcinoma p16 positive cells, a concerned expression of $\beta 1,4$ -galactosyltransferases as well as a decreased sialylation of O-/N-glycans, were observed. These aspects correlate with increased $\beta 1$ -integrin maturation, subunit assembly and increased binding activity of the $\alpha 5\beta 1$ -integrin. Besides, as a result of the reduced sialylation, that normally masks terminal galactoside residues for lectins, the presentation of glycan binding sites is

increased along with the cells capacity to bind Gal-1 (a galectin that favours anoikis), that was also increased at the transcription level (André et al. 2007). Moreover, in addition to altering α 2,6-sialyltransferase expression, p16 acts through the regulation of enzymes on the pathway of sialic acid biosynthesis (Amano et al. 2012).

The concerned effects of p16 to restore tumour cells anoikis susceptibility also affect Gal-3. As already mentioned, Gal-3 is important to protect cells from anoikis induction, effect that is exerted intracellularly and at the cell surface by antagonizing Gal-1 pro-anoikis effects. Likewise, forced expression of Gal-3 in p16-positive cells reduces their susceptibility to anoikis but the presence of p16 decreases Gal-3 mRNA levels and cell surface presentation (Sanchez-Ruderisch et al. 2010). In addition, it was shown that this tumour suppressor controls oncogenic KRAS function in human pancreatic cancer cells: restitution of p16 downregulates KRAS^{G12V} activity, decreases its stability and expression, event that is necessary for p16-mediated restoration of anoikis resistance and suppression of cells clonogenicity (phenomena that was also verified in CRC cells- SW480 cell line) (Rabien et al. 2012). In this model, reduced levels of Gal-3 were found (Rabien et al. 2012), and in the light of the exposed information one might speculate that those could be a result of p16 expression and might also have contributed for the observed effects on KRAS. In summary, p16 coordinately orchestrates important changes to suppress the transformed phenotype with relevant impact in the galectin network and on the oncogenic KRAS.

As far as the p16 role in senescence is concerned, besides being involved in other senescence mechanisms, namely the ones induced by telomere erosion or DNA damage, p16 is involved in prematurely oncogenic stimuli-induced senescence (OIS). This mechanism was firstly referred by Serrano et al. 1997 and has been suggested to have a tumour suppressive function in a variety of different tumours (Collado & Serrano 2013). p16 levels increase in response to prolonged oncogenic HRAS^{G12V} expression/activation and provoke permanent cell cycle arrest in G1 phase. The mechanism underlying this requires RAS-mediated MAPK activation, which can produce two precisely opposite effects: cell-cycle arrest or forced mitogenesis, depending on the integrity of the senescence cooperative program controlled by p53 and p16, thereby reinforcing the tumour suppressor status of these genes (Serrano et al. 1997; Lin et al. 1998). This duality of effects seems to depend on the level of RAS activation: low levels led to hyperplasia, whereas high levels induce irreversible cellular senescence. This oncogene-induced senescence is followed by RAS downregulation and subsequent apoptosis, which could be explained by the so called “RAS addiction” hypothesis: once established, oncogenic RAS activation may be required

for the survival of the growth-arrested cells or in other words, the cells may become “addicted” to the RAS oncogenic stimulus (Sarkisian et al. 2007). As for oncogenic KRAS^{G12V}, it has been shown that it induces senescence-related markers following MAPK pathway activation in colon cancer Caco-2 cells. However, in this cell line, p16 is hypermethylated and p53 mutated and although pRb and p19ARF were working to induce senescence-related markers, they were not sufficient to induce growth arrest, demonstrating the importance of p16 and p53 tumour suppressors (Oikonomou et al. 2009). In a serrated colon cancer mice model, KRAS^{G12D} has been demonstrated to be capable of induce tumour suppressive senescence and deletion of Ink4a/Arf locus prevents senescence and leads to invasive, metastasizing carcinomas (Bennecke et al. 2010). Once again, this emphasizes the relevance of the cellular context in which a given molecular alteration occurs.

In conclusion p16 exerts its tumour suppression activity not only by its CKI function, but also by interfering with other tumour progression mechanisms, including anoikis and senescence, in which it is indirectly connected to Gal-3 and KRAS.

1.5. Rationale and aims

Gal-3 and KRAS seem to have a mutual and dual relationship: Gal-3 is necessary for KRAS membrane nanoclusters formation and signal output (Shalom-feuerstein et al. 2008), and increases its expression, stability and activity by downregulating let-7 miRNA (Levy et al. 2011); in its turn, Gal-3 transformation effects have been described as being mediated by its interaction with KRAS and subsequent activation of its downstream signalling pathways, namely in models of breast (Shalom-Feuerstein et al. 2005), thyroid (Levy et al. 2010), pancreatic (Song et al. 2012) and colon cancer (Wu et al. 2013). Furthermore, it is possible to postulate the existence of a relation between p16, downregulating both Gal-3, and KRAS (Sanchez-Ruderisch et al. 2010; Rabien et al. 2012) (Fig. 1.9). Gathering all the data from the literature, it is possible to infer that Gal-3, KRAS and p16 are all important players in the carcinogenesis. To the best of our knowledge, the Gal-3/KRAS/p16 triple axis interplay has never been brought together in a study and the connection among these proteins in the CRC model is poorly understood, requiring further investigation.

The general aim of this work is to understand, in the CRC model, the interaction between Gal-3/KRAS/p16 proteins and to explore the effect of silencing Gal-3 and/or KRAS on the triple interplay and on tumour-associated phenotypic alterations.

Specifically we aim to answer the following questions:

- (1) Is there a direct interaction between *KRAS^{mut}*, Gal-3 and p16 in the CRC model?
- (2) Which is the effect of silencing Gal-3 and/or KRAS in the Gal-3/KRAS/p16 expression levels regulation and interplay in the CRC model?
- (3) What are the tumour-associated phenotypic alterations induced by inhibition of KRAS and/or Gal-3 in CRC cell lines?

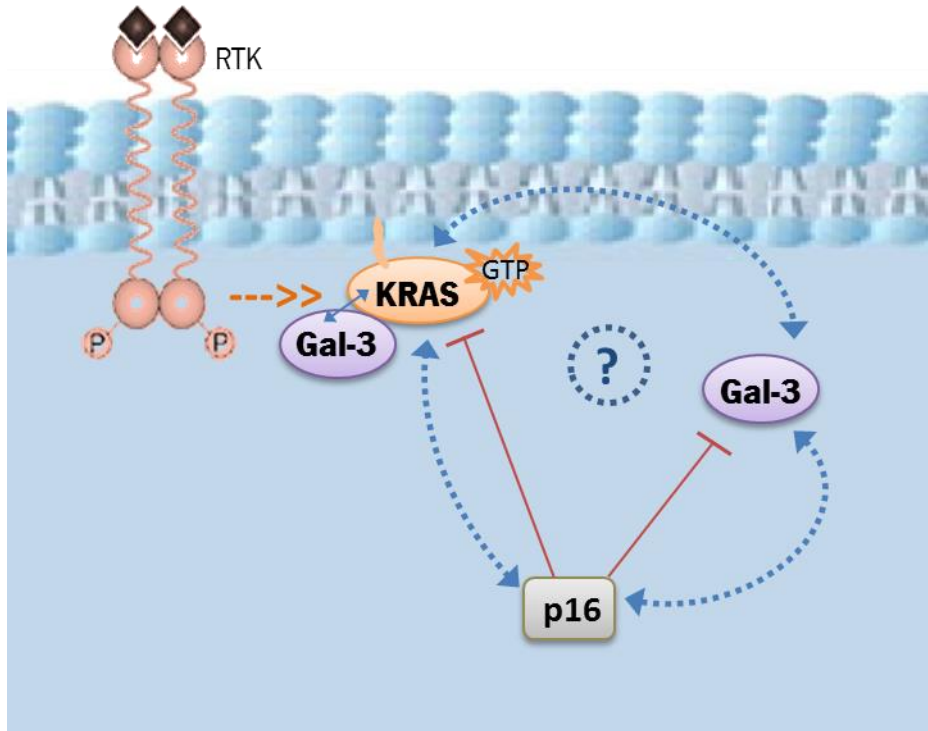


Fig. 1.9. Rationale of the project. Gal-3 and KRAS seem to have a mutual and dual relationship and are known to interact in KRAS membrane nanoclusters formation (blue arrows). Some evidences have shown that p16 is capable of downregulate both Gal-3, and KRAS (red lines). The main goal of this project is to understand if there is a direct interaction (blue interrupted arrows) between Gal-3, KRAS and p16.

II.

MATERIALS AND METHODS

2.1. Cell lines and culture conditions

In order to achieve the aims proposed for this work, cell lines with different genetic backgrounds were used: SW480 (ATCC-CCL-228), HCT116 (ATCC-CCL-247), NCM460 parental (transfected with an empty vector) and 4 others NCM460-derived cell lines previously transfected with Flag-KRAS^{wt} and FLAG-KRAS harbouring hotspot mutations: Flag-KRAS^{G12V}, Flag-KRAS^{G12D} and Flag-KRAS^{G13D}.

SW480 cell line was kindly provided by Maria José Oliveira (IBMC-INEB). This cell line was established from a colorectal primary adenocarcinoma and harbours a KRAS^{G12V} mutation (Ahmed et al. 2013). HCT116 cell line was kindly ceded by Muriel Priault (IBGC, CNRS). This cell line was established from a colorectal primary carcinoma and harbours a KRAS^{G13D} mutation (Ahmed et al. 2013). NCM460, the normal colon-derived cell line (Moyer et al. 1996), was received by a material transfer agreement with INCELL Corporation, San Antonio, TX and the stable transfected cell lines, Flag-KRAS^{wt}, Flag-KRAS^{G12V}, Flag-KRAS^{G12D} and Flag-KRAS^{G13D} were established by Sara Alves during her PhD (CBMA-UMinho).

SW480 and all NCM460 and NCM460-derived cell lines were maintained in RPMI-1640 medium (Biowest) while the HCT116 cell line was maintained in McCoy's 5A medium (Biowest). For all cell lines, the medium was supplemented with 10% heat inactivated fetal bovine serum (FBS; Gibco) and 1% penicillin/streptomycin (Biowest). The medium was renewed twice a week and the cells were subcultured every week, when the confluence reached values close to 80%, by detachment with 0,05% trypsin (Sigma-Aldrich). All cells were grown at 37°C in a humidified incubator with 5% carbon dioxide.

2.2. Western Blotting analysis

2.2.1. Total protein extraction

For the analysis of basal expression levels of Gal-3, KRAS and p16, total protein extracts were prepared. Cells were plated in 60mm Petri dishes at a density of 1.5x10⁵ cells/ml for HCT116 cells and of 3.0x10⁵ cells/ml for SW480 cells in a final volume of 3ml; and 1.2x10⁶ cells/ml for NCM460 and NCM460-transfected cell lines, in a final volume of 2,5ml. After 24h, the culture medium was changed and after 48h, the protein extraction protocol was performed.

Cells were scraped and harvested for the respective 15ml tube on ice. To minimize cell loss, the plate was washed 2 times with PBS 1×, scraped again and the suspension harvested for the assigned tube. Cell suspension was centrifuged for 10 min, at 2000 rpm, at 4°C, the

supernatant was removed until the mark of 500 μ l and the pellet was gently resuspended and transferred to an eppendorf tube on ice. 500 μ l of cold PBS 1 \times were added and the eppendorf tube was centrifuged for 5 min, at 2000 rpm, at 4 $^{\circ}$ C. The supernatant was removed and a mixture of ice-cold radioimmunoprecipitation assay (RIPA) buffer (50mM of Tris-HCl pH=7.5, 150mM NaCl, 2mM EDTA and 1% NP-40) supplement with 20mM NaF, 20mM Na₃VO₄, 1mM PMSF and 40 μ l/ml proteases inhibitor cocktail (Roche) was added until covering the pellet. The pellet was strongly resuspended to promote cell lysis and left to rest on ice for 20 min. After that time, cells were centrifuged for 15 min at 14000 rpm, at 4 $^{\circ}$ C. The supernatant was transferred into another eppendorf and stored at -80 $^{\circ}$ C until sample quantification and preparation for western blot analysis.

2.2.2. Protein Quantification

In this work total protein extracts were quantified using the Bio-Rad *DC Protein Assay Kit*-a colorimetric method for protein concentration determination.

Protein standards of crescent bovine serum albumin (BSA) concentrations (0.25, 0.5, 1, 2, 3 and 5mg/ml) were prepared in RIPA buffer from a 10% BSA stock solution. In a 96 wells plate, 5 μ l of RIPA buffer (blank), 5 μ l of each BSA standard and 1 μ l of each sample diluted 5 times in RIPA buffer, were added in the respective well. Then, the colorimetric assay is based on two steps: the addition of 25 μ l of A' reagent (20 μ l S reagent and 1000 μ l of A reagent), followed by the addition of 200 μ l of B reagent to each well. At that point, the plate was incubated in the dark, at room temperature (RT), for 15 min and the absorbance values were read at 720nm in the *SpectraMax Plus 384* (Molecular Devices).

A calibration curve was designed using the absorbance values of the BSA standards and the concentration of the samples was extrapolated.

2.2.3. Western Blotting

After quantification, an equal protein amount (30 or 50 μ g) of each sample was mixed with 5 μ l Laemmli Buffer 4 \times (0.25M Tris-HCl, 9.2% SDS, 40% glycerol, 5% β -mercaptoethanol, 5% bromophenol blue) and deionized H₂O to obtain the final volume of 20 μ l. In order to denature proteins, samples were heated at 95 $^{\circ}$ C for 5 min, followed by a short spin. Then 20 μ l of each sample and 3 μ l of molecular weight marker (Thermo Scientific) were loaded into the respective well of a 5% polyacrylamide stacking gel (125 mM Tris-HCl pH 6.8 SDS 0.4%, 0.1% TEMED,

0.05% APS), and separated in a 15% polyacrylamide resolving gel (375 mM Tris-HCl pH 8.8 SDS 0.4%, 0.1% TEMED, 0.05% APS), using running buffer (10x: 0.25 M Tris base, 1.92 M Glycine, 1% SDS, final concentration of 1x) in a Mini-Protean III electrophoresis system (Bio-Rad) at 100V for about 2h (until the dye front reached the bottom of the gel).

The proteins were then transferred to a polyvinylidene difluoride (PVDF) membrane (Thermo Scientific) in a Mini Trans-Blot System (Bio-Rad) at 100V and 400mA for 2h, using Transfer Buffer (10x: 0.25 M Tris base, 1.92 M Glycine, final concentration 1x + 10% methanol) and a cooling coil. Next, membranes were removed from the system and blocked for a minimum of 2h at RT with moderate stirring, in 2.5% soy milk in PBST (PBS 1x + 0,1% Tween-20), in order to block nonspecific binding sites. After blocking, membranes were briefly washed in PBST and then incubated overnight with primary antibody (Table 2.1) at 4°C under agitation, or, in the case of β -actin antibody, at RT for 1h. After 3 washes of 5 min in PBST, with moderate stirring, membranes were incubated for 1h at RT with the respective secondary antibody (Table 2.1), conjugated with IgG horseradish peroxidase. Membranes were washed 5 times for 7-10 min in PBST and finally, immunoreactive bands were detected using the immobilon solutions (Millipore) under the Chemi Doc XRS (Bio-Rad) chemiluminescence detection system.

Table. 2.1. Primary and secondary antibodies used in this study and their respective dilutions

Primary antibody	Primary antibody Dilution	Protein Size (kDa)	Secondary antibody	Secondary antibody Dilution
Anti-KRAS (Santa Cruz Biotechnology)	1:100	21	Goat anti-mouse (Jackson Laboratory)	1:2000 In 2,5% soy milk
Anti-Flag (Sigma-Aldrich)	1:1000	25	Goat anti-mouse (Jackson Laboratory)	1:2000 In 2,5% soy milk
Anti-p16 (Santa Cruz Biotechnology)	1:250	16	Goat-anti-rabbit (Jackson Laboratory)	1:2000 In 2,5% soy milk
Anti-Gal-3 (Santa Cruz Biotechnology)	1:1000	31	Rabbit anti-goat (Santa Cruz Biotechnology)	1:3000 In 2,5% soy milk
Anti-β-actin (Sigma-Aldrich)	1:500	42	Goat anti-mouse (Jackson Laboratory)	1:2000 In 5% BSA

When needed, for re-incubation with different antibodies, the membranes were stripped by washing twice with glycine stripping solution (25mM Glycine pH=2.5 and 1% SDS) for 10 min and then with PBS1× (2×10 min) at RT with moderate stirring. Membranes were blocked again and incubated with the desired primary antibody.

Densitometry analysis was performed using the Quantity one software (Bio-Rad) and protein expression levels for each sample were normalized to the level of β -actin.

2.3. Immunofluorescence Assay

In order to assess protein cellular localization immunofluorescence assay was performed. Therefore, SW480 and HCT116 cells were seeded in 12mm glass coverslips (Thermo Scientific) with no treatment at 2 different densities: 1) to obtain low confluent cells, SW480 cells were plated at 1.5×10^5 cells/ml and HCT116 at 6.7×10^4 cells/ml in 12 well plates (final volume of 1ml) and were allowed to grow for 2 days; 2) to obtain high confluent cells, SW480 cells were plated at 2.5×10^5 cells/ml and HCT116 at 1×10^5 cells/ml in 24 well plates (final volume of 500 μ l) and were allowed to grow for 4 days. NCM460-derived cell lines were plated at a density of 4×10^5 cells/ml in 12 well plates (final volume of 750 μ l).

Cells lines were fixed using 2 different methods: fixation in methanol and fixation in 4% paraformaldehyde (PFA). The immunofluorescence protocol varied depending on the fixation method.

All the images were acquired in a Leica TCS SP5II confocal microscope using the HCX PL APO CS 63.0x1.40 OIL UV objective, and processed with the LAS AF TCS SP5 software. The lasers: Diode (405-excitation), Argon (488-excitation) and DPSS (561-excitation) were used to obtain images from DAPI, Alexa fluor-488 and Alexa fluor-594 fluorochromes, respectively. In each condition the images were acquired with identical laser power, gain and offset.

2.3.1. Cells fixation in methanol

The coverslips were washed 3 times for 5 min with PBS 1× and fixed with ice-cold methanol, at -20°C, for 30 min. The coverslips were left at RT, dried and stored at -20°C, until use.

To initiate the single staining protocol, the coverslips were re-hydrated by being washed 3 times for 5min in PBS 1× under agitation and blocked with a 5% BSA solution for 30 min at RT. Next they were incubated overnight, at 4°C in a humidified chamber, with the respective primary

antibody (Table 2.2) or with PBS 1× for the negative control. On the next day, the coverslips were washed 3 times for 5 min in PBS 1× under agitation and incubated with the respective secondary antibody (Table 2.2) for 1h, at RT, in a dark chamber. Finally, the last 3 washes of 5 min in PBS 1× were performed, and the coverslips were mounted in Vectashield+DAPI mounting media (Vector Laboratories) onto a microscope slide.

The double staining protocol was done sequentially, in other words, the single staining was repeated twice (with one additional step). After blocking with 5% BSA, the coverslips were incubated overnight at 4°C with anti-p16 antibody, washed and incubated with the secondary biotinylated swine anti-rabbit antibody for 1h at RT. Subsequently, the coverslips were incubated overnight with anti-Gal-3 antibody, washed and incubated with Alexa fluor-488 donkey anti-goat antibody for 1h at RT in a dark chamber, followed by a 20 min incubation with streptavidin Alexa fluor-594 conjugated (Molecular Probes). Finally, after another round of washes, coverslips were mounted in Vectashield+DAPI mounting media onto a microscope slide.

2.3.2. Cells fixation in 4% paraformaldehyde

The coverslips were washed 3 times for 5 min with PBS 1× and fixed with 4% PFA for 40 min at RT. After fixation, PFA was removed and the coverslips were washed five times for 5 min with PBS 1× and stored in sterile PBS 1× at 4°C until use.

To start the immunofluorescence, the coverslips were washed 3 times for 5 min in PBS 1× under agitation and quenched for 10 min with a NH_4Cl 50mM solution, followed by another round of washes. Then, the cells were permeabilized for 5min with TritonX-100 0,2%, washed again and blocked for 30 min in 5% BSA solution at RT. The coverslips were then incubated overnight, at 4°C in a humidified chamber, with the respective primary antibody (Table 2.2) or with PBS 1× for the negative control. Afterwards, the coverslips were washed 3 times for 5 min in PBS 1×, under agitation and incubated with the respective secondary antibody (Table 2.2) for 1h, at RT, in a dark chamber. Finally, the last 3 washes of 5min in PBS 1× were performed and the coverslips were mounted in Vectashield+DAPI mounting media onto a microscope slide.

Double staining was done sequentially in order to minimize secondary antibodies interaction. After blocking with 5% BSA, the coverslips were incubated overnight at 4°C with the respective anti-Gal-3 or anti-p16 antibody, washed and incubated with the assigned secondary-conjugated antibody for 1h at RT. Subsequently, the coverslips were incubated for 1h at RT with primary anti-FLAG antibody, washed and incubated with Alexa fluor-594 goat

anti-mouse antibody (Invitrogen) for 1h at RT in a dark chamber. Lastly, after another round of washes, coverslips were mounted in Vectashield+DAPI mounting media onto a microscope slide.

Table. 2.2. Primary and secondary-conjugated antibodies and the respective dilutions used in immunofluorescence, with reference to cell lines and fixation methods

	Primary antibody	Dilution	Secondary antibody (1:100)		
			Single staining	Double staining	
SW480 and HCT116 cell lines	Anti-KRAS (Santa Cruz Biotechnology)	1:50	Alexa Fluor-488 goat anti-mouse (Invitrogen)	—	Methanol or 4% -PFA-fixed cells
	Anti-p16 (Santa Cruz Biotechnology)	1:50	Alexa Fluor-488 goat anti-rabbit (Invitrogen)	Swine anti-rabbit biotinylated (Dako)	Methanol-fixed cells
	Anti-Gal-3 (Santa Cruz Biotechnology)	1:100	Alexa Fluor-488 donkey anti-goat (Invitrogen)		
NCM460 Flag-KRAS-transfected cell lines	Anti-Flag (Sigma-Aldrich)	1:100	—	Alexa Fluor-594 goat anti-mouse (Invitrogen)	4% PFA-fixed cells
	Anti-p16 (Santa Cruz Biotechnology)	1:50	—	Alexa Fluor-488/594 goat anti-rabbit (Invitrogen)	
	Anti-gal-3 (Santa Cruz Biotechnology)	1:100	—	Alexa Fluor-488 donkey anti-goat (Invitrogen)	

2.4. Co-Immunoprecipitation

Immunoprecipitation (IP) is a routinely used technique to isolate target proteins from complex samples (e.g. cell lysates or serum) taking advantage of antibodies specificity. Co-immunoprecipitation (Co-IP) is an effective IP strategy to study protein-protein interactions. The traditional method basically consists of incubating the IP antibody with the sample, establishing an antigen-antibody complex, and subsequently with Protein A or G beads, which bind to the antibody via the Fc region, facilitating antigen and antigen-bound proteins recovery. The results are typically analyzed via one or two-dimensional gel electrophoresis followed by mass spectrometry or immunoblotting (Kaboord & Perr 2008).

For Co-IP experiments, SW480 cells were plated in 25cm² culture flasks until reaching approximately 90% confluence. Cells were washed twice with PBS 1× and lysed for 15 min at 4°C in RIPA buffer with 3mM Na₃VO₄, 20mM NaF, 1mM PMSF and 10µg/ml of aprotinin and

leupeptin. After that, the monolayer was scraped, resuspended and collected for an eppendorf. Cell suspension was centrifuged for 10 min at 14000rpm at 4°C and the supernatant was transferred to another eppendorf. After this procedure total protein concentration was determined using the Bio-Rad *DC Protein Assay Kit* (as described in 2.2.2).

Protein G sepharose beads (GE Healthcare) were centrifuged, for 12sec at 14000rpm at 4°C, to remove the ethanol fraction, and then washed twice with buffer C (Catenin lysis buffer- 1% Triton X-100+1%NP-40 in PBS 1×+ Na₄P₂O₇+ NaF 1× in PBS 1×) with short spins between the washes to remove supernatant. In order to block unspecific binding to the beads, these were incubated with 1% BSA overnight at 4°C under agitation.

Afterwards, samples were pre-cleared by adding 25µl of bead suspension to each sample with 1250µg protein and shaken for 30 to 45 min at 4°C. The supernatant was collected to a new eppendorf, the respective antibodies- anti-Gal-3, anti-KRAS or anti-p16- were added (2µg antibody/250µg protein) to the respective tubes, and incubated overnight, at 4°C, under agitation. 55µl of loading buffer 1,5× were added to each pre-clear sample. These samples were denatured during 5 min at 95°C and frozen.

On the following day, 50-75µl of beads suspension was added to each sample (antibody-antigen complexes) and after an incubation of 45 min, at 4°C under agitation, a short spin was made and the supernatant discarded. The pellet (beads-antibody-antigen complexes) was washed 3 times with 750µl of buffer C, and in the last wash, supernatants were completely removed. Finally, 38µl of loading buffer 1,5× were added to the samples which were then subjected to denaturing conditions (5 min at 95°C), to dissociate the complexes. All samples, including the pre-clear samples, were centrifuged for 5 min, at 14000 rpm, at 4°C and 20µl of the supernatant (antibody, antigen and all antigen-bound proteins) were loaded to the respective lane of a 5% polyacrylamide gel. Proteins were then separated in 16% polyacrylamide gel (western blot protocol detailed in 2.2.3.). Membranes were incubated with anti-Gal-3, anti-KRAS and anti-p16 antibodies in order to assess the presence of these proteins in the immunoprecipitated samples.

2.5. RNA Interference: silencing of KRAS and galectin-3

Experimental RNA interference (RNAi) takes advantage of the conserved cellular machinery that regulates gene expression in a sequence-dependent manner. *In vitro* this technique requires the use of short RNA molecules, short interfering RNA (siRNA), to inhibit the expression of a target gene. These double-stranded sequences are recognized by the cell enzymatic RNAi

machinery (namely the RISC complex) and used as a guide to destroy specific mRNA transcripts, based on sequence homology, resulting in targeted and transient post-transcriptional gene silencing (Fellmann & Lowe 2014).

In order to obtain KRAS and Gal-3 silencing, specific siRNA molecules (designed by Qiagen) with the target sequences: 5`-AAGGAGAATTTAATAAAGATA-3` (Hs_KRAS2_8) and 5`-CACGGTGAAGCCCAATGCAAA-3` (Hs_LGALS3_3), were used for KRAS and Gal-3, respectively. As negative control siRNA the AllStars negative control siRNA (Qiagen) with the target sequence 5`-AATTCTCCGAACGTGTCACGT-3`, was employed while Lipofectamine 2000 (Invitrogen) was used as transfection reagent.

SW480 cells were transfected using the reverse transfection method. The desired volume of OptiMEM (reduced serum medium; Gibco) and Lipofectamine 2000 were mixed and 5 min after the siRNA was gently added to the mixture for a total volume of 250µl. After 20 min at RT, the transfection mix and 750µl of cell suspension, 4x10⁵ cells/well in RPMI-1640 medium supplemented with 10% FBS, were added into the respective well in a 6 well plate. In order to mix the cells and the transfection mix, the plate was gently shaken back and forth. After 24 h (time 0) the medium was replaced by RPMI-1640 complete medium (10% FBS and 1% penicillin/streptomycin) and cells were allowed to grow in optimal conditions for additional 48 h. All procedures were performed under RNase free conditions.

In all experiments cells were harvested at the end of 48h and processed for western blot analysis (as described in 2.2.3) to confirm silencing.

2.6. Gelatin Zymography

Zymography is a widely used technique to study hydrolytic enzymes on the basis of substrate degradation. The standard method requires the copolymerization of the enzymatic substrate (in this case gelatin) with acrylamide. After non-reducing SDS-PAGE, the SDS is replaced by a non-ionic detergent allowing the enzymes to partially refold to their active conformation. The gel is then incubated in a buffer with essential cofactors, which permits the enzymes to degrade the copolymerized substrate. Staining procedures reveal proteolytic white zones on a Coomassie-blue stained gelatin-zymogram (Vandooren et al. 2013).

At the end of RNAi experiments (48 h after medium exchange), the supernatant of each condition was collected and the proteins from these conditioned media were quantified using the Bio-Rad *DC Protein Assay Kit* (as described in 2.2.2.). 20µg of protein were mixed with 3µL of non-reducing sample loading buffer (10% SDS, 4% sucrose and 0.03% in 0.25M Tris-HCl pH 6.8)

and PBS 1× to a final volume of 12µL. Samples were loaded into a 2.5% polyacrylamide gel and separated in a 10% polyacrylamide gel with 0.1% gelatin (Difco) as a substrate using running buffer 1× in a Mini- Protean III electrophoresis system (Bio-Rad) at 80V until the 25kDa band from the molecular marker reached the bottom of the gel (approximately 3 h).

After electrophoresis, gels were washed twice with 2% Triton X-100 for 15 min, to remove the SDS, washed once with deionized H₂O, and incubated with MMP substrate buffer (50mM Tris-HCL, pH 7.5; 10mM CaCl₂; 0.5% NaN₃) for 16 h at 37°C. Next, the gels were washed once with deionized H₂O and stained with Coomassie Blue solution (0.2% Coomassie blue; 7.5% acetic acid; 50% ethanol) for ½ h in the shaker. The staining solution was removed and the gels were washed with deionized H₂O until proteolytic bands were clear. Zymograms were scanned and bands intensities were quantified using imageJ software.

2.7. Trypan Blue exclusion assay

Trypan blue exclusion assay is based on the principle that live cells have intact cell membranes excluding trypan blue dye, whereas dead cells incorporate the dye acquiring a blue cytoplasm, thus making them easily distinguishable.

At the end of the RNAi experiments (48 h after medium exchange), cells were trypsinized and cell suspension was transferred to an identified 15ml tube corresponding to each condition (in duplicate) - control, cells transfected with scramble siRNA and cells transfected with Gal-3 siRNA and/or KRAS siRNA. 20µl of cell suspension were mixed with 0,4% trypan blue dye solution (Sigma-Aldrich) in a 1:1 ratio. The viable (unstained) and nonviable (stained) cells were counted separately in a Neubauer chamber. The percentage of viability was determined following the formula: % Viability = (Number of total viable cells ÷ Number of total cells) × 100.

2.8. Time-lapse microscopy

To analyze cell motility, bright field images of control cells and cells transfected with scramble siRNA, Gal-3 siRNA and/or KRAS siRNA, were taken every 5 min during the last 24 h of the RNAi experiment, using the 20x objective of an high-resolution inverted Leica DMI 6000B time-lapse microscope and the LAS AF (Leica) software. Results were analyzed using the ImageJ software.

2.9. Statistical analysis

All experiments, performed in triplicate, were treated as means \pm SEM. The results were statistically analyzed using the One-way ANOVA test followed by Bonferroni multiple comparison test with 95% confidence intervals (* $p \leq 0.05$; ** $p \leq 0.01$; *** $p \leq 0.001$). All statistical analyses were performed through to the GraphPad Prism 5.0 software.

III.

RESULTS

3.1. Basal expression levels of galectin-3, p16 and KRAS in colorectal cancer cells

Aiming to evaluate the expression levels of Gal-3, KRAS and p16 in CRC-derived cell lines - SW480 and HCT116 - harbouring different KRAS hotspot mutations, we performed western blot analysis using specific antibodies. While the anti-KRAS antibody was already routinely used in Ana Preto's group, the optimal dilution for anti-p16 and anti-Gal-3 antibodies, needed however to be determined. Therefore, we tested three different concentrations, within the range advised by the manufacture (1:1000, 1:500 and 1:100; data not shown). After a comparative analysis, for anti-Gal-3 antibody the selected dilution was 1:1000 while for anti-p16 was the intermediate dilution of 1:250.

Western blot results showed that both SW480 and HCT116 cells express indeed Gal-3, KRAS and p16 (Fig. 3.1). SW480 cells express higher levels of Gal-3 and KRAS in comparison with HCT116 cells. Conversely, the p16 protein is less expressed in SW480 and HCT116 cells in comparison to the other two proteins, being the higher p16 levels detected in HCT116 cells. Our results suggested that the expression levels of Gal-3 and KRAS inversely correlate with p16 levels.

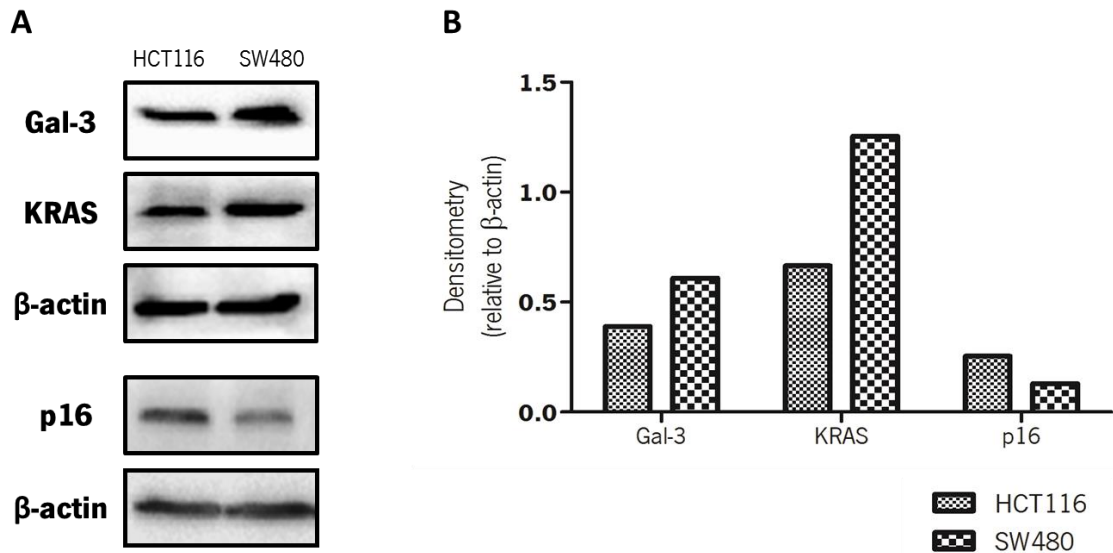


Fig. 3.1. Expression pattern of Gal-3, KRAS and p16 levels in CRC-derived cells HCT116 and SW480. (A) Representative western blot analysis of Gal-3, KRAS and p16 basal expression levels in both HCT116 and SW480 cell lines. (B) Densitometry analysis of Gal-3, KRAS and p16 expression levels normalized to the loading control β -actin.

In these experiments we faced some problems regarding the anti-p16 antibody, as it did not function in a regular way, evidencing an high background and the presence of unspecific bands which made the results interpretation unclear. A claim report was presented to the

manufacture however, by the time we received an answer, all the anti-p16 antibodies produced by the company had been discontinued. Some optimizations were made in the western blot protocol, mainly concerning the amount of protein used, membrane blocking and time of washes in PBST, and total protein extracts from Hela cells were used as a positive control (as indicated in the antibody datasheet). Despite the fact that the optimizations solved the background problems, the band we obtained, closer to 16 kDa, did not perfectly match the only band observed in the positive control. Therefore, we decided to confirm our results, sending the band for sequencing by an exterior service. However, by the time this manuscript was delivered the results were not available yet.

3.2. Galectin-3, KRAS and p16 localization patterns in normal colon and colorectal cancer cells

3.2.1. Galectin-3, KRAS and p16 immunostaining in colorectal cancer cells

After the confirmation that SW480 and HCT116 cell lines expressed KRAS, p16 and Gal-3 we performed immunofluorescence (IF) to analyze the subcellular localization patterns. Anti-KRAS, anti-Gal-3 and anti-p16 antibodies were all recommended for IF experiences however, only the anti-Gal-3 and the anti-p16 antibodies had a manufacture advice for cells fixation in methanol, while the anti-KRAS antibody had no specifications on the fixation method. For that reason, cells were fixed using two different methods to test the KRAS antibody recognition: fixation in methanol and fixation in 4% paraformaldehyde (PFA).

As far as KRAS staining is concerned, we started by testing the IF protocol in SW480 cells as these are the cells that express higher levels of this protein. Representative images of the staining are seen in Fig. 3.2. For both types of fixation, when the negative control is compared with the staining condition no differences are observed, indicating that the anti-KRAS immunostaining did not work. The dilution used in these experiments (1:50) was already the lowest dilution recommended by the manufacture. Additionally, after research in literature, we found a study in which several anti-KRAS antibodies, including our specific antibody, were tested, and the authors reached the conclusion that the appropriate antibodies for western blot analysis were not adequate for immunofluorescence protocols, and even the ones that were, displayed false positive results (Fuentes-Calvo et al. 2010). Thus, we concluded that the anti-KRAS antibody

was not adequate for immunofluorescence being wrongly recommended for this type of studies by the manufacture.

For Gal-3 and p16 single staining, cells were plated at low density and fixed after 48 h using ice-cold methanol. We could observe a positive Gal-3 staining, both in SW480 and HCT116 cells, when compared to the negative controls (Fig.3.3 and Fig. 3.4).

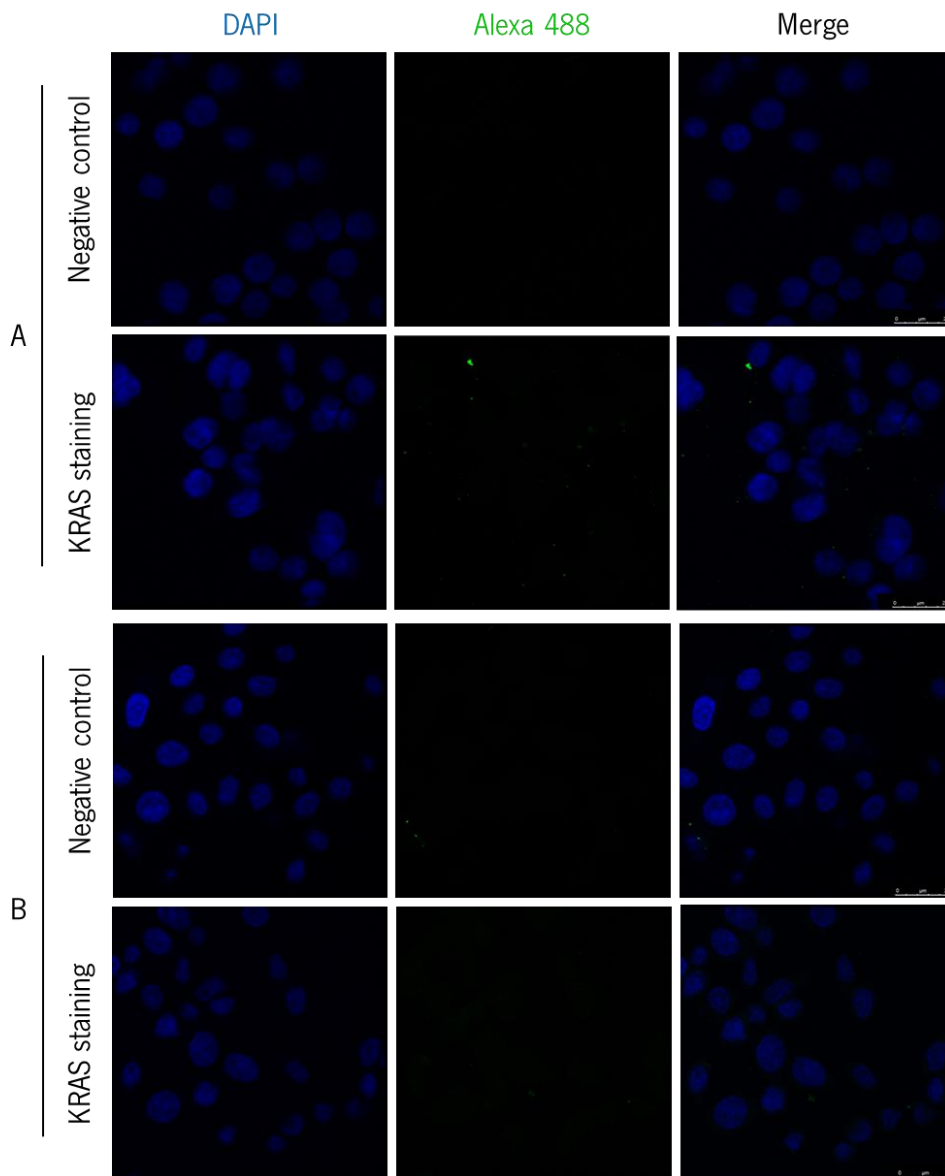


Fig. 3.2. Confocal fluorescence microscopy analysis of KRAS localization shows no positive staining. SW480 cells were cultured on coverslips with no treatment and fixed with A) methanol or B) 4% paraformaldehyde. KRAS was stained with an Alexa fluor-488 secondary antibody (green) and cell nuclei were counterstained with DAPI (blue). KRAS staining conditions (lower panels) showed no differences when compared to the negative controls (incubated only with secondary antibody). Right bottom scale bars correspond to 25 μ m.

Gal-3 localization in low confluent SW480 cells (Fig. 3.3) is cytoplasmic and perinuclear, with nuclear exclusion, being the cytoplasmic staining more evident at the cell-cell junctions. To evaluate the staining in more confluent cells, cells were plated in a higher density and allowed to

grow and differentiate for a longer time (4 days) (lower panel of Fig. 3.3). Interestingly, the Gal-3 localization pattern is different than the observed in low confluent cells: the staining is heterogeneous, with a punctuated pattern dispersed through the cytoplasm and nucleus, with nucleolus exclusion.

Instead in HCT116 cells (Fig. 3.4), Gal-3 staining is similar in low and high confluent cells, presenting a disperse pattern through the whole cytoplasm and nucleus, being however more heterogeneous in high confluent cells.

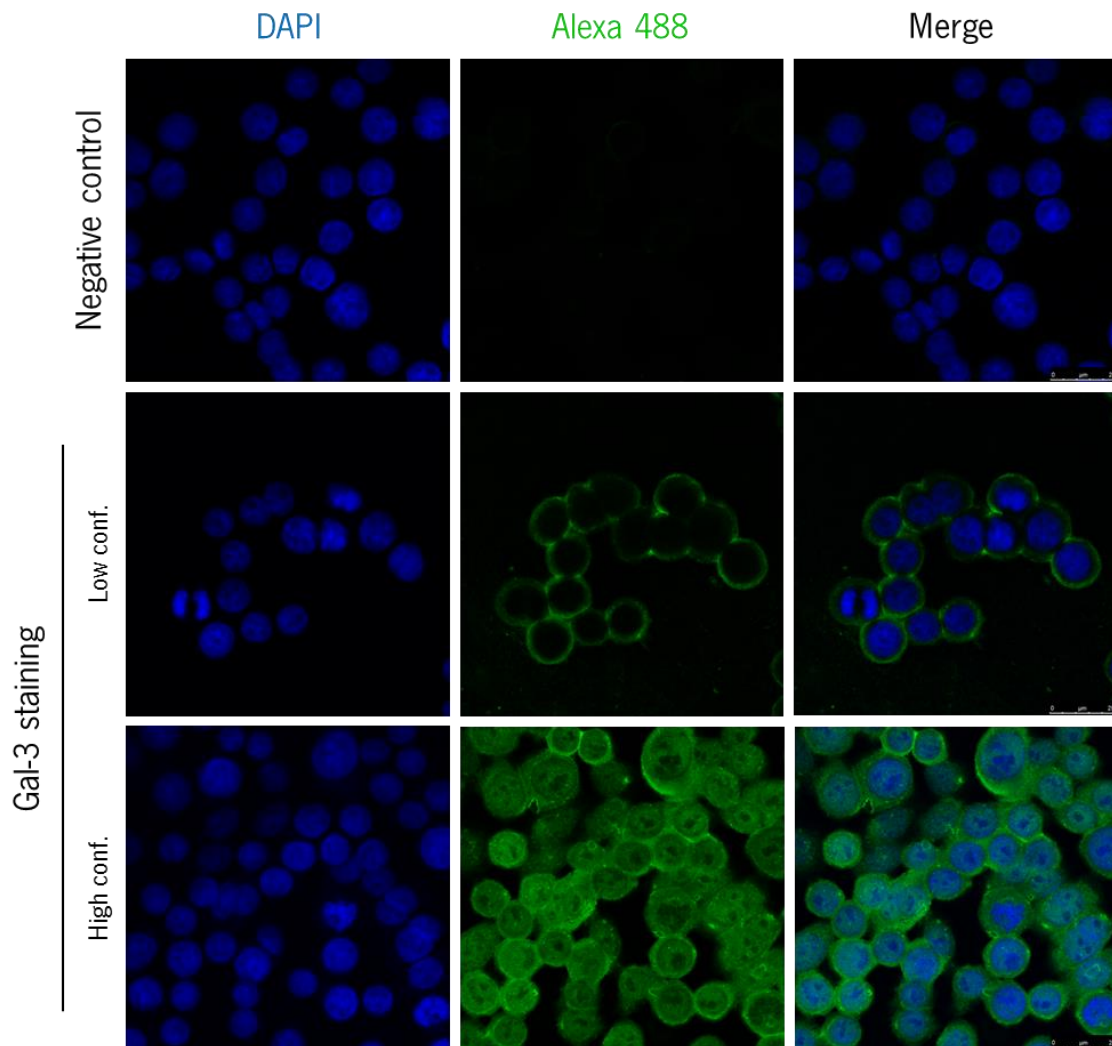


Fig. 3.3. Confocal fluorescence microscopy analysis of Gal-3 staining in SW480 cells evidences differences between Gal-3 localization in low and high confluent cells. In low confluent cells, Gal-3 (stained in green) exhibits perinuclear localization with nuclear exclusion pattern, whereas in more confluent cells it is also found in the nucleus (counterstained in blue with DAPI). Negative control (of low confluent cells; negative control of high confluent cells can be seen in Fig. S1) corresponds to a condition incubated only with secondary antibody. Bottom right scale bars correspond to 25 μ m.

Concerning p16 localization in SW480 cells (Fig. 3.5), it is also different in cells with different confluence levels: in low confluent cells, p16 localization is cytoplasmic, essentially concentrated at the perinuclear region, and with a faint nuclear punctuated staining in some cells; instead, in more confluent cells, p16 seems to suffer a delocalization and the staining follows the entire cellular body, with more intense dots in the nucleus.

In HCT116 cells (Fig. 3.6), p16 is localized in the cytoplasm and nucleus, with a dispersed and heterogeneous punctuated pattern, both in low and high confluent cells. Taking into account that p16 detection by western blot was being a little ineffective, immunofluorescence proved to be a successful method to demonstrate p16 expression. Additionally, these results seem to corroborate the ones obtained in western blot, since Gal-3 expression appears to be more intense in SW480 cells, whereas p16 is much fainter in both cell lines.

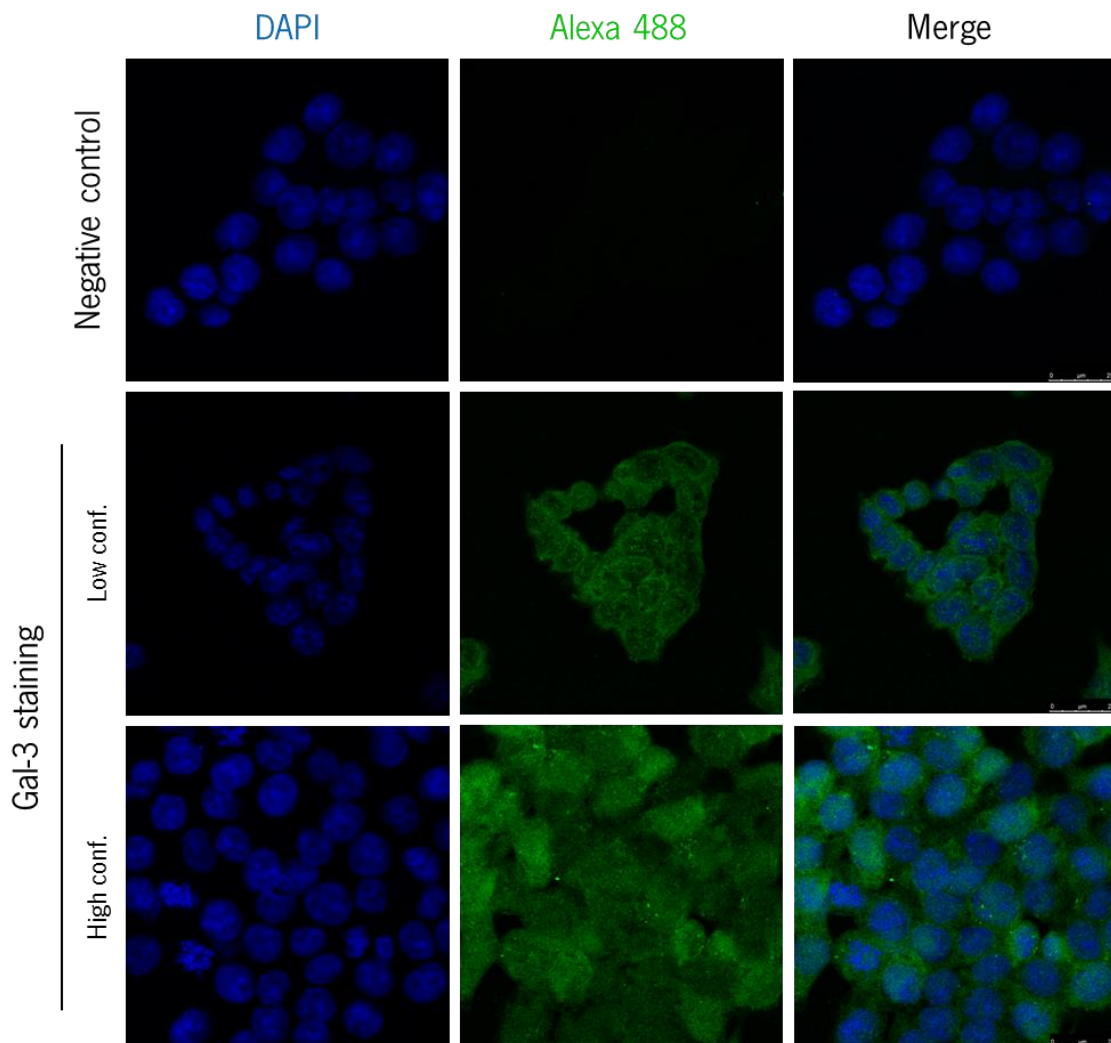


Fig. 3.4. Confocal fluorescence microscopy analysis of Gal-3 staining in HCT116 cells evidences a similar Gal-3 localization pattern in low and high confluent cells. In HCT116 cells, Gal-3 (stained in green) is localized both in the cytoplasm and nucleus (counterstained in blue with DAPI), exhibiting a more diffuse and heterogeneous pattern in high confluent than in low confluent cells. Negative control (of low confluent cells; negative control of high confluent cells can be seen in Fig. S1) corresponds to a condition incubated only with secondary antibody Bottom right scale bars correspond to 25 μ m.

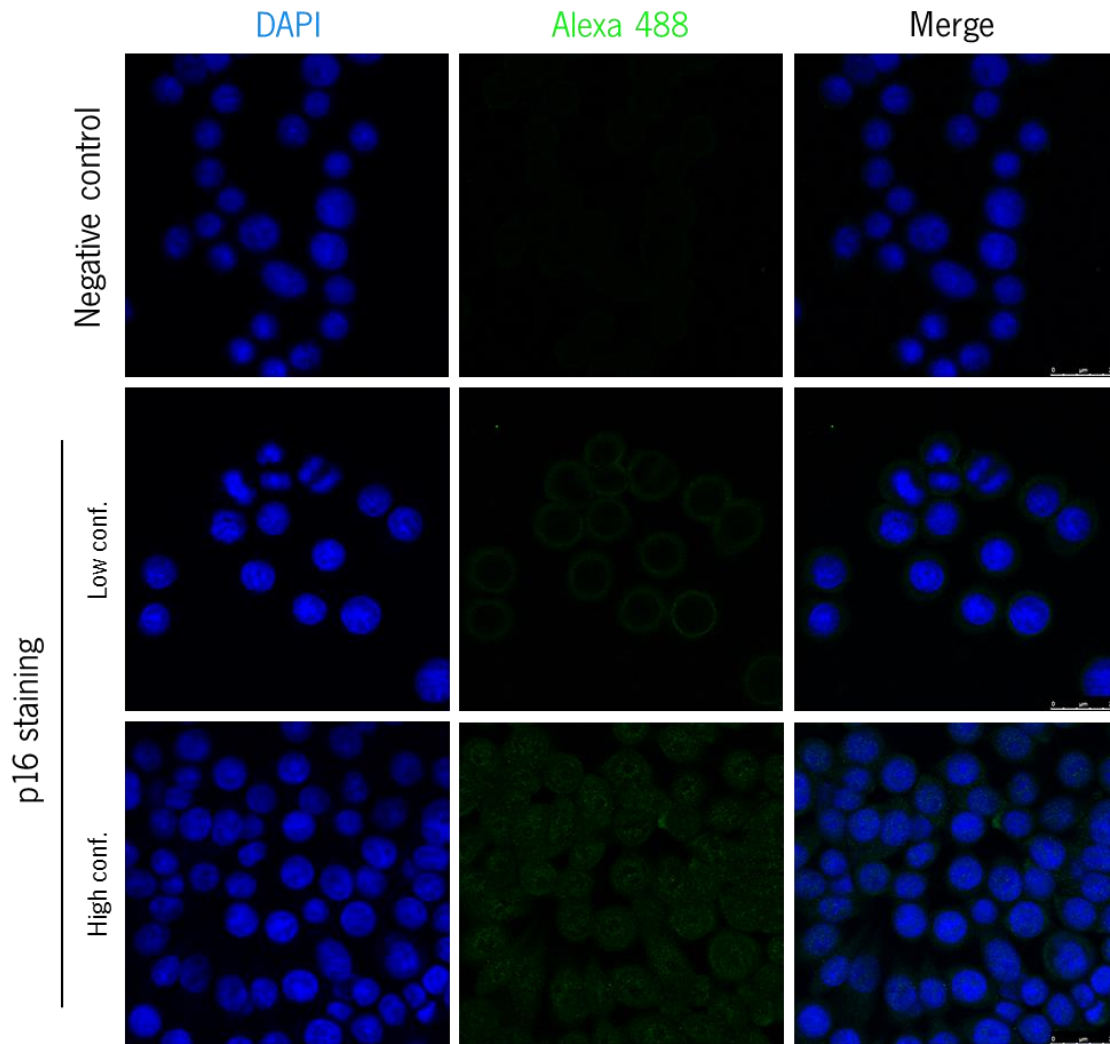


Fig. 3.5. Confocal fluorescence microscopy analysis of p16 staining in SW480 cells evidences differences between p16 localization in low and high confluent cells. In low confluent cells p16 (stained in green) exhibits perinuclear localization whereas in more confluent cells it is also found in the nucleus (counterstained in blue with DAPI) and follows the entire cellular body. Negative control (of low confluent cells; negative control of high confluent cells can be seen in Fig. S1) corresponds to a condition incubated only with secondary antibody. Bottom right scale bars correspond to 25 μ m.

Since the localization patterns of these proteins demonstrated to have some differences in low and high confluent cells, we questioned whether the results obtained could be justified by a delocalization of the proteins induced by monolayer maturation and differentiation or simply by an increased expression. To clarify this question, cells were seeded in the same conditions and total protein extractions were performed. Since high confluent cells were plated at higher density and spent more time growing in culture we also evaluated if the nutritional availability had some interference in our results: in low confluent cells the medium was changed for HBSS (low nutrient content medium), while in high confluent cells the medium was refreshed 6 h before protein extraction. Western blot analysis was performed, but unfortunately results on p16 expression could not be obtained due to problems with the antibody. Concerning Gal-3 (supplementary data

Fig S2), similar levels were observed independently of the condition, leading us to conclude that the protein levels were not altered despite the delocalization observed and that the nutritional availability were not interfering with our results, at least at the protein level.

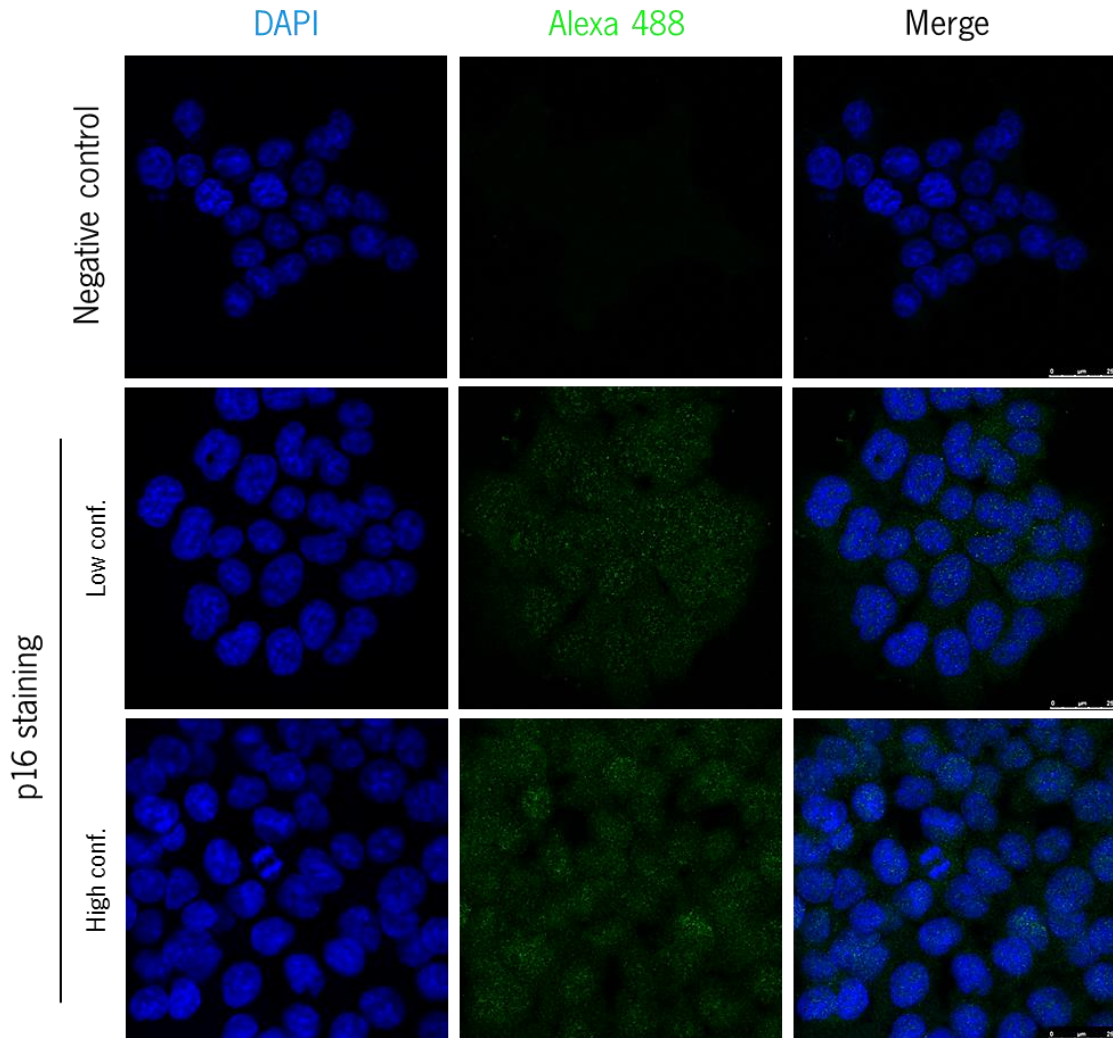


Fig. 3.6. Confocal fluorescence microscopy analysis of p16 staining in HCT116 cells evidences a similar p16 localization pattern in low and high confluent cells. In HCT116 cells, p16 (stained in green) is localized both at the cytoplasm and nucleus (counterstained in blue with DAPI). Negative control (of low confluent cells; negative control of high confluent cells can be seen in Fig. S1) corresponds to a condition incubated only with secondary antibody. Bottom right scale bars correspond to 25 μ m.

3.2.2. Galectin-3 and p16 double immunostaining in colorectal cancer cells

Gal-3 and p16 displayed a similar cellular distribution patterns, thus to test if they in fact co-localize we performed a double immunostaining. Such staining was, once more, performed in low and high confluent SW480 and HCT116 cells. Additional controls regarding the secondary antibodies were considered: coverslips incubated only with the two secondary antibodies (plus streptavidin Alexa-594 conjugated), Gal-3 complete staining plus the anti-rabbit biotinylated

secondary antibody+streptavidin Alexa-594 conjugated and p16 complete staining plus the Alexa fluor-488 donkey anti-goat secondary antibody. Image acquisition settings were optimized for each fluorochrome and according to the cell line.

Analyzing the panel with the controls for SW480 and HCT116 cells (Fig. 3.7), it is possible to observe that the anti-rabbit biotinylated antibody+streptavidin Alexa-594 conjugated (lines 1 and 2) is giving some unspecific signal. This unspecific signal is confined to the perinuclear region, and is fainter than the positive staining condition (line 3), in which the staining also includes the nucleus. The control concerning the secondary antibody against anti-Gal-3 antibody (line 1 and 3), displayed a faint background noise. Overall the observation of the images corresponding to the double immunostaining in SW480 cells (Fig. 3.8) revealed that the patterns of Gal-3 and p16 localization are identical in low and high confluent cells, which was not the case in the simple staining. However, we had already discarded the hypothesis of secondary antibody cross-reaction and this observation can only intensify the instability and heterogeneity of Gal-3 localization. A careful analysis of double staining images (Fig. 3.8 and Fig. 3.9) reveals that Gal-3 and p16 localization patterns are very similar to the ones observed in single staining experiments (just in high confluent cells for the SW480 cell line). The localization of these two proteins appears to be similar and in the inset photos we can observe the presence of orange staining as well as some discreet yellow dots, more evident in HCT116 cell line (Fig. 3.9). The yellow/orange staining results from the overlap/close proximity of green and red signals, being indicative of a close association and co-localization between Gal-3 and p16. This staining seems to be more evident at the cells nuclei, meaning that the unspecific staining given by the secondary antibody/streptavidin almost has no interference in the co-localization observed. Despite the need of further optimization of the anti-rabbit antibody/streptavidin concentration to obtain more reliable evidences, these results constitute our first indication that Gal-3 and p16 could directly interact in these CRC cell models.

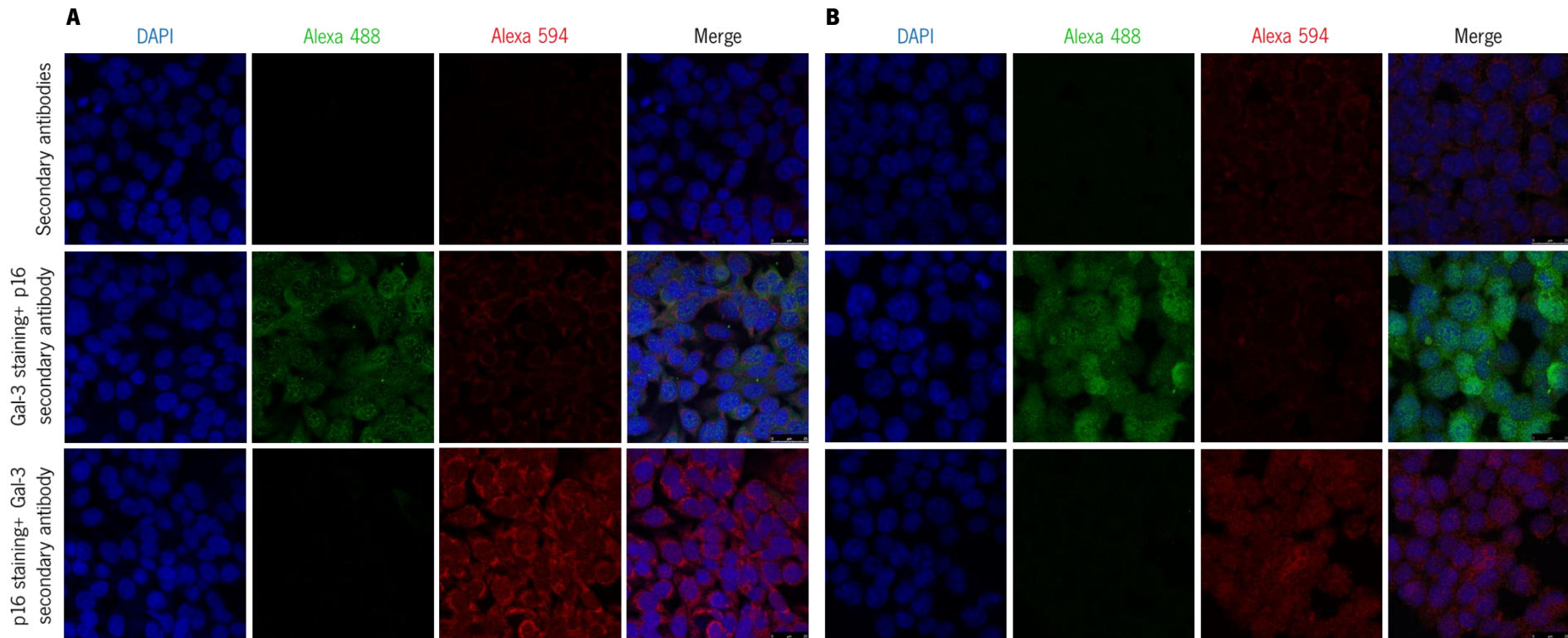


Fig. 3.7. Confocal fluorescence microscopy analysis of Gal3+p16 double immunostaining secondary antibodies control conditions in SW480 (A) and HCT116 cells (B). In both cell lines the anti-rabbit secondary antibody+streptavidin Alexa-fluor 594 (red) is conferring some perinuclear staining in the absence of primary antibody; anti-goat Alexa-488 secondary antibody demonstrated no unspecificity. Gal-3 is stained in green, p16 is stained in red and cells nuclei are counterstained in blue with DAPI. Bottom right scale bars correspond to 25 μ m.

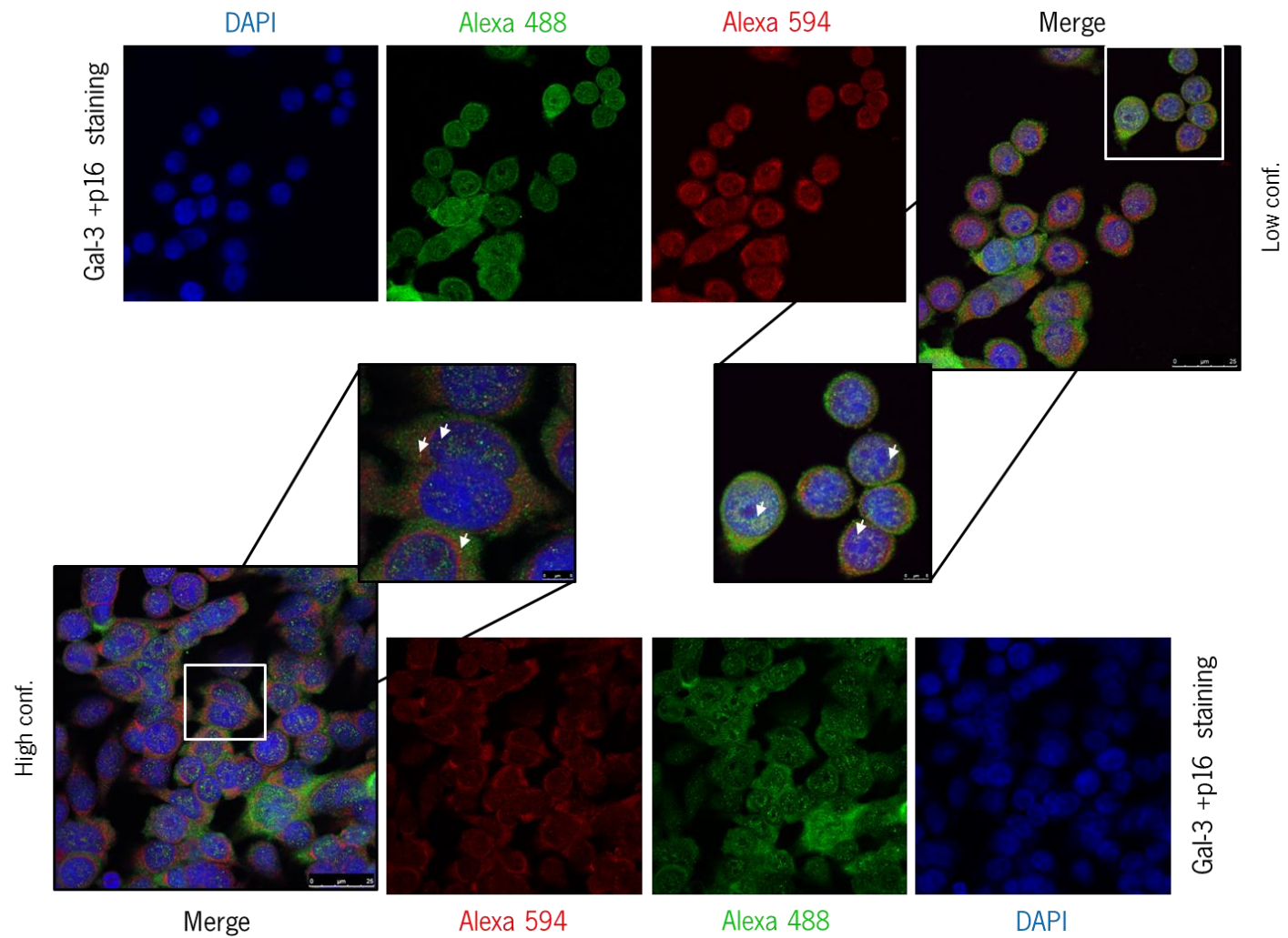


Fig. 3.8. Confocal fluorescence microscopy analysis of Gal-3+p16 double immunostaining in low and high confluent SW480 cells reveals the presence of some discreet yellow dots indicative of close proximity and co-localization of these proteins. Gal-3 is stained in green, p16 is stained in red and cell nuclei are counterstained in blue with DAPI. White arrows evidence some yellow stained areas. Right bottom scale bars correspond to 25 μm in the merged images and to 5 μm in the centre zoomed images.

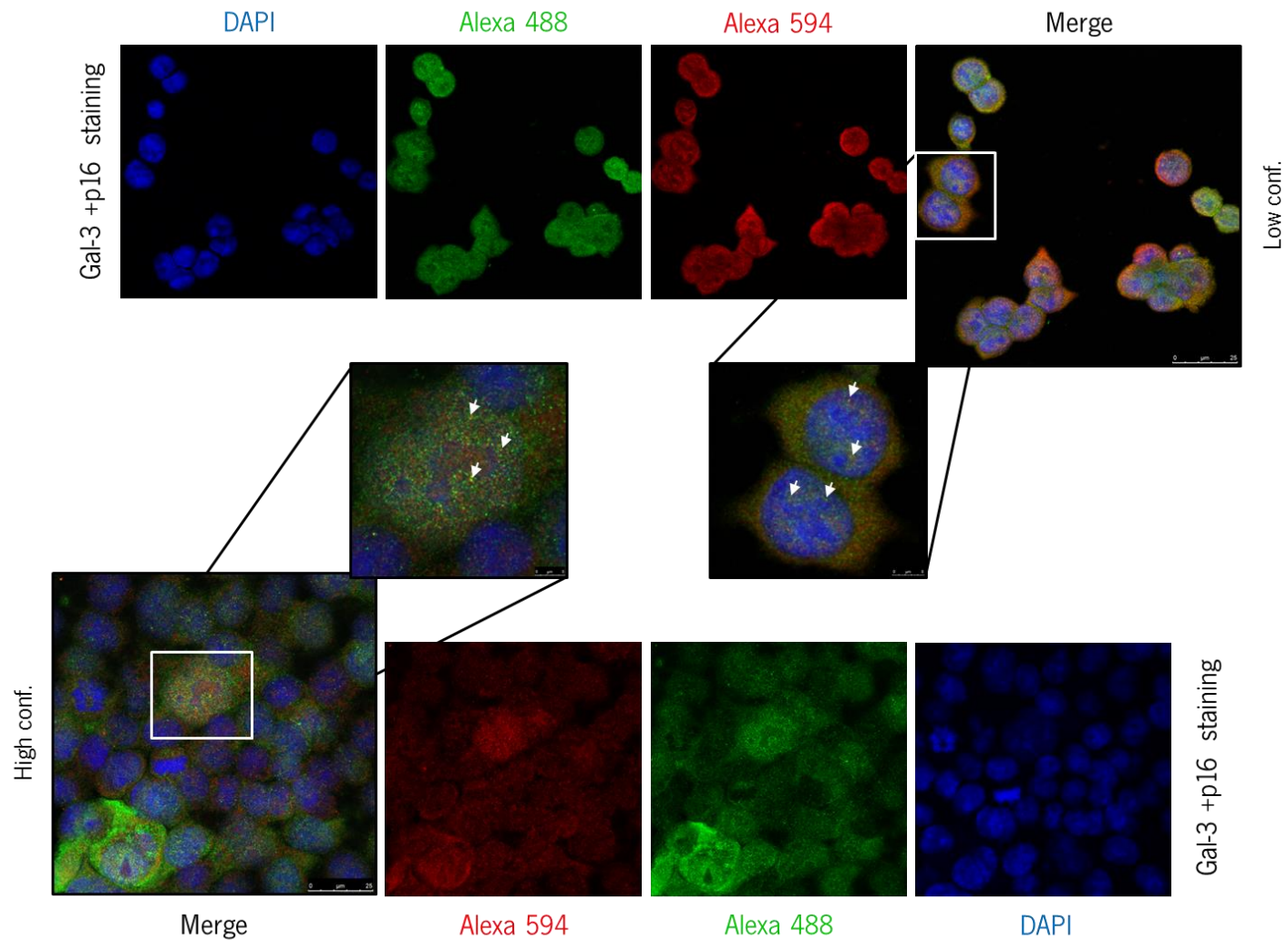


Fig. 3.9. Confocal fluorescence microscopy analysis of Gal-3+p16 double immunostaining in low and high confluent HCT116 cells reveals the presence of some discreet yellow dots mainly localized at the cells nuclei and suggestive of co-localization. Gal-3 is stained in green, p16 is stained in red and cell nuclei are counterstained in blue with DAPI. White arrows evidence some yellow stained areas. Right bottom scale bars correspond to 25 μ m in the merged images and to 5 μ m in the centre zoomed images.

3.2.3. Galectin-3, KRAS and p16 immunostaining in NCM460-transfected cells

To solve the problem with KRAS localization we used a valuable research model previously established in our lab - NCM460 Flag-KRAS transfected cells (Flag-KRAS^{wt}, Flag-KRAS^{G12V}, Flag-KRAS^{G12D}, Flag-KRAS^{G13D}) - in which KRAS localization can be assessed using an anti-Flag antibody. These cell lines constitute a “clean” model allowing us to study possible interactions established between Gal3, KRAS and p16 in the context of KRAS hotspot mutations in a normal genetic background. Before performing the immunofluorescence staining, we confirmed the expression of these proteins by western blot. Results revealed that all cell lines, including the NCM460 parental, expressed Gal-3, p16, as well as endogenous KRAS; and the transfected cell lines stably expressed Flag-KRAS (Fig. 3.10).

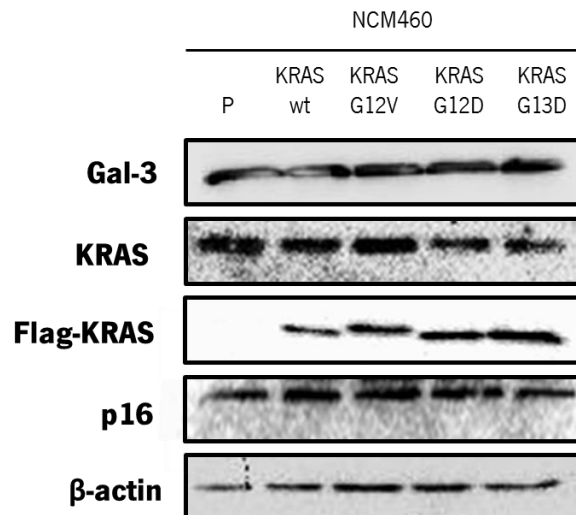


Fig. 3.10. Representative western blot analysis of Gal-3, endogenous KRAS, Flag-KRAS and p16 basal expression levels in NCM460 parental (P) cell line and NCM460 transfected with Flag-KRAS^{wt}, Flag-KRAS^{G12V}, Flag-KRAS^{G12D} and Flag-KRAS^{G13D}.

The primary anti-Flag antibody only worked in cells fixed with 4% PFA and fortunately anti-Gal-3 and anti-p16 antibodies, besides being effective in cells fixed in methanol, also work in cells fixed in 4% PFA. Therefore, NCM460 cells transfected with Flag-KRAS^{wt}, Flag-KRAS^{G12V}, Flag-KRAS^{G12D} and Flag-KRAS^{G13D} cells were fixed in 4% PFA and the double staining of Flag-KRAS+Gal-3/or p16 and Gal-3+p16 was carried out as described in materials and methods (2.3.2). Negative controls to exclude secondary antibodies cross-reaction were performed in NCM460 Flag-KRAS^{wt} for each double staining (Fig. 3.11, 3.12 and 3.13 A).

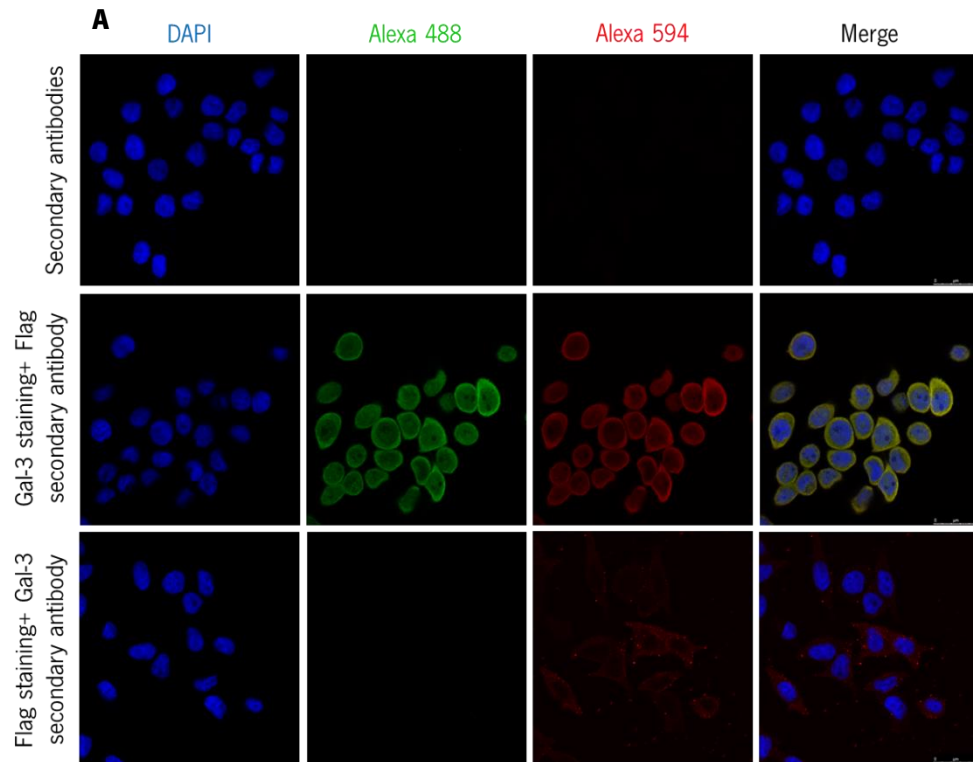
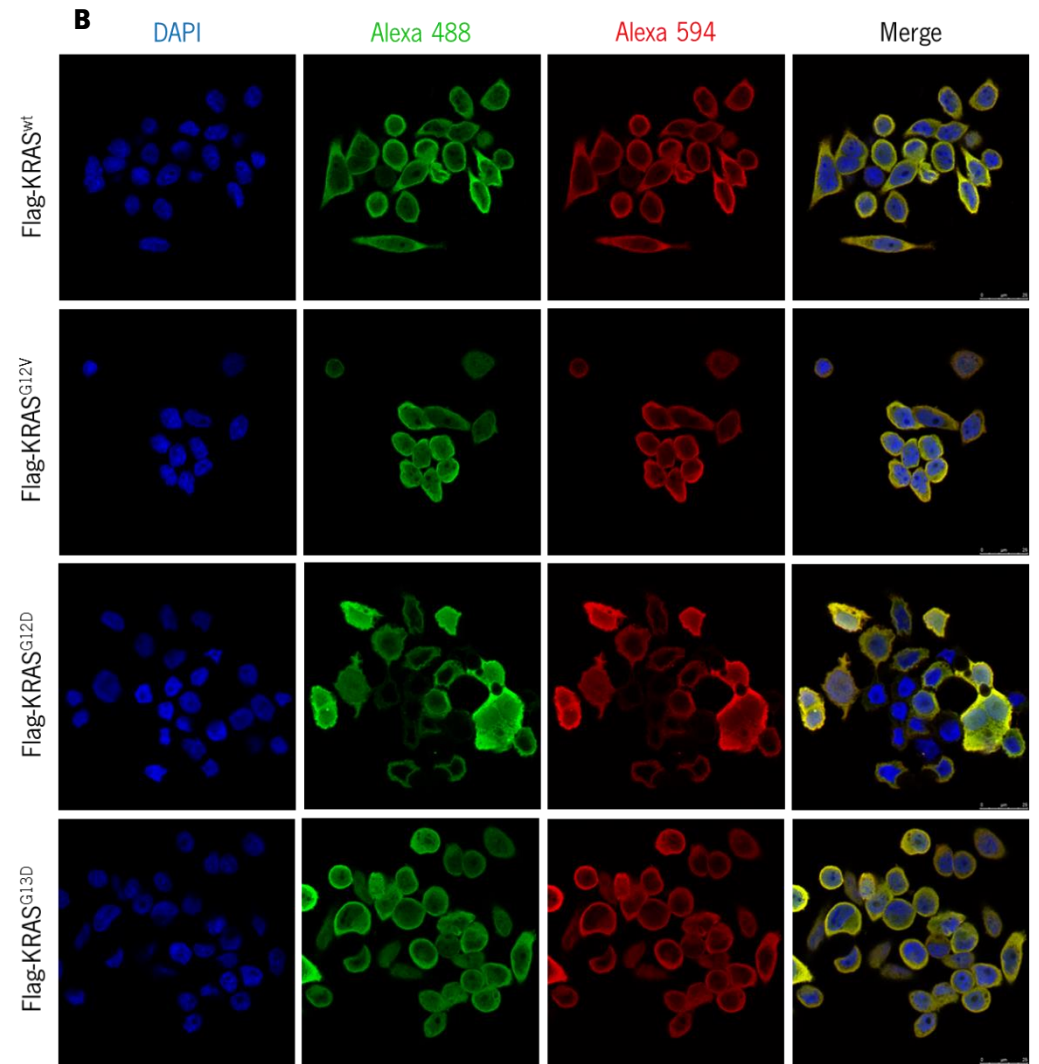
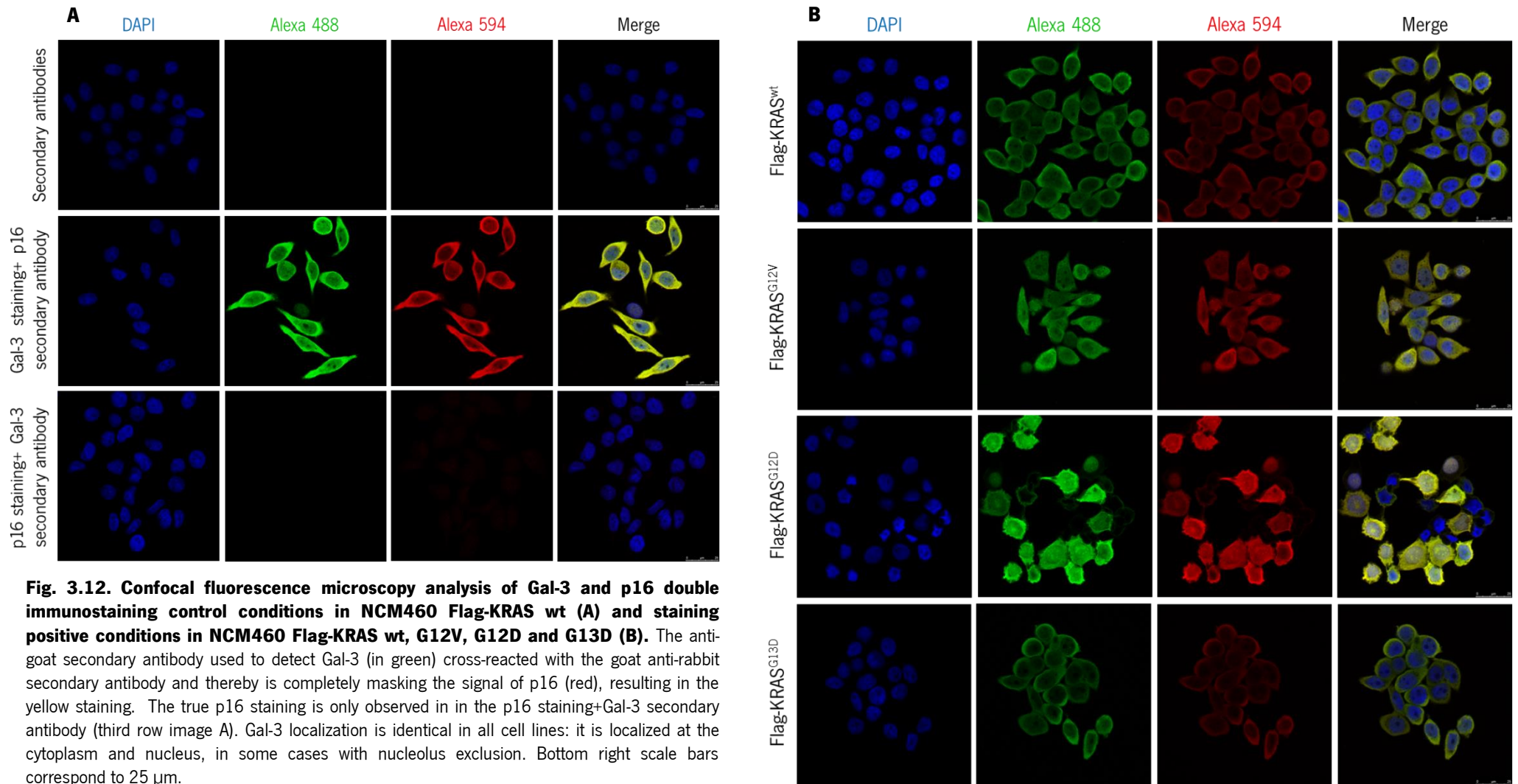
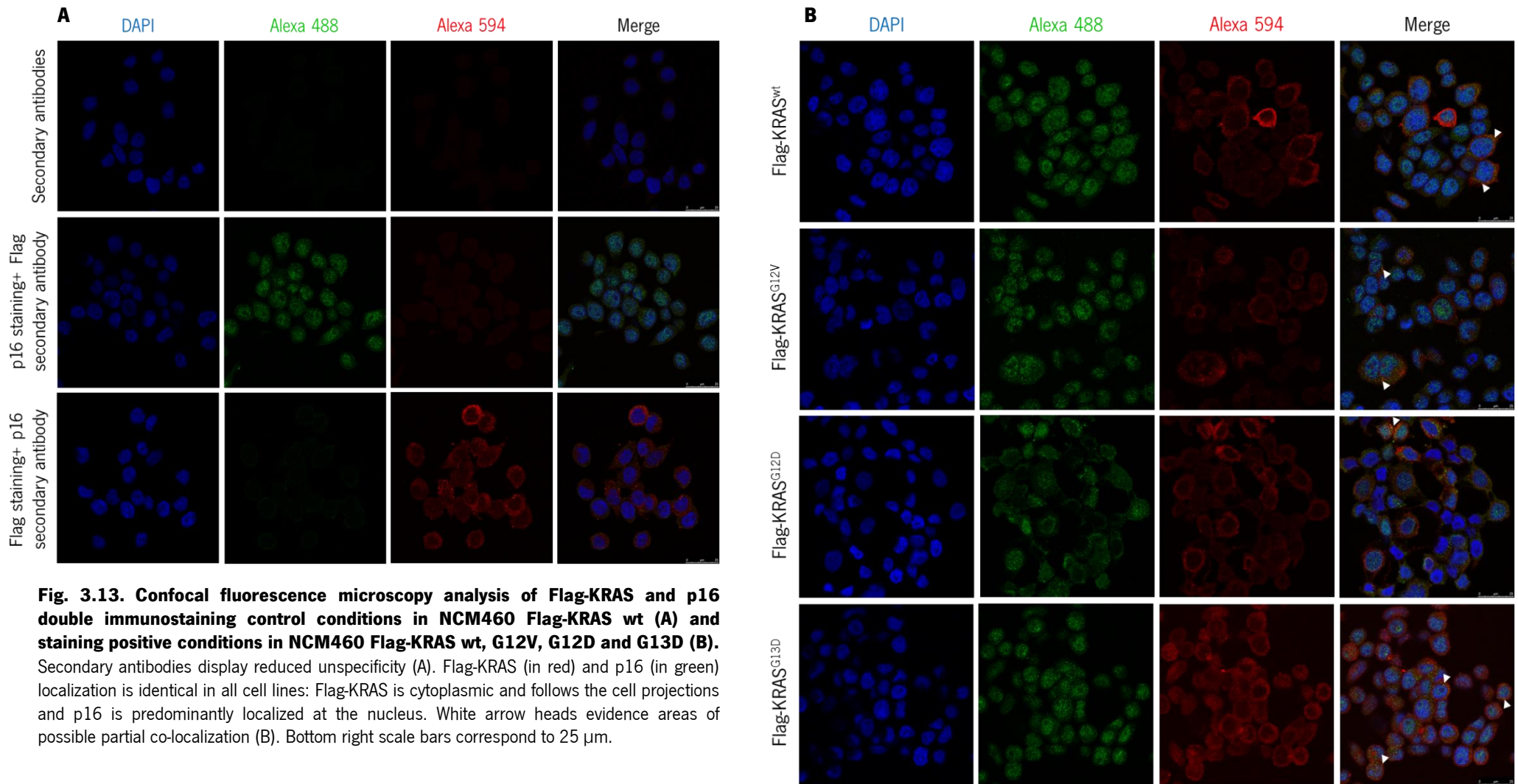


Fig. 3.11. Confocal fluorescence microscopy analysis of Flag-KRAS and Gal-3 double immunostaining control conditions in NCM460 Flag-KRAS wt (A) and staining positive conditions in NCM460 Flag-KRAS wt, G12V, G12D and G13D (B).

The anti-goat secondary antibody used to detect Gal-3 (in green) cross-reacted with the goat anti-mouse secondary antibody and thereby is completely masking the signal of Flag-KRAS (red), resulting in the yellow staining. The true Flag-KRAS staining is only observed in the Flag staining+Gal-3 secondary antibody (third row image A). Gal-3 localization is identical in all cell lines: it is localized at the cytoplasm and nucleus, in some cases with nucleolus exclusion. Bottom right scale bars correspond to 25 μm .







Examining the images of Gal-3 complete staining+Flag-KRAS or p16 secondary antibodies (second rows of Fig. 3.11 and 3.12 A) it is clear that our donkey anti-goat antibody cross-reacted with the goat anti-mouse and the goat anti-rabbit secondary antibodies and, thereby the signal in green and red channels both correspond to Gal-3 staining. Thus, the sequential immunofluorescence, proved to be inefficient to avoid antibodies cross-reactions. Thereby we can only explore Gal-3 staining pattern, which seems to be identical in the four cell lines: it follows the entire cellular body, being more intense at the perinuclear region and in some cases, it appears to exclude the nucleoli. Among the NCM460 cell lines, the one that harbours the mutation G12D is the one that exhibits a more heterogeneous staining, showing that in some cells the staining is very strong while in others it is very weak. From these set of experiments the only double immunostaining we can indeed analyze is the Flag-KRAS/p16 (Fig. 3.13). It is important to refer that for the acquisition of these images we had to increase the gain values, since in the previous experiments we were working with reduced values for Flag-KRAS and p16 to avoid the overexposition of the unspecific yellow staining. In Fig. 3.13 A, in the negative controls we can observe that they display some unspecific signal that is undoubtedly different from the positive condition and therefore does not interfere with the staining results. The observed patterns are identical independently of the cell line (Fig. 3.13 B), showing that p16 is localized mainly at the nucleus (more dispersed in NCM460 Flag-KRAS^{G12D}). Flag-KRAS, exhibits a heterogeneous staining probably related to transfection efficiency issues, being localized at the cytoplasm (perinuclear region) and along the cellular projections. These proteins are mainly localized in different cellular compartments, making them unlikely to co-localize in these models. Nevertheless, a low level/partial co-localization is not totally excluded since orange/yellow dots and stained areas are visible in some cells.

Gal-3 localization pattern in these KRAS transfected models is very similar to what had been demonstrated in SW480 and HCT116 cell lines, however its punctuated distribution is not visible. p16 localization seems to be different than the previously observed: in CRC cells it is expressed in the whole cell and in NCM460 cells it is predominantly localized at the nucleus, evidencing a difference between normal colon and CRC cells. It was also observed that among the NCM460-transfected cells, the NCM460 harbouring Flag-KRAS with the G12D mutation is phenotypically distinguishable from the others by its different cellular architecture. This observation suggests a KRAS implication in the cytoskeleton cells shape regulation, for example by interfering with some cellular cytoskeleton components, like actin or tubulin.

Table 3.1 summarizes the most important results obtained on p16, Gal-3 and Flag-KRAS localization patterns in CRC and normal colon KRAS-transfected cells.

Table. 3.1. Localization patterns of Gal-3 and p16 in SW480 and HCT116 cells and Gal-3, p16 and (Flag-)KRAS in NCM460 cells transfected with KRAS^{wt} and the three KRAS hotspot mutations.

Cell line	Gal-3 localization	p16 localization	(Flag-)KRAS localization	Co-localization
SW480	Cytoplasmic and nuclear with nucleolus exclusion	Cytoplasmic and nuclear	—	Gal-3 and p16 co-localize in the nucleus
HCT116	Dispersed through the whole cytoplasm and nucleus	Dispersed through the whole cytoplasm and nucleus	—	
NCM460 Flag-KRAS transfected	Cytoplasmic/nuclear	Mainly nuclear	Cytoplasmic and along cells projections	- (Flag-)KRAS and p16 partial co-localization is not totally discarded. - No conclusion can be taken concerning Gal-3 and p16 co-localization

3.3. Study of galectin-3, KRAS and p16 interaction by co-immunoprecipitation in SW480 cells

Considering that Gal-3 and p16 had been demonstrated to be in closer proximity in immunofluorescence experiments, we decided to perform co-immunoprecipitation (Co-IP) to assess if these proteins physically interact. With this approach we could evaluate KRAS interaction with Gal-3 and p16, what constitutes an advantage relatively to immunofluorescence. These experiments were only performed in SW480 cell line.

Gal-3, p16 and KRAS were immunoprecipitated from SW480 total cell lysates and the presence of the three proteins in each of the immunoprecipitates was assessed by western blot analysis. Representative results of these experiments are presented in Fig. 3.14.

The pre-clear (sample incubated with protein G sepharose beads, without antibody) is important to discard unspecific binding of proteins directly to the beads. In the case of Gal-3 and KRAS western blot, one band appears in the pre-clear sample and in the p16 western blot at least 4 bands are observed, being relevant to highlight that in this specific case the membrane was

overexposed, due to the fact that our specific band of interest only developed after a minimum of 30min to 1h of exposure. These unspecific bands and the observed background can be explained by unspecific signal due to the secondary antibody or to free immunoglobulin-like proteins present in the sample.

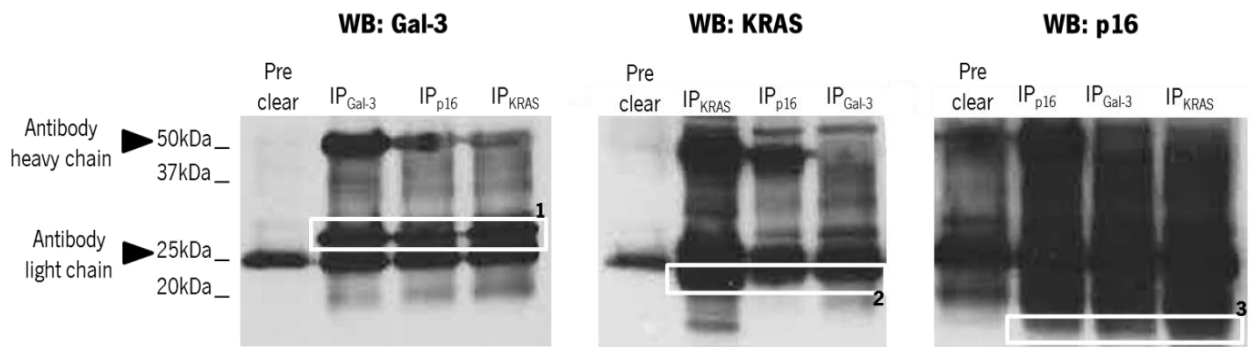


Fig. 3.14. Gal-3, KRAS and p16 co-immunoprecipitate. Gal-3, KRAS and p16 were immunoprecipitated from SW480 total cell lysates using protein G sepharose beads and the samples were analysed by western blot using specific antibodies against the three proteins. White boxes are surrounding the bands corresponding to the proteins Gal-3 (1), KRAS (2) and p16 (3). These results were reproduced twice.

In this type of traditional Co-IP the antibody is eluted with the immunoprecipitated sample at the end of the procedure. Since we had to use the same antibody in IP and in western blot detection, IgG corresponding to the light (25kDa) and heavy (50kDa) denatured chains of the antibody were detected by the secondary antibody. These bands difficult the results interpretation, especially in the cases of KRAS and Gal-3, which have a closer molecular weight to the 25kDa immunoglobulin light chain band, presenting 21kDa and 31kDa, respectively. However, based on protein molecular weight and in the bands obtained at IP_{Gal-3}/WB_{Gal-3} , IP_{KRAS}/WB_{KRAS} , IP_{p16}/WB_{p16} we believe that bands corresponding to Gal-3 (1), KRAS (2) and p16 (3) are visible in each of the immunoprecipitated samples. These bands are stronger in each combination of IP/WB, e.g. band corresponding to KRAS are stronger in the sample of IP_{KRAS} when western blotted for KRAS, and none of them are visible in the preclear, i.e. no unspecific binding of these proteins to the beads was detected. Summing up, our results showed that Gal-3, KRAS and p16 are co-immunoprecipitating with each other, corroborating the IF findings and suggesting that these proteins could form a complex.

3.4. Optimization of galectin-3 silencing conditions by RNA interference

In these experiments we used the SW480 cell line, in which the number of cells, the transfection reagent concentration and the transfection method had already been optimized in our lab. We set forward to evaluate the optimal siRNA concentration to obtain an efficient Gal-3 silencing. Three different concentrations: 50, 100 and 150nM, prepared from a 20 μ M stock of specific Gal-3 siRNA, were tested for their silencing efficiency. We achieved an efficiency of Gal-3 silencing superior to 80% with all the tested concentrations and in a concentration dependent manner (Fig. 3.15). The exact silencing percentages were 81.2% for the lowest concentration (50nM), 90.2% for the intermediated 100nM concentration and 94.6% for the highest concentration (150nM). The differences observed on silencing efficiency where not significant when compared to the increasing concentrations of siRNA. Taking into account that high amounts of siRNA can be toxic to the cells and also because it is an expensive reagent, we decided to choose a work concentration of 50nM siRNA to be used in the subsequent RNAi experiments.

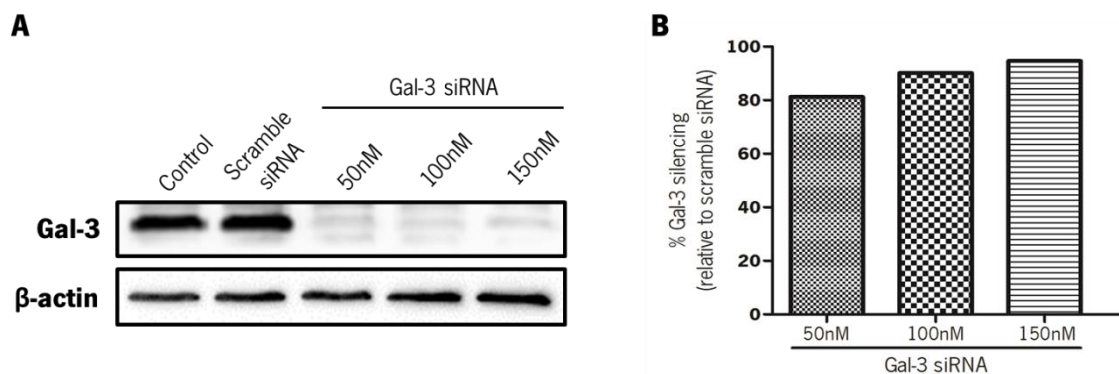


Fig. 3.15. A concentration of 50nM of Gal-3 siRNA is enough to obtain a silencing percentage of 81.2%. A) Three different concentrations- 50, 100 and 150nM of Gal-3 siRNA were tested in order to determine the working concentration. Gal-3 silencing was confirmed by western blot analysis. **B)** Band intensity was quantified relatively to β -actin and the % of Gal-3 silencing was calculated relatively to the scramble siRNA condition.

3.5. Phenotypic alterations induced by galectin-3 and/or KRAS silencing in SW480 cells

Since KRAS/Gal-3 interaction has been repeatedly associated with the tumourigenic process (Elad-Sfadia et al. 2004; Shalom-Feuerstein et al. 2005; Levy et al. 2010; Song et al. 2012; Wu et al. 2013), we wanted to assess the effects of Gal-3 and/or KRAS silencing on specific cellular activities. For that reason, we evaluated some phenotypic characteristics upon Gal-3 and/or KRAS silencing, namely cell morphology, cell viability, variations on Gal-3, KRAS

and p16 expression levels, MMPs production and cell migration. Silencing was confirmed at the protein level, by western blot, in all the experiments performed.

3.5.1. Effect of galectin-3 and/or KRAS silencing on cell morphology

With the purpose of evaluating the effects on cell morphology upon Gal-3 and/or KRAS silencing, phase contrast images of each condition were taken at time 0h (after medium exchange) and at time 48h (the time when the maximum silencing efficiency is achieved). Representative images of these experiments can be seen in Fig. 3.16.

At time 0h, the majority of the cells from all the conditions are undifferentiated, i.e. round shaped, with few cells (mostly in the control condition) starting to gain their characteristic spindle/stellar-like morphology. After 48h of transfection, when compared to the control condition (non-transfected cells), scramble siRNA transfected cells do not display any significant differences in morphology. In contrast, when we look to Gal-3 and/or KRAS transfected cells some evident differences stand out. In the condition of cells transfected with Gal-3 siRNA, cells are in general characteristically-shaped but a great number seems to be more rounded and even the more elongated ones seem to assume smoothed edges instead of “sharped” ones. In this condition, although in a much reduced number, larger cells with vacuolar structures are also encountered. In its turn, KRAS silenced cells almost totally lose their shape; they adopted a flat enlarged morphology and developed large vacuole-like structures. Double silenced cells do not display evident and generalized morphology changes, still some rounder and some larger vacuolated cells can be observed.

Hereupon, it is possible to conclude that the inhibition of Gal-3 and/or KRAS expression has a visible impact in SW480 cells, inducing alterations in their normal morphology.

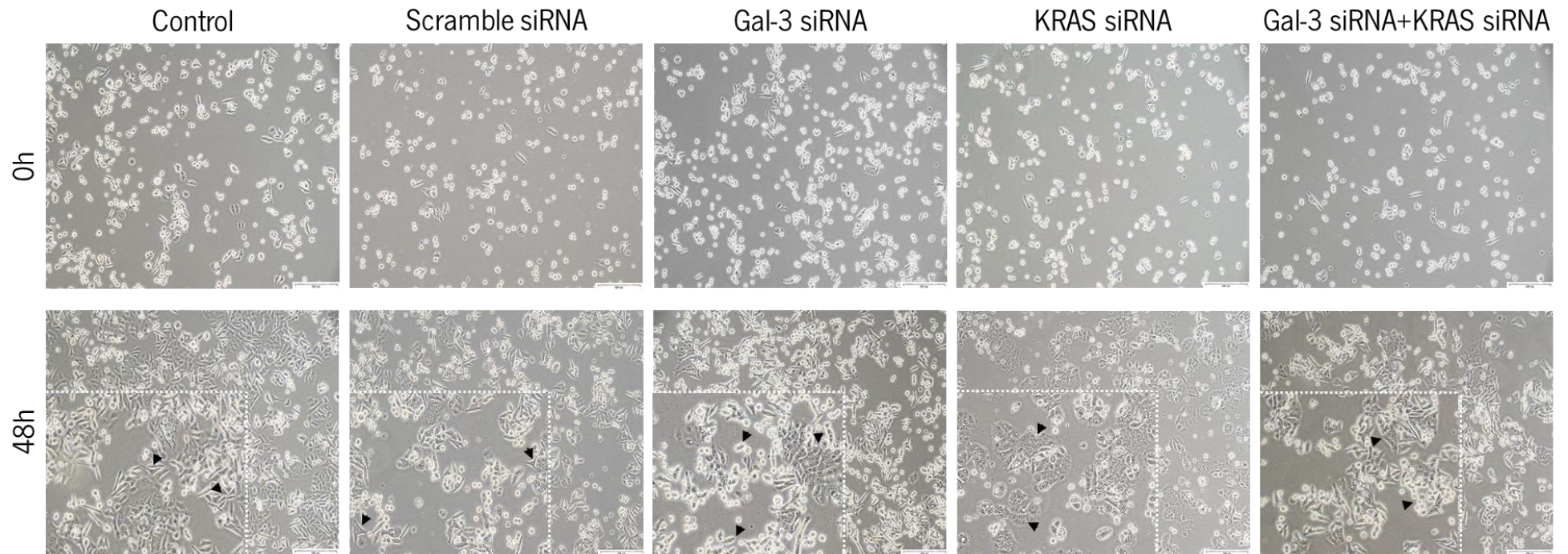


Fig. 3.16. Gal-3 and/or KRAS silencing induce morphology changes in SW480 cells. Representative phase contrast photographs of three independent RNAi experiments. Cells from the control conditions (control and scramble siRNA) differentiate into spindle/stellar shaped cells whereas in Gal-3 silencing condition, cells acquire a more rounded shape. In turn, KRAS silenced cells adopt a flat enlarged morphology and develop large vacuole-like structures. Double silenced cells do not evidence so pronounced changes but some round and vacuolated cells are visible. Black head arrows evidence the aforementioned cell' shape characteristics. Right bottom bars represent a 200 μ m scale.

3.5.2. Effect of galectin-3 and/or KRAS silencing on cell viability

To assess the effect of Gal-3 and/or KRAS silencing on cellular viability we opted to perform trypan blue exclusion assay, a simple and rapid technique which allowed to conclude about the number of viable/nonviable cells in a given cell suspension. The results of these experiments are presented in terms of percentage of cell viability and are summarized in Fig. 3.17.

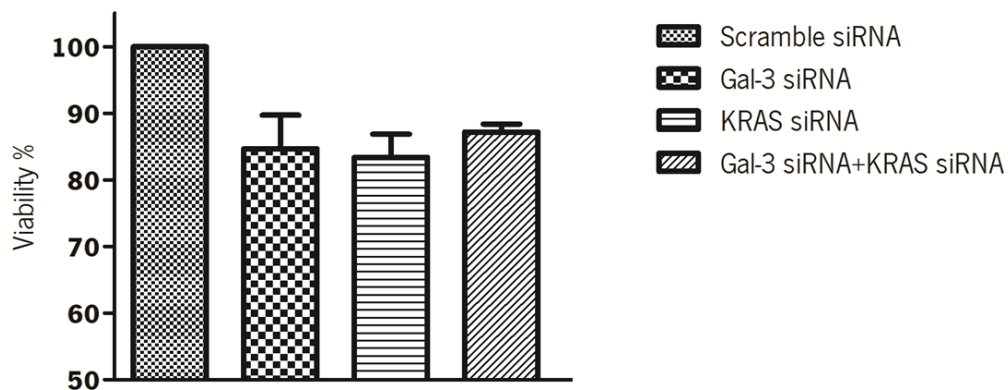


Fig. 3.17. Gal-3 and/or KRAS silencing decrease cell viability of SW480 cells. 48h after medium change, silenced cells were mixed with trypan blue dye and counted in a Neubauer chamber. Results show that Gal-3 and KRAS silencing induce a decrease in cell viability of $15.3\% \pm 8.6$ and $16.6\% \pm 6.0$, respectively, when compared to the scramble siRNA condition. In its turn, the double silencing of Gal-3 and KRAS decrease the viability only in $12.8\% \pm 2.0$. None of the observed results proved to be statistically significant. The results display the mean values \pm SEM of 3 independent experiments.

A decrease in cell viability was observed in the 3 silencing conditions (normalized values to the scramble siRNA condition), however none of those values demonstrated to be statistically significant. Gal-3 inhibition culminated in a decrease of $15.3\% \pm 8.6$ in cellular viability, a similar value to the one obtained with KRAS silencing, $16.6\% \pm 6.0$. Strikingly, the double silencing resulted in a slightly inferior impact on cell viability, registering a difference of $12.8\% \pm 2.0$ when compared to the scramble siRNA control condition. These results indicate that Gal-3 and KRAS silencing might have little impact on cell viability and when double silenced they do not display a synergistic effect but instead have a reduced effect on cell viability. This method has to be complemented with other more accurate techniques like cell cycle and annexin V/Propidium iodide (PI) analysis by flow cytometry.

3.5.3. Effect of galectin-3 and/or KRAS silencing on galectin-3, KRAS and p16 expression levels

We analyzed the expression of Gal-3, KRAS and p16 upon Gal-3 and/or KRAS silencing by RNAi. Our results show that Gal-3 and KRAS expression levels significantly ($p < 0.05$; silencing percentage $> 80\%$) decrease when cells are transfected with Gal-3 siRNA or KRAS siRNA, respectively, demonstrating that the specific designed siRNA molecules are effective in silencing their targets (Fig. 3.18). However, when we examine the double silencing condition, the effectiveness of the Gal-3 siRNA is maintained, but regarding KRAS, the efficiency of its specific siRNA is decreased. This result can be justified with the fact that Gal-3 silencing upregulates KRAS expression levels, meaning that KRAS inhibition is partially masked (in the double silencing condition) by the increase on its levels induced by Gal-3 silencing. In opposition, KRAS silencing causes a reduction in Gal-3 expression levels. These results suggest that KRAS and Gal-3 regulate their expression in an opposite manner, which needs further investigation.

Concerning p16 expression levels, the results presented on Fig. 3.18 (A and B) represent the only successful result obtained in these range of experiments, due to problems with the primary anti-p16 antibody. The results showed that p16 expression seems to change depending on the protein silenced: a modest increase is registered when Gal-3 is silenced and contrariwise KRAS and Gal-3+KRAS silencing led to a decrease in p16 levels. However, as these results are only from one experiment, no final conclusions can be drawn.

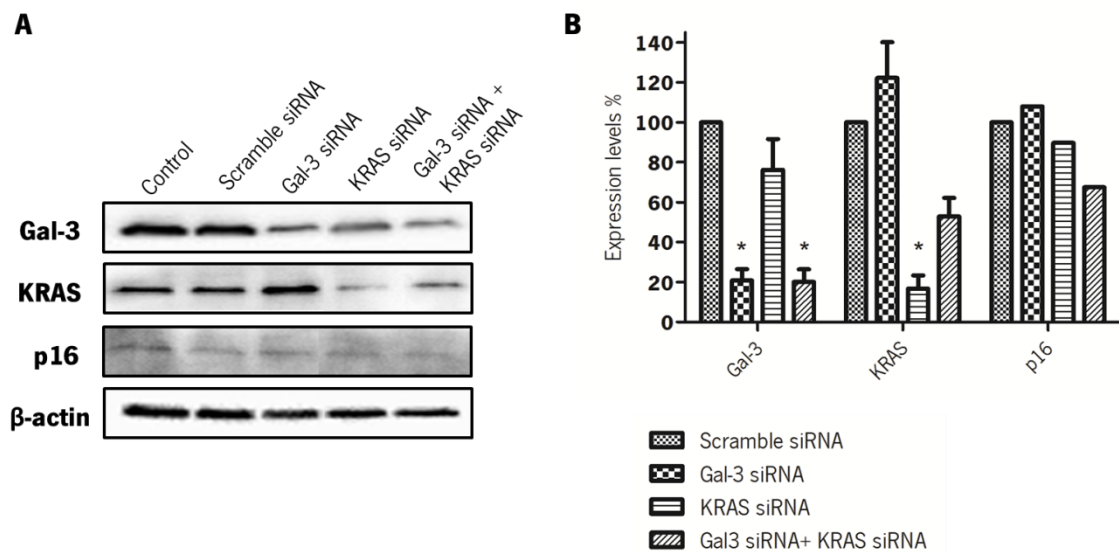


Fig. 3.18. Gal-3 silencing induces an increase in KRAS expression levels whereas KRAS silencing slightly decrease Gal-3 expression. **A)** Representative western blot of the RNAi experiments, evaluating changes in Gal-3, KRAS and p16 expression. **B)** Densitometry analysis values are presented as means \pm SEM of three independent experiments (* $p < 0.05$). Bars corresponding to p16 represent one isolated experiment.

3.5.4. Effect of galectin-3 and/or KRAS silencing on MMPs production/activity

Proteolytic enzymes, particularly MMPs, are involved in the degradation of extracellular matrix (ECM), facilitating tumour growth, invasion and metastasis (Herszényi et al. 2014). In order to elucidate the effect of Gal-3 and/or KRAS inhibition on secreted MMPs production and potential activity profile, gelatin zymography was performed using as samples the conditioned media (CM) from each of the RNAi experimental conditions. Gelatin zymography particularly detects MMP-2 and MMP-9 activities, which possess higher gelatin-degrading activity than other MMPs. These proteinases are secreted as inactive zymogens (pro-MMPs) with an inhibitory pro-peptide domain and are activated by other proteinases that remove the pro-peptide. During electrophoresis, the pro-peptide is unfolded and its inhibitory segment is pushed away from the enzyme catalytic site by SDS. In the post-run treatment the pro-peptides are only partially refolded, which results in a catalytically active enzyme and visualization of not only the active forms but also the originally inactive enzymes pro-forms (Vandooren et al. 2013).

Our results (Fig. 3.19 A) reveal the presence of bands corresponding to Pro-MMP-9 and Pro-MMP-2 and an additional band corresponding to the active form of MMP-9 that was not possible to quantify. The inhibition of Gal-3 seems to have almost no impact on Pro-MMP-9 and Pro-MMP-2 production; in opposition, KRAS and Gal-3+KRAS silencing led to a decrease of both Pro-MMP-9 and Pro-MMP-2 production, yet no significant value was detected (Fig. 3.19 B). Concerning the MMP-9 band, it is visible in the control, scramble siRNA and Gal-3 siRNA conditions, but there is a significant decrease on MMP-9 activity in KRAS and Gal3+KRAS silencing conditions, as no band appears between the pro-forms of MMP-9 and MMP-2 (Fig. 3.19 A).

In conclusion, Gal-3 silencing seems to have no effect on MMPs production and activity, inversely KRAS silencing and Gal-3/KRAS double silencing led to a decrease in MMP-9 and MMP-2 pro-forms and in MMP-9 active form.

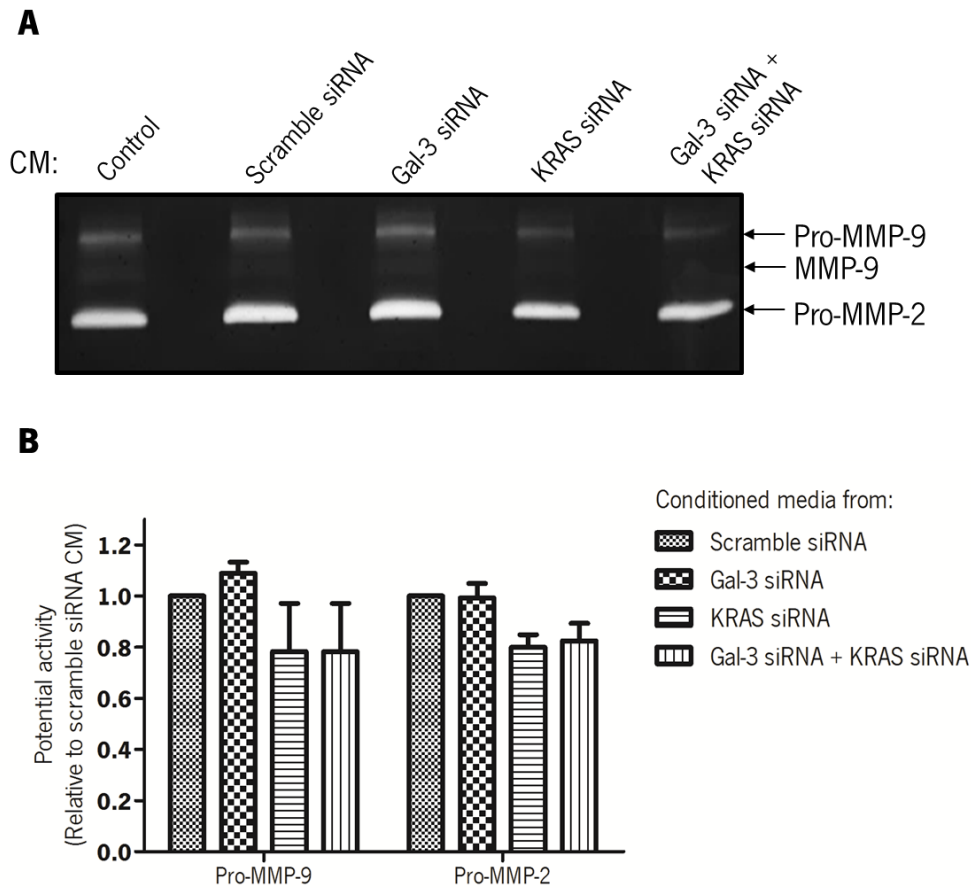


Fig. 3.19. KRAS silencing and Gal-3/KRAS double silencing led to a decrease in Pro-MMP-9, MMP-9 and Pro-MMP-2 levels. A) Conditioned media from - SW480 cells (negative control), SW480 transfected with scramble siRNA, Gal-3 siRNA, KRAS siRNA and Gal3 siRNA+KRAS siRNA- was collect and assessed for MMP-9 and MMP-2 potential activity by gelatin zymography. **B)** Band intensity was quantified relatively to the scramble siRNA condition. Bars represent the mean values \pm SEM of 3 independent experiments.

3.5.5. Effect of galectin-3 and/or KRAS silencing on cell migration

Cancer cell migration is an important step for the disruption of the basement membrane (BM) and the ECM, which is essential for the process of invasion and metastasis (Herszényi et al. 2014). We use a time-lapse microscope with a stage CO₂ incubator and cells were photographed every 5min during the last 24h of transfection (when the maximum of transfection is attained) to track cell trajectories and evaluate differences in cell motility/capacity of migration caused by silencing Gal-3 and KRAS alone or at the same time.

Representative images of the cells at 0h (24h post-transfection), 12h (36h post-transfection) and 24h (48h post-transfection) are shown in Fig. 3.20 A. Results show that control SW480 cells display a reduced migration that did not change in any of the evaluated conditions: no differences in the migration capability, between the silencing conditions and the

controls, were observed. These results correspond only to one isolated experiment, however we can infer that SW480 cells exhibit a reduced migration capacity and that neither Gal-3 nor KRAS silencing are able of influence that capacity.

At the end of this experiment, total cell lysates from each condition were prepared and Gal-3/KRAS silencing were confirmed by western blot analysis (Fig. 3.20 B).

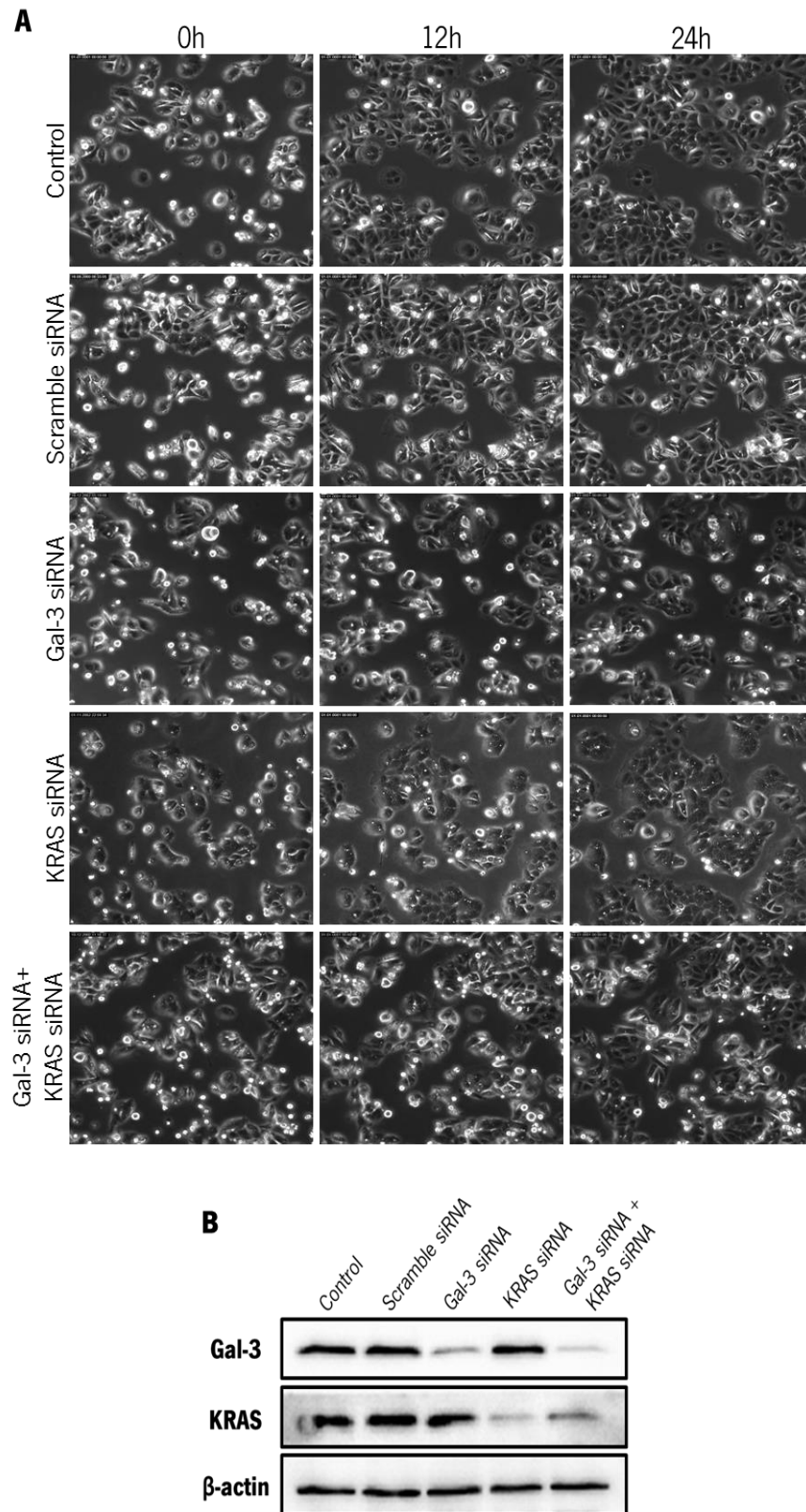


Fig. 3.20. Gal-3 and/or KRAS silencing have no effect on colon cancer SW480 cells migration. A) Representative images of each condition at 0h, 12h and 24h show that SW480 control cells present reduced motility and no differences in that capacity were observed among any of the experimental conditions (Magnification 20x). **B)** Gal-3 and KRAS silencing were confirmed by western blot analysis. These results represent one isolated experiment.

IV.

DISCUSSION

CRC is a very frequent type of cancer and one of the leading causes of death worldwide (GLOBOCAN, 2012). The last decades witnessed remarkable progress in screening, diagnosis and therapy that improved the overall survival of patients. Nevertheless, the great majority of the patients develop secondary tumours due to metastasis that are frequently fatal, being the five-year survival rate of curatively resected patients no more than 60%. Therefore, the development of new therapies and the focus on personalized treatment, to improve patient survival and reduce the side effects, are emerging fields in oncology (De Stefano & Carlomagno 2014). For the successful design of new therapies there is an urgent need of scientific research to get deeper knowledge on CRC carcinogenesis and to unveil new eligible cancer markers and prognostic predictors.

KRAS mutations are an important feature of CRC and are considered a therapeutic predictive biomarker (De Stefano & Carlomagno 2014). Gal-3 expression has increasingly been recognized to be altered in a variety of cancers and to be connected to tumour progression, including in CRC (Povegliano et al. 2011). The interaction between KRAS and Gal-3 has been demonstrated to be associated with transformation and malignant phenotype characteristics in many cancers (Shalom-Feuerstein et al. 2005; Levy et al. 2010; Song et al. 2012; Wu et al. 2013) being a potential therapeutic target. As already mentioned, p16 seems to be related to KRAS and Gal-3, exerting its tumour suppressor function by downregulating both proteins to achieve cancer cell anoikis resistance reversion (Sanchez-Ruderisch et al. 2010; Rabien et al. 2012). In this work, we aimed to study if there is a direct KRAS/Gal-3/p16 interaction and what are the phenotypic alterations induced by the absence of Gal-3 and/or KRAS in the CRC model.

In order to answer our first question, we started by evaluating the levels of expression KRAS, Gal-3 and p16 in the two selected patient-derived cell models. Concerning p16 expression, it is important to refer that confirmation based on band sequencing and maybe the reproduction of the results with another antibody will totally clarify any existing doubts. SW480 and HCT116 cells expressed different levels of Gal-3, KRAS and p16 as determined by western blot and confirmed by IF staining. Our observations showed a concordant association in both cell lines: KRAS and Gal-3 levels positively correlate and, in turn, are inversely related with the levels of p16. In accordance with these results, Sanchez-Ruderisch et al. 2010 had already demonstrated preliminary evidences for a negative correlation between Gal-3 and p16 in human pancreatic tissue and pancreatic cancer, as a support of their *in vitro* data in pancreatic cancer cells. Additionally, mutant KRAS (Song et al. 2012) and KRAS^{wt}-GTP (Levy et al. 2010) have been

related with high Gal-3 expression in pancreatic and thyroid cancer models, respectively. Using the SW480 cell line, two authors (Herman et al. 1995; Kim et al. 2005) demonstrated that p16 gene promoter is methylated and that the protein is not expressed in these cells. However, we and others (Hartman et al. 2009) using the same anti-p16 antibody, have detected p16 expression in SW480 cells. HCT116 cells seem to be an interesting case among CRC cell lines: p16 promoter is hemimethylated but the protein is expressed (Kim et al., 2005). Moreover, it is important to mention that these two CRC cell lines harbour different KRAS mutations: SW480 cell line harbours a G12V mutation and HCT116 harbours a G13D mutation, which might be involved in the differences observed.

Our results on IF experiments also evidenced a difference between SW480 and HCT116 cell lines: both Gal-3 and p16 reveal a more generalized and dispersed localization pattern in HCT116 in comparison to SW480 cells. Concerning Gal-3 localization, it has already been shown to be very variable depending on many factors, including: cell type, culture conditions and proliferative state of the cells (Haudek et al. 2010) but recent data on this subject is scarce. For example, Moutsatsos et al. 1987 reported that in 3T3 fibroblasts, Gal-3 localization and expression was different depending on the confluence levels of the stained cells, on the proliferative state of the cells (serum starved quiescent cells or proliferating cells) or on the cell cycle phase. Thus, culture conditions (namely the levels of confluency and nutrient availability), the number of cell passages, the cell cycle phase (as the cells were not synchronized) or the different levels of confluency, are some of the factors that can support the discrepancy in results obtained in low vs high confluent cells and in the single staining to the double staining experiments in SW480 cells. As for p16, it seems that the levels of confluence can alter p16 localization in SW480 cells. Since this protein participates in cell cycle regulation, these results might be a consequence of cells being in different cell cycle phases upon fixation that could originate different p16 localizations. These two proteins seem to partially co-localize in these cell models, providing an encouraging indication of their interaction.

In normal colon Flag-KRAS transfected cells, p16 localization demonstrated to be different (mainly nuclear) than the one observed in CRC cells, suggesting that changes in its subcellular localization can be a characteristic of tumour progression. Gal-3 staining pattern also seems to suffer some alterations from cancer to normal cells, as its punctuated pattern is lost and the staining is stronger in the cytoplasm than in the nucleus. In normal colon Gal-3 has been reported to be expressed both in the cytoplasm and nucleus, but more strongly in the nucleus

(Lotz et al. 1993; Sanjuán et al. 1997), and along CRC progression its localization has been reported to be variable, being its cytoplasmic rather than its nuclear localization, considered a poor prognostic factor (Povegliano et al. 2011). In these cell lines, in spite of being mainly localized in different subcellular compartments, the hypothesis of a, at least partial, co-localization of Flag-KRAS and p16 is not totally discarded (some yellow/orange areas are observed) and needs further exploration.

As there was a good indication of a potential Gal-3 and p16 co-localization, we carried out Co-IP experiments, which allowed the confirmation of such interaction and also gave insights about the interaction with KRAS. Results of these experiments provided good evidence that Gal-3, KRAS and p16 are physically interacting in the CRC SW480 cell line. As mentioned, Gal-3 is known to directly bind KRAS, and co-immunoprecipitation of Gal-3 and KRAS^{G12V} was already demonstrated (Elad-Sfadia et al. 2004; Shalom-Feuerstein et al. 2005), however, we were not able to find any literature reference regarding the direct interaction of these two proteins with p16. In our work, due to protocol inherent drawbacks, the bands corresponding to the denatured IgG difficult a clear observation of the results. Therefore, some strategies should be applied to reduce the interference of the IgG bands. We have already tried to increase the resolution, using a longer and more concentrated gel (18%, 13.3x8.7cm; Bio-Rad). However, the separation between the 25-35kDa was not significantly different from what we had in a regular 16% polyacrylamide gel, additionally there are some commercial kits to remove the IgG from the sample and some specific secondary antibodies that selectively bind the non-denatured form of the primary antibody, which could be worth to try. Despite the need of further protocol optimizations, our Co-IP results showed a new underexplored biochemical interaction between Gal-3, KRAS and p16. This set of results constitutes preliminary evidences that answer our first aim.

In the second and third aims, we intended to study the effect of silencing Gal-3 and/or KRAS in Gal-3/KRAS/p16 expression levels regulation and in some cancer-associated phenotypic characteristics. The interaction between Gal-3 and KRAS and the subsequent activation of KRAS signalling pathways, particularly the RAF/MEK/ERK pathway, are known to be responsible for many cancer-related features, for example proliferation (Song et al. 2012; Levy et al. 2010), apoptosis and anchorage independent growth resistance (Shalom-Feuerstein et al. 2005), migration and invasion (Song et al. 2012; Wu et al. 2013). Variations on Gal-3, KRAS or p16 proteins expression levels, when Gal-3 and/or KRAS are inhibited, constitute an indirect

indication of their interplay. Variations on p16 levels were detected in Gal-3 and/or KRAS silencing conditions: an increase was observed when Gal-3 was silenced and a decrease when KRAS or Gal-3+KRAS were silenced, although further experiences should be performed in order to confirm the results obtained. Gal-3 silencing induced an upregulation of KRAS levels and conversely KRAS silencing resulted in a decrease of Gal-3 expression levels. These results suggest the existence of an opposite regulation mechanism between these proteins, which as far as we are aware, has never been reported before. Song et al. 2012 demonstrated that the silencing of Gal-3 decreases total RAS and active RAS levels in Panc-1 and MPanc96 pancreatic cancer cells, however they evaluated total RAS, meaning that all RAS isoforms contribute to their results. Additionally, in thyroid cancer cells, stable transfection of MRO cells with Gal-3 shRNA decreased KRAS-GTP levels, but in this case the authors were considering the active form of KRAS^{wt} (Levy et al. 2010). In DLD-1 colon cancer cells, which harbour a KRAS^{G13D} mutation (Ahmed et al. 2013), Gal-3 stable silencing had no effect on KRAS levels, but instead significantly decreased p-RAF and p-EKR1/2 expression (Wu et al. 2013). The mechanism observed in our model, can be governed either at transcription or at protein degradation levels. The KRAS increased expression induced by Gal-3 silencing may justify the poorer impact of the double silencing on cell morphology and cell viability.

Silencing of Gal-3 and/or KRAS induce visible changes on cells morphology. Gal-3 silenced cells are more rounded, feature that was also reported by Cheong et al. (2010), upon Gal-3 silencing in AGS gastric cancer cells. This change in morphology can indicate a decrease in lamellipodia formation (movement-propulsion structures, usually connected with the invasion capacity), which has been demonstrated by Wu et al. (2013) after Gal-3 silencing in DLD-1 colon cancer cells. KRAS silencing is the condition that exerts more dramatic effects on cell morphology as cells became enlarged, flat and acquire vacuolar structures. These results support once again the already suggested role of KRAS in the regulation of the cellular cytoskeleton. The vacuolar structures can be indicative of death processes, however, deeper analysis, namely by electronic microscopy should be performed.

Gal-3 and KRAS silencing, reduced the viability of SW480 cells. Given the relevance of these two proteins in cell fate regulation, a decrease in cell viability, after their inhibition, was predictable. In pancreatic cancer *in vitro* and *in vivo* models, Gal-3 knockdown was reported to decrease cell viability and tumour volume, respectively (Song et al. 2012). On the other hand, other reports showed no visible effects of Gal-3 silencing on the viability of pancreatic (Kobayashi

et al. 2011) and tongue cancer (Zhang et al. 2013) cells. Furthermore, Gal-3 silencing has been shown to induce G1 phase cell cycle arrest in gastric cancer cells and, when combined with therapeutic drugs it decreases cancer cell viability and augments apoptosis levels (Cheong et al. 2010). Mutant KRAS silencing has been shown to reduce pancreatic adenocarcinoma (model in which KRAS mutations are even more frequent than in CRC) cells proliferation and to induce apoptosis (Fleming et al. 2005). All these aforementioned studies determined cell viability/proliferation using MTT/MTS-reduction based assays, which are dependent on mitochondrial metabolism integrity, and therefore cannot be compared with our results that instead reflect the cellular membrane integrity. Hence, it is important to mention that trypan blue exclusion assay despite being simple and rapid, only constitutes an indirect assessment of cell viability based on membrane integrity and to supplement our results, more refined techniques, namely annexinV/PI staining and cell cycle analysis by flow cytometry, should be performed. Recent results of our group demonstrate that KRAS inhibition leads to cell death in SW480 cells (Alves et al. 2014).

Tumour (or host tumour-induced) secretion of proteolytic enzymes, responsible for the degradation of BM and ECM components, and the migration of tumour cells across the BM and tumour stroma, are essential events for tumour invasion and metastasis (Herszényi et al. 2014). These two tumour cell capabilities, MMPs production and migration, were analyzed in this work upon silencing of Gal-3 and/or KRAS. MMPs, in particular MMP-9, play important roles in colorectal carcinogenesis and are considered independent prognostic biomarkers and potential diagnostic and therapeutic tools (Herszényi et al. 2014). Our data evidenced that KRAS silencing induces a decrease in Pro-MMP-2/-9 and MMP-9. KRAS was found to regulate the expression of MMP-2 in fibroblasts (Liao et al. 2003), which supports our result. This data probably deserves more attention and further exploration if we take into account that Gal-3 is a substrate of MMP-9 and MMP-2, and that the cleaved form is more effective in improving angiogenesis and invasion (Nangia-Makker et al. 2007; Nangia-Makker et al. 2010). Hence, one might speculate that KRAS silencing can indirectly act by reducing the levels and the activity of MMP-2/-9 which consequently will lead to a decrease in Gal-3 ND-cleavage, impairing the effects of cleaved Gal-3 form and thereby reducing angiogenesis and invasion capacity of tumour cells. In this extent, we have confirmed that in our models, SW480 and HCT116, Gal-3 is secreted to the cell culture medium (supplementary data Fig. S3) in normal culture conditions, though we failed to detect the cleaved form because the antibody we have available recognizes an epitope mapping at the

N-terminus of Gal-3. Altogether these results support the notion that KRAS silencing can be considered a good therapeutic approach as its inhibition can have effect not only on viability but also on invasion capacity, a relevant clinical problem.

A connection between Gal-3 and the capacity of migration has been established for example in models of pancreatic (Kobayashi et al. 2011), colon (Wu et al. 2013), and tongue (Zhang et al. 2013) cancers, where Gal-3 silencing is capable of decrease the cells migration rate. KRAS silencing has also been shown to reduce the levels of migration of MiaPaca-2 and Panc-1 pancreatic adenocarcinoma cells in about 70% (Fleming et al. 2005). Regardless the fact that in these reports the evaluation of cancer cell migration rates was done by different techniques (wound-healing assays and modified Boyden chamber assays) than the one we employed in our work, our results showed a reduced mobility capacity in all the experimental conditions. Importantly, Kasem et al. 2014 recently used SW480 cells in migration assays (radius cell migration assays, very similar to wound-healing assay) to study the role of JK1 in colon cancer cell migration. The authors stably silenced JK1 in SW480 cells and observed that when plated in regular non-coated plates these cells displayed no differences in migration capacity, but when plated in matrix components (collagen, fibronectin or laminin) coated plates the migration rates were significantly altered.

Overall, our work provides the first evidence of a direct interplay between Gal-3, KRAS and p16. The outcomes of this interaction should definitely constitute a research subject, as novel therapeutic strategies can arise from its understanding. KRAS and Gal-3 silencing are capable of induce changes in SW480 cells, and considering our results, KRAS silencing could constitute a good therapeutic approach. An integrative outline of the findings and hypothesis resulting from this thesis project are summarized at Fig.4.1.

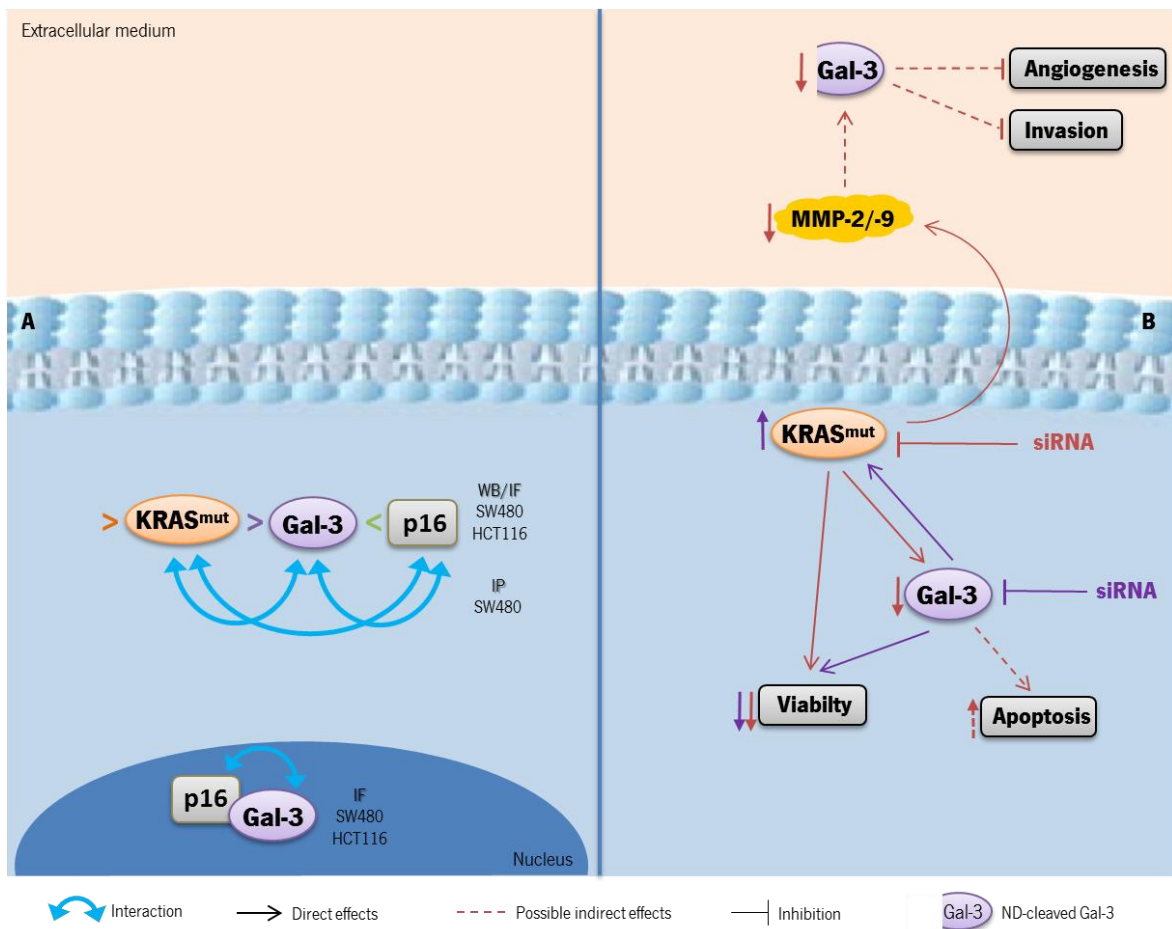


Fig. 4.1. Results outline of this project. A) Answering our first aim, we were able to establish a relation among the expression levels of the three proteins under study. Resorting to IF and Co-IP assays, our preliminary results showed a interaction between Gal-3, KRAS and p16, being the interaction between Gal-3 and p16 most likely to occur at the nucleus, according to our IF results. **B)** As for our second/third aims we demonstrated the existence of an opposite regulation between KRAS and Gal-3 upon their silencing and also that the inhibition of these proteins reduce cell viability. Additionally, KRAS inhibition was found to decrease the levels of MMPs, and therefore, we suggest that KRAS silencing could be a good therapeutic strategy, which could indirectly impair cancer cell survival, angiogenesis and metastasis.

V.

**CONCLUDING REMARKS AND
FUTURE PERSPECTIVES**

The main goal of this project was to explore the Gal-3/KRAS/p16 interplay in CRC *in vitro* models and at this point we can set many important conclusions, which not only can help to uncover our initial questions but also constitute the basis for some protocol improvements and future experiments.

We demonstrated the existence of a positive correlation between KRAS and Gal-3 levels and of an inverse correlation between those and p16 levels in CRC cells. Through IF experiments we found Gal-3 in the nucleus and cytoplasm with a punctuate pattern, more dispersed in the case of HCT116 cells. Gal-3 and p16 double staining in SW480 and HCT116, showed a partial co-localization of these proteins, more pronounced at the nuclear compartment. Taking into account that anti-KRAS antibodies appear not to be considered good tools for IF experiments (Fuentes-Calvo et al. 2010) and as Gal-3 has been shown to selectively bind KRAS (Elad-Sfadia et al. 2002; Elad-Sfadia et al. 2004) the use of an anti-pan RAS antibody could be a valid approach to search for Gal-3 and KRAS co-localization in these cell lines. In normal colon cells transfected with Flag-KRAS^{wt} and the three KRAS hotspot mutations, p16 demonstrated to be mainly localized at the nucleus and Flag-KRAS instead was localized at the cytoplasm and along cellular-projections. However, a level of partial co-localization between these proteins is not totally rejected and therefore, needs further investigation, for example resorting to Co-IP or proximity-ligation assays (PLA). Gal-3 seems to have a similar cellular distribution in normal and CRC cells, but in the former, the punctuated pattern is lost. Also, it is important to notice from these experiments that commercial antibodies validation is very important; a careful selection of antibodies is an essential part of IF experiments, and the sequential staining, in spite of being an accepted procedure is ineffective to avoid secondary antibodies cross-reaction.

Moreover, as SW480 and HCT116 cell lines harbour different KRAS mutations, in the future it could be of most interest to explore the role of the distinct KRAS hotspot mutations in the regulation of Gal-3 and p16 expression, and its consequent effects in the CRC model. Understanding if this correlation is maintained in human tumours could bring valuable new insights to understand CRC biology and help explaining for example, why the patients that harbour a G13D mutation are more responsive to EGFR inhibitors-based therapy.

The main conclusion of this work is that for the first time we showed a physical interaction of Gal-3/KRAS/p16 in SW480 cells, establishing a totally new concept. Even though some relations between these proteins had been described, it was never mentioned that they could establish a physical interaction. This opens a new field of research to study the functions of

this interaction in colorectal carcinogenesis and, once again, to try to understand the effect of the different KRAS mutations in its regulation. After protocol optimization, band isolation and sequencing, sequential immunoprecipitation (immunoprecipitate one protein, confirm its presence and immunoprecipitate the other from the initial immunoprecipitate and so on) and a control condition with the naive IgG from the specific antibody used in IP, can be performed in order to confirm the results.

RNAi experiments demonstrated that the specific targeting of KRAS and Gal-3 with siRNA were effective to achieve their silencing (confirmed at the protein level) in SW480 cells. The inhibition of these proteins evidenced an opposite regulation: when Gal-3 is silenced KRAS is upregulated and when KRAS is silenced Gal-3 is downregulated. This justifies the poorer effectiveness of KRAS silencing, and the consequently results obtained on the effect on morphological characteristics and on cell viability, when the double silencing of these proteins was performed. From our point of view, explore KRAS protein localization, activity and phosphorylation levels of its downstream effectors (p-ERK, p-AKT), when Gal-3 is silenced, will be important to understand how Gal-3 regulates KRAS signalling. Gal-3 or KRAS silencing alone demonstrated to have a noticeable effect on SW480 cell morphology, which can be related to a decrease in the migration/invasion-essential structures, associated with Gal-3, and with cell death characteristics associated with KRAS. Electronic microscopy analysis and study of the cytoskeleton organization following a phalloidin staining of actin fibers constitute complementary approaches to be considered. Despite not very pronounced, Gal-3 or KRAS silencing induced a reduction on cell viability. KRAS silencing in SW480 cells has been shown by our group to induce an increase in annexinV positive cells (Alves et al. 2014). Nevertheless, the effect of Gal-3 silencing in cell proliferation and viability should be more explored in the future, using flow cytometry analysis of cell cycle and annexinV/PI staining.

Concerning the gelatin zymography results, KRAS silencing and Gal-3/KRAS double silencing demonstrated to have impact on MMPs production/activity, what *per se* constitutes a good result, since MMPs are considered important players in colorectal carcinogenesis, but also could represent an indirect way to impair extracellular Gal-3 tumour promotion effects. Thus, matrigel invasion assays and assessment of Gal-3 and cleaved-Gal-3 levels in the conditioned media (for example using the ELISA) constitute complementary experiments to explore this question. Regardless the fact that SW480 cells showed to have a reduced motility capacity and that no alterations were found among our experimental conditions, we should perform this

experiment again. The use of matrix coated plates can be an important strategy to apply in our work, which could allow us to conclude about the effect of Gal-3 and/or KRAS silencing on SW480 CRC cells migration.

In summary, future work will focus on completing the presented results in HCT116 cells, addressing the role of KRAS mutations on Gal-3/KRAS/p16 interplay regulation, and also on an extensive characterization of the phenotypic alterations (on proliferation, apoptosis, clonogenic survival and anchorage independent growth, migration, invasion and cytoskeleton organization) induced by silencing Gal-3 and/or p16 and/or KRAS.

Moreover, considering the different morphology of NCM460 Flag-KRAS^{G12D} and the effects of KRAS inhibition on SW480 cells morphology, which suggest the involvement of KRAS in cytoskeleton organization, it should be interesting to assess this hypothesis. We should also highlight that considering the relevance of KRAS and Gal-3 interaction in tumour progression, there is a visible lack in literature of studies analysing if there is a connection between KRAS expression and mutation status and Gal-3 expression in CRC tissues. Thus, this underexplored field could constitute a good opportunity of scientific research. Besides, as RAS has been found to function in other signalling platforms, in addition to the membrane (e.g. lysosomes and mitochondria) (Omerovic & Prior 2009), it could be worth to search for Gal-3 presence and interaction with KRAS in those cellular organelles.

Summing up, this work represents the first and, as far as we are aware, unique evidence of a physical Gal-3/KRAS/p16 interaction, and supports the notion that KRAS^{mut} silencing can be a good approach in CRC therapy, especially in metastatic CRCs resistant to anti-EGFR therapy. Furthermore, this project highlights new questions that could be worth to explore and may constitute important clues to the understanding of the biology of CRC harbouring KRAS mutations, in order to identify new cancer markers for potential targeted therapy.

VI.

REFERENCES

- Abankwa, D., A.A. Gorfe, and J.F. Hancock. 2007. Ras nanoclusters : molecular structure and assembly. *Semin Cell Dev Biol.* 18:599–607.
- Ahmed, D., P.W. Eide, I.A. Eilertsen, S. Danielsen, M. Eknæs, M. Hektoen, G. Lind, and R. Lothe. 2013. Epigenetic and genetic features of 24 colon cancer cell lines. *Oncogenesis.* 2:e71.
- Akahani, S., P. Nangia-makker, H. Inohara, H.-R.C. Kim, and A. Raz. 1997. Galectin-3: A Novel Antiapoptotic Molecule with A Functional BH1 (NWGR) Domain of Bcl-2 Family Bcl-2 Family. *Cancer Res.* 57:5272–5276.
- Alhaja, E., J. Adan, R. Pagan, F. Mitjans, M. Cascalló, M. Rodríguez, V. Noé, C.J. Ciudad, A. Mazo, S. Vilaró, and J. Piulats. 2004. Anti-migratory and anti-angiogenic effect of p16: a novel localization at membrane ruffles and lamellipodia in endothelial cells. *Angiogenesis.* 7:323–33.
- Al-Mohanna, M. a, P.S. Manogaran, Z. Al-Mukhalafi, K. A Al-Hussein, and A. Aboussekhra. 2004. The tumor suppressor p16(INK4a) gene is a regulator of apoptosis induced by ultraviolet light and cisplatin. *Oncogene.* 23:201–12.
- Al-Sohaily, S., A. Biankin, R. Leong, M. Kohonen-Corish, and J. Warusavitarne. 2012. Molecular pathways in colorectal cancer. *J. Gastroenterol. Hepatol.* 27:1423–31.
- Alves, S., L. Castro, M.S. Fernandes, P. Castro, M. Priault, S.R. Chaves, M.P. Moyer, C. Oliveira, R. Seruca, M. Côrte-Real, M.J. Sousa, and A. Preto. 2014. Hotspot mutations in the KRAS oncogene function as positive regulators of autophagy. *Submitted.*
- Amano, M., H. Eriksson, J.C. Manning, K.M. Detjen, S. André, S.-I. Nishimura, J. Lehtiö, and H.-J. Gabius. 2012. Tumour suppressor p16(INK4a) - anoikis-favouring decrease in N/O-glycan/cell surface sialylation by down-regulation of enzymes in sialic acid biosynthesis in tandem in a pancreatic carcinoma model. *FEBS J.* 279:4062–80.
- André, S., H. Sanchez-Ruderisch, H. Nakagawa, M. Buchholz, J. Kopitz, P. Forberich, W. Kemmer, C. Böck, K. Deguchi, K.M. Detjen, B. Wiedenmann, M. von Knebel Doeberitz, T.M. Gress, S.-I. Nishimura, S. Rosewicz, and H.-J. Gabius. 2007. Tumor suppressor p16INK4a—modulator of glycomic profile and galectin-1 expression to increase susceptibility to carbohydrate-dependent induction of anoikis in pancreatic carcinoma cells. *FEBS J.* 274:3233–3256.
- Andreyev, H.J.N., A.R. Norman, D. Cunningham, J. Oates, B.R. Dix, B.J. Iacopetta, J. Young, T. Walsh, R. Ward, N. Hawkins, M. Beranek, P. Jandik, R. Benamouzig, E. Jullian, P. Laurent-Puig, S. Olschwang, O. Muller, I. Hoffmann, H. Rabes, C. Zietz, C. Troungos, C. Valavanis, S. Yuen, J. Ho, C. Croke, D. O'Donoghue, W. Giaretti, A. Rapallo, A. Russo, V. Bazan, M.T. Tanaka,, K. Omura, T. Azuma, T. Ohkusa, T. Fujimori, Y. Ono, M. Pauly, C. Faber, R. Glaesener, A. de Goeij, J. Arends, S. Andersen, T. Lövig, J. Breivik, G. Gaudernack, O. Clausen, P. De Angelis, G. Meling, T. Rognum, R. Smith, H.-S. Goh, A. Font, R. Rosell, X. Sun, H. Zhang, J. Benhattar, L. Losi, J. Lee, S. Wang, P. Clarke, S. Bell, P. Quirke, V. Bubb, J. Piris, N. Cruickshank, D. Morton, J. Fox, F. Al-Mulla, N. Lees, C. Hall, D. Snary, K. Wilkinson, D. Dillon, J. Costa, V. Pricolo, S. Finkelstein, J. Thebo, A. Senagore, S. Halter, S. Wadler, S. Malik, K. Krtolica, and N. Urosecvic. 2001. Kirsten ras mutations in patients with colorectal cancer : the “ RASCAL II ” study. *Br. J. Cancer.* 85:692–696.
- Andreyev, H.J.N., A.R. Norman, D. Cunningham, J.R. Oates, and P.A. Clarke. 1998. Kirsten ras Mutations in Patients With Colorectal Cancer : the Multicenter ““ RASCAL ”” Study. *J. Natl. Cancer Inst.* 90:675–684.
- Armaghany, T., J.D. Wilson, Q. Chu, and G. Mills. 2012. Genetic alterations in colorectal cancer. *Gastrointest. cancer Res.* 5:19–27.
- Arrington, A.K., E.L. Heinrich, W. Lee, M. Duldulao, S. Patel, J. Sanchez, J. Garcia-Aguilar, and J. Kim. 2012. Prognostic and Predictive Roles of KRAS Mutation in Colorectal Cancer. *Int. J. Mol. Sci.* 13:12153–12168.
- Barboni, E. a. M., S. Bawumia, K. Henrick, and R.C. Hughes. 2000. Molecular modeling and mutagenesis studies of the N-terminal domains of galectin-3: evidence for participation with the C-terminal carbohydrate recognition domain in oligosaccharide binding. *Glycobiology.* 10:1201–1208.

- Barondes, S.H., V. Castronovo, D.N.W. Cooper, R.D. Cummings, K. Drickamer, T. Feizi, M.A. Gitt, J. Hirabayashi, C. Hughes, K. Kasai, H. Leffler, F.-T. Liu, R. Lotan, A.M. Mercurio, M. Monsigny, S. Pillai, F. Poirer, A. Raz, P.W.J. Rigby, J.M. Rini, and J.L. Wang. 1994. Galectins: A Family of Animal B-Galactoside-Binding Lectins. *Cell*. 76:597–598.
- Barrow, H., X. Guo, H.H. Wandall, J.W. Pedersen, B. Fu, Q. Zhao, C. Chen, J.M. Rhodes, and L.-G. Yu. 2011. Serum galectin-2, -4, and -8 are greatly increased in colon and breast cancer patients and promote cancer cell adhesion to blood vascular endothelium. *Clin. cancer Res.* 17:7035–7046.
- Barrow, H., J.M. Rhodes, and L.-G. Yu. 2013. Simultaneous determination of serum galectin-3 and -4 levels detects metastases in colorectal cancer patients. *Cell. Oncol.* 36:9–13.
- Bennecke, M., L. Kriegl, M. Bajbouj, K. Retzlaff, S. Robine, A. Jung, M.C. Arkan, T. Kirchner, and F.R. Greten. 2010. Ink4a/Arf and oncogene-induced senescence prevent tumor progression during alternative colorectal tumorigenesis. *Cancer Cell*. 18:135–46.
- Bihl, M.P., A. Foerster, A. Lugli, and I. Zlobec. 2012. Characterization of CDKN2A(p16) methylation and impact in colorectal cancer: systematic analysis using pyrosequencing. *J. Transl. Med.* 10:173.
- Blanchard, H., X. Yu, P.M. Collins, and K. Bum-Erdene. 2014. Galectin-3 inhibitors: a patent review (2008-present). *Expert Opin. Ther. Pat.* 24:1053–1065.
- Bresalier, R.S., N. Mazurek, L.R. Sternberg, J.C. Byrd, C.K. Yunker, P. Nangia-Makker, and A. Raz. 1998. Metastasis of Human Colon Cancer Is Altered by Modifying Expression of the B-Galactoside-Binding Protein Galectin 3. *Gastroenterology*. 115:287–296.
- Brown, E.R., T. Doig, N. Anderson, T. Brenn, V. Doherty, Y. Xu, J.M.S. Bartlett, J.F. Smyth, and D.W. Melton. 2012. Association of galectin-3 expression with melanoma progression and prognosis. *Eur. J. Cancer*. 48:865–874.
- Van Den Br ule, F.A., D. Waltregny, F. Llu, and V. Castronovo. 2000. Alteration of the cytoplasmic / nuclear expression pattern of galectin-3 correlates with prostate carcinoma progression. *Int. J. cancer (Pred. Oncol.)*. 89:361–367.
- Califice, S., V. Castronovo, M. Bracke, and F. van den Br ule. 2004. Dual activities of galectin-3 in human prostate cancer: tumor suppression of nuclear galectin-3 vs tumor promotion of cytoplasmic galectin-3. *Oncogene*. 23:7527–7536.
- Castellano, E., and E. Santos. 2011. Functional specificity of ras isoforms: so similar but so different. *Genes Cancer*. 2:216–31.
- Cejas, P., M. L pez-G mez, C. Aguayo, R. Madero, J. de C. Carpen , C. Belda-Iniesta, J. Barriuso, V.M. Garc a, J. Larrauri, R. L pez, E. Casado, M. Gonzalez-Bar n, J. Feliu, and M. Gonzalez-baro. 2009. KRAS Mutations in Primary Colorectal Cancer Tumors and Related Metastases: A Potential Role in Prediction of Lung Metastasis. *PLoS One*. 4:e8199.
- Chen, C., C.A. Duckworth, Q. Zhao, D.M. Pritchard, J.M. Rhodes, and L.-G. Yu. 2013b. Increased circulation of galectin-3 in cancer induces secretion of metastasis-promoting cytokines from blood vascular endothelium. *Clin Cancer Res.* 19:1693–1704.
- Chen, C., T. Er, Y. Liu, J. Hwang, M.J. Barrio, M. Rodrigo, E. Garcia-toro, and M. Herreros-villanueva. 2013a. Computational Analysis of KRAS Mutations: Implications for Different Effects on the KRAS p . G12D and p . G13D Mutations. *PLoS One*. 8:e55793.
- Cheong, T.-C., J.-Y. Shin, and K.-H. Chun. 2010. Silencing of galectin-3 changes the gene expression and augments the sensitivity of gastric cancer cells to chemotherapeutic agents. *Cancer Sci*. 101:94–102.
- Chiu, C.G., S.S. Strugnell, O.L. Griffith, S.J.M. Jones, A.M. Gown, B. Walker, I.R. Nabi, and S.M. Wiseman. 2010. Diagnostic utility of galectin-3 in thyroid cancer. *Am. J. Pathol.* 176:2067–2081.
- Collado, M., and M. Serrano. 2013. Senescence in tumours: evidence from mice and humans. *Nat. Rev. Cancer*. 10:51–57.
- Cooper, D.N.W. 2002. Galectinomics: finding themes in complexity. *Biochim. Biophys. Acta*. 1572:209–231.

- Dai, C.Y., E.E. Furth, R. Mick, J. Koh, T. Takayama, Y. Niitsu, and G.H. Enders. 2000. p16INK4a expression begins early in human colon neoplasia and correlates inversely with markers of cell proliferation. *Gastroenterology*. 119:929–942.
- Duffy, M.J. 2013. The war on cancer: are we winning? *Tumour Biol*. 34:1275–84.
- Dumic, J., S. Dabelic, and M. Flögel. 2006. Galectin-3: an open-ended story. *Biochim. Biophys. Acta*. 1760:616–35.
- Elad-Sfadia, G., R. Haklai, E. Balan, and Y. Kloog. 2004. Galectin-3 augments K-Ras activation and triggers a Ras signal that attenuates ERK but not phosphoinositide 3-kinase activity. *J. Biol. Chem*. 279:34922–34930.
- Elad-Sfadia, G., R. Haklai, E. Ballan, H.-J. Gabius, and Y. Kloog. 2002. Galectin-1 augments Ras activation and diverts Ras signals to Raf-1 at the expense of phosphoinositide 3-kinase. *J. Biol. Chem*. 277:37169–37175.
- Endo, K., S. Kohnoe, E. Tsujita, A. Watanabe, H. Nakashima, H. Baba, and Y. Maehara. 2005. Galectin-3 Expression is a Potent Prognostic Marker in Colorectal Cancer. *Anticancer Res*. 25:3117–3121.
- Fearon, E.R., and B. Vogelstein. 1990. A Genetic Model for Colorectal Tumorigenesis. *Cell*. 61:759–767.
- Fellmann, C., and S.W. Lowe. 2014. Stable RNA interference rules for silencing. *Nat. Cell Biol*. 16:10–18.
- Fleming, J.B., G. Shen, S.E. Holloway, M. Davis, and R.A. Brekken. 2005. Molecular Consequences of Silencing Mutant K- ras in Pancreatic Cancer Cells : Justification for K- ras – Directed Therapy. *Mol Cancer Res*. 3:413–423.
- Floor, S.L., J.E. Dumont, C. Maenhaut, and E. Raspe. 2012. Hallmarks of cancer: of all cancer cells, all the time? *Trends Mol. Med*. 18:509–515.
- Fuentes-Calvo, I., A.M. Blázquez-Medela, E. Santos, J.M. López-Novoa, and C. Martínez-Salgado. 2010. Analysis of k-ras nuclear expression in fibroblasts and mesangial cells. *PLoS One*. 5:e8703.
- Fukumori, T., H. Kanayama, and A. Raz. 2007. The role of galectin-3 in cancer drug resistance. *Drug Resist Updat*. 10:101–108.
- Funasaka, T., V. Balan, A. Raz, and R.W. Wong. 2013. Nucleoporin Nup98 mediates galectin-3 nuclear-cytoplasmic trafficking. *Biochem. Biophys. Res. Commun*. 434:155–161.
- Funasaka, T., A. Raz, and P. Nangia-Makker. 2014. Galectin-3 in angiogenesis and metastasis. *Glycobiology*. 24:886–891.
- GLOBOCAN. 2012. Estimated Cancer Incidence, Mortality and Prevalence Worldwide in 2012. <http://globocan.iarc.fr/Default.aspx>, Accessed on 2nd Novembre 2014.
- Gong, H.C., Y. Honjo, P. Nangia-makker, V. Hogan, N. Mazurak, R.S. Bresalier, and A. Raz. 1999. The NH 2 Terminus of Galectin-3 Governs Cellular Compartmentalization and Functions in Cancer Cells. *Cancer Res*. 59:6239–6245.
- Greco, C., R. Vona, M. Cosimelli, P. Matarrese, E. Straface, P. Scordati, D. Giannarelli, V. Casale, D. Assisi, M. Mottolese, A. Moles, and W. Malorni. 2004. Cell surface overexpression of galectin-3 and the presence of its ligand 90k in the blood plasma as determinants in colon neoplastic lesions. *Glycobiology*. 14:783–792.
- Haggar, F.A., and R.P. Boushey. 2009. Colorectal cancer epidemiology: incidence, mortality, survival, and risk factors. *Clin. Colon Rectal Surg*. 22:191–197.
- Hanahan, D., and R.A. Weinberg. 2000. The Hallmarks of Cancer. *Cell*. 100:57–70.
- Hanahan, D., and R.A. Weinberg. 2011. Hallmarks of cancer: The next generation. *Cell*. 144:646–674.
- Hancock, J.F. 2003. Ras proteins: different signals from different locations. *Nat. Rev. Mol. Cell Biol*. 4:373–384.

- Hara, E., R. Smith, D. Parry, H. Tahara, S. Stone, and G. Peters. 1996. Regulation of p16 CDKN2 Expression and Its Implications for Cell Immortalization and Senescence. *Mol. Cell. Biol.* 16:859–867.
- Hartman, J., K. Edvardsson, K. Lindberg, C. Zhao, C. Williams, A. Ström, and J.-A. Gustafsson. 2009. Tumor repressive functions of estrogen receptor beta in SW480 colon cancer cells. *Cancer Res.* 69:6100–6106.
- Haudek, K.C., K.J. Spronk, P.G. Voss, R.J. Patterson, L. John, and E.J. Arnoys. 2010. Dynamics of Galectin-3 in the Nucleus and Cytoplasm. *Biochim. Biophys. Acta.* 1800:1–20.
- Heinemann, V., S. Stintzing, T. Kirchner, S. Boeck, and A. Jung. 2009. Clinical relevance of EGFR- and KRAS-status in colorectal cancer patients treated with monoclonal antibodies directed against the EGFR. *Cancer Treat. Rev.* 35:262–271.
- Herman, J.G., A. Merlo, L. Mao, G. Herman, G. Lapidus, J. Issa, E. Davidson, D. Sidransky, and S.B. Baylin. 1995. Inactivation of the CDKN2 / p16 / MTS1 Gene Is Frequently Associated with Aberrant DNA Methylation in All Common Human Cancers. *Cancer Res.* 55:4525–4530.
- Herszényi, L., L. Barabás, I. Hritz, G. István, and Z. Tulassay. 2014. Impact of proteolytic enzymes in colorectal cancer development and progression. *World J. Gastroenterol.* 20:13246–13257.
- Hill, M., D. Mazal, V.A. Biron, L. Pereira, L. Ubillos, E. Berriel, H. Ahmed, T. Freire, M. Rondán, G.R. Vasta, F.-T. Liu, M.M. Iglesias, and E. Osinaga. 2010. A novel clinically relevant animal model for studying galectin-3 and its ligands during colon carcinogenesis. *J. Histochem. Cytochem.* 58:553–565.
- Hittlet, A., H. Legendre, N. Nagy, Y. Bronckart, J.-C. Pector, I. Salmon, P. Yeaton, H.-J. Gabius, R. Kiss, and I. Camby. 2003. Upregulation of galectins-1 and -3 in human colon cancer and their role in regulating cell migration. *Int. J. cancer.* 103:370–379.
- Ho, M.-K., and T.A. Springer. 1982. Mac-2 , a novel 32 , 000 m , mouse macrophage subpopulation-specific antigen defined by monoclonal antibodies. *J. Immunol.* 128:1221–1228.
- Honjo, Y., H. Inohara, S. Akahani, H. Yoshii, Y. Takenaka, J. Yoshida, K. Hattori, Y. Tomiyama, A. Raz, and T. Kubo. 2000. Expression of Cytoplasmic Galectin-3 as a Prognostic Marker in Tongue Carcinoma. *Cancer Res.* 6:4635–4640.
- Honjo, Y., P. Nangia-makker, H. Inohara, and A. Raz. 2001. Down-Regulation of Galectin-3 Suppresses Tumorigenicity of Human Breast Carcinoma Cells. *Cancer Res.* 7:661–668.
- Hsu, D.K., A.I. Chernyavsky, H. Chen, L. Yu, A. Sergei, and F. Liu. 2009. Endogenous Galectin-3 Is Localized in Membrane Lipid Rafts and Regulates Migration of Dendritic Cells. *J Invest Dermatol.* 129:573–583.
- Hughes, R.C. 1999. Secretion of the galectin family of mammalian carbohydrate-binding proteins. *Biochim. Biophys. Acta.* 1473:172–185.
- Hughes, R.C. 2001. Galectins as modulators of cell adhesion. *Biochimie.* 83:667–676.
- Irimura, T., Y. Matsushita, R.C. Sutton, D. Carralero, D. V Ohannesian, K.R. Cleary, D.M. Ota, G.L. Nicolson, and R. Lotan. 1991. Increased Content of an Endogenous Lactose-binding Lectin in Human Colorectal Carcinoma Progressed to Metastatic Stages. *Cancer Res.* 51:387–393.
- Jacobs, J.J.L., and T. De Lange. 2004. Significant Role for p16 INK4a in p53-Independent Telomere-Directed Senescence. *Curr. Biol.* 14:2302–2308.
- Jass, J.R. 2007. Classification of colorectal cancer based on correlation of clinical, morphological and molecular features. *Histopathology.* 50:113–130.
- Jia, W., H. Kidoya, D. Yamakawa, H. Naito, and N. Takakura. 2013. Galectin-3 accelerates M2 macrophage infiltration and angiogenesis in tumors. *Am. J. Pathol.* 182:1821–1831.
- Jiang, S.-S., D.-S. Weng, Q.-J. Wang, K. Pan, Y.-J. Zhang, Y.-Q. Li, J.-J. Li, J.-J. Zhao, J. He, L. Lv, Q.-Z. Pan, and J.-C. Xia. 2014. Galectin-3 is associated with a poor prognosis in primary hepatocellular carcinoma. *J. Transl. Med.* 12:273.
- Kaboord, B., and M. Perr. 2008. Isolation of proteins and protein complexes by immunoprecipitation. *Methods Mol. Biol.* 424:349–64.

- Kasem, K., E. Sullivan, V. Gopalan, A. Salajegheh, R. a Smith, and A.K.-Y. Lam. 2014. JK1 (FAM134B) represses cell migration in colon cancer: a functional study of a novel gene. *Exp. Mol. Pathol.* 97:99–104.
- Kim, B.N.O., H. Yamamoto, K. Ikeda, B. Damdinsuren, Y. Sugita, C.Y.E.E. Ngan, Y. Fujie, M. Ogawa, T. Hata, M. Ikeda, M. Ohue, M. Sekimoto, T. Monden, N. Matsuura, and M. Monden. 2005. Methylation and expression of p16 INK4 tumor suppressor gene in primary colorectal cancer tissues. *Int. J. Oncol.* 26:1217–1226.
- Kim, M.K., C.O. Sung, I.-G. Do, H.-K. Jeon, T.J. Song, H.S. Park, Y.-Y. Lee, B.-G. Kim, J.-W. Lee, and D.-S. Bae. 2011. Overexpression of Galectin-3 and its clinical significance in ovarian carcinoma. *Int. J. Clin. Oncol.* 16:352–358.
- Knapp, J.S., S.D. Lokeshwar, U. Vogel, J. Hennenlotter, C. Schwentner, M.W. Kramer, A. Stenzl, and A.S. Merseburger. 2013. Galectin-3 expression in prostate cancer and benign prostate tissues: correlation with biochemical recurrence. *World J. Urol.* 31:351–358.
- Kobayashi, T., T. Shimura, T. Yajima, N. Kubo, K. Araki, S. Tsutsumi, H. Suzuki, H. Kuwano, and A. Raz. 2011. Transient gene silencing of galectin-3 suppresses pancreatic cancer cell migration and invasion through degradation of β -catenin. *Int. J. cancer.* 129:2775–2786.
- Lee, E.C., H. Woo, C.A. Korzelius, G.D. Steele, and A.M. Mercurio. 1991. Carbohydrate-Binding Protein 35 Is the Major Cell-Surface Laminin-Binding Protein in Colon Carcinoma. *Arch Surg.* 126:1498–1502.
- Legendre, H., C. Decaestecker, N. Nagy, A. Hendlisz, M.-P. Schüring, I. Salmon, H.-J. Gabius, J.-C. Pector, and R. Kiss. 2003. Prognostic values of galectin-3 and the macrophage migration inhibitory factor (MIF) in human colorectal cancers. *Mod. Pathol.* 16:491–504.
- Levy, R., A. Biran, F. Poirier, A. Raz, and Y. Kloog. 2011. Galectin-3 mediates cross-talk between K-Ras and Let-7c tumor suppressor microRNA. *PLoS One.* 6:e27490. doi:10.1371/journal.pone.0027490.
- Levy, R., M. Grafi-Cohen, Z. Kraiem, and Y. Kloog. 2010. Galectin-3 promotes chronic activation of K-Ras and differentiation block in malignant thyroid carcinomas. *Mol. Cancer Ther.* 9:2208–2219.
- Liang, J.-T., K.-J. Chang, J.-C. Chen, C.-C. Lee, Y.-M. Cheng, H.-C. Hsu, M.-S. Wu, S.-M. Wang, J.-T. Lin, and A.-L. Cheng. 1999. Hypermethylation of the p16 Gene in Sporadic T3N0M0 Stage Colorectal Cancers: Association with DNA Replication Error and Shorter Survival. *Oncology.* 57:149–156.
- Liao, J., J.C. Wolfman, and A. Wolfman. 2003. K-ras regulates the steady-state expression of matrix metalloproteinase 2 in fibroblasts. *J. Biol. Chem.* 278:31871–8.
- Liggett, B.W.H., and D. Sidransky. 1998. Role of the p16 Tumor Suppressor Gene in Cancer. *J. Clin. Oncol.* 16:1197–1206.
- Lin, a. W., M. Barradas, J.C. Stone, L. van Aelst, M. Serrano, and S.W. Lowe. 1998. Premature senescence involving p53 and p16 is activated in response to constitutive MEK/MAPK mitogenic signaling. *Genes Dev.* 12:3008–3019.
- Lin, H.-M., R.G. Pestell, A. Raz, and H.-R.C. Kim. 2002. Galectin-3 enhances cyclin D(1) promoter activity through SP1 and a cAMP-responsive element in human breast epithelial cells. *Oncogene.* 21:8001–10.
- Liu, F., R.J. Patterson, and J.L. Wang. 2002. Intracellular functions of galectins. *Biochim. Biophys. Acta.* 1572:263–273.
- Liu, F., and G.A. Rabinovich. 2005. Galectins as modulators of tumour progression. *Nat. Rev. Cancer.* 5:29–41. doi:10.1038/nrc1527.
- Liu, L., T. Sakai, N. Sano, and K. Fukui. 2004. Nucling mediates apoptosis by inhibiting expression of galectin-3 through interference with nuclear factor κ B signalling. *Biochem. J.* 380:31–41.
- Lotan, R., Y. Matsushita, D. Ohannesian, D. Carralero, M. David, K.R. Cleary, G.L. Nicolson, and T. Irimura. 1991. Lactose-binding lectin expression in human colorectal carcinomas . Relation to tumor progression. *Carbohydr. Res.* 213:47–57.

- Lotz, M.M., C.W. Andrews, C.A. Korzelius, E.C. Lee, G.D. Steele, A. Clarke, and A.M. Mercurio. 1993. Decreased expression of Mac-2 (carbohydrate binding protein 35) and loss of its nuclear localization are associated with the neoplastic progression of colon carcinoma. *Proc. Natl. Acad. Sci. U. S. A.* 90:3466–3470.
- Lu, Y., X. Zhang, and J. Zhang. 2012. Inhibition of Breast Tumor Cell Growth by Ectopic Expression of p16/INK4A Via Combined Effects of Cell Cycle Arrest, Senescence and Apoptotic Induction, and Angiogenesis Inhibition. *J. Cancer.* 3:333–344.
- Lukyanov, P., V. Furtak, and J. Ochieng. 2005. Galectin-3 interacts with membrane lipids and penetrates the lipid bilayer. *Biochem. Biophys. Res. Commun.* 338:1031–1036.
- Malumbres, M., and M. Barbacid. 2003. RAS oncogenes: the first 30 years. *Nat. Rev. Cancer.* 3:459–465.
- Mao, C., Y.-F. Huang, Z.-Y. Yang, D.-Y. Zheng, J.-Z. Chen, and J.-L. Tang. 2013. KRAS p . G13D Mutation and Codon 12 Mutations Are Not Created Equal in Predicting Clinical Outcomes of Cetuximab in Metastatic Colorectal Cancer. *Cancer.* 119:714–721.
- Markowska, A.I., F.-T. Liu, and N. Panjwani. 2010. Galectin-3 is an important mediator of VEGF- and bFGF-mediated angiogenic response. *J. Exp. Med.* 207:1981–1993.
- Matarrese, P., N. Tinari, M. Letizia, C. Natoli, S. Iacobelli, and W.M. Y. 2000. Galectin-3 overexpression protects from cell damage and death by influencing mitochondrial homeostasis. *FEBS Lett.* 473:311–315.
- Mazurek, N., J. Conklin, J.C. Byrd, A. Raz, and R.S. Bresalier. 2000. Phosphorylation of the beta-galactoside-binding protein galectin-3 modulates binding to its ligands. *J. Biol. Chem.* 275:36311–5.
- Mccubrey, J.A., L.S. Steelman, W.H. Chappell, S.L. Abrams, W.T. Wong, F. Chang, B. Lehmann, D.M. Terrian, M. Milella, A. Tafuri, F. Stivala, M. Libra, J. Basecke, C. Evangelisti, M. Alberto, and R.A. Franklin. 2007. Roles of the raf/mek/erk pathway in cell growth, malignant transformation and drug resistance. *Biochim. Biophys. Acta.* 1773:1263–1284.
- Moutsatsos, I.K., M. Wadet, M. Schindler, and J.L. Wang. 1987. Endogenous lectins from cultured cells: Nuclear localization of carbohydrate-binding protein 35 in proliferating 3T3 fibroblasts. *Proc. Natl. Acad. Sci. U. S. A.* 84:6452–6456.
- Moyer, M.P., L.A. Manzano, R.L. Merriman, J.S. Stauffer, and L.R. Tanzer. 1996. NCM460, A normal human colon mucosal epithelial cell line. *InVitr. Cell. Dev. Biol. - Animal.* 13:315–317.
- Nakahara, S., V. Hogan, H. Inohara, and A. Raz. 2006b. Importin-mediated nuclear translocation of galectin-3. *J. Biol. Chem.* 281:39649–39659.
- Nakahara, S., N. Oka, Y. Wang, V. Hogan, H. Inohara, and A. Raz. 2006a. Characterization of the nuclear import pathways of galectin-3. *Cancer Res.* 66:9995–10006.
- Nangia-Makker, P., T. Raz, L. Tait, V. Hogan, R. Fridman, and A. Raz. 2007. Galectin-3 Cleavage: A Novel Surrogate Marker for Matrix Metalloproteinase Activity in Growing Breast Cancers. *Cancer Res.* 67:11760–11768.
- Nangia-Makker, P., Y. Wang, T. Raz, V. Balan, V. Hogan, and A. Raz. 2010. Cleavage of galectin-3 by matrix metalloproteases induces angiogenesis in breast cancer. *Int. J. cancer.* 127:2530–2541.
- Nash, G.M., M. Gimbel, J. Shia, D.R. Nathanson, M.I. Ndubuisi, Z. Zeng, N. Kemeny, and P.B. Paty. 2010. KRAS Mutation Correlates With Accelerated Metastatic Progression in Patients With Colorectal Liver Metastases. *Ann. Surg. Oncol.* 17:572–578.
- Normanno, N., S. Tejpar, F. Morgillo, A. De Luca, E. Van Cutsem, and F. Ciardiello. 2009. Implications for KRAS status and EGFR-targeted therapies in metastatic CRC. *Nat. Rev. Clin. Oncol.* 6:519–27.
- Norrie, M.W.A., N.J. Hawkins, A. V. Todd, A.P. Meagher, T.W. O'Connor, and R.L. Ward. 2003. Inactivation of p16INK4a by CpG hypermethylation is not a frequent event in colorectal cancer. *J. Surg. Oncol.* 84:143–50.

- Ochieng, J., V. Furtak, and P. Lukyanov. 2004. Extracellular functions of galectin-3. *Glycoconjugate J.* 19:527–535.
- Ochieng, J., B. Green, S. Evans, O. James, and P. Warfield. 1998. Modulation of the biological functions of galectin-3 by matrix metalloproteinases. *Biochim. Biophys. Acta.* 1379:97–106.
- Ohannesian, D.W., D. Lotan, P. Thomas, G.- Human, C. Carcinoma, D.V. V Ohannesian, J.M. Jessup, M. Fukuda, and R. Lotan. 1995. Carcinoembryonic Antigen and Other Glycoconjugates Act as Ligands for Galectin-3 in Human Colon Carcinoma Cells. *Cancer Res.* 55:2191–2199.
- Ohhara, M., M. Esumi, and Y. Kurosu. 1996. Activation but Not Inactivation of the MTS1 Gene Is Associated with Primary Colorectal Carcinomas. *Biochem. Biophys. Res. Commun.* 226:791–795.
- Oikonomou, E., E. Makrodouli, M. Evagelidou, T. Joyce, L. Probert, and A. Pintzas. 2009. BRAF V600E Efficient Transformation and Induction of Microsatellite Instability Versus KRAS G12V Induction of Senescence Markers in Human Colon. *Neoplasia.* 11:1116–1131.
- Oliveira, C., M. Pinto, A. Duval, C. Brennetot, E. Domingo, E. Espi, M. Armengol, H. Yamamoto, R. Hamelin, R. Seruca, and S.S. Jr. 2003. BRAF mutations characterize colon but not gastric cancer with mismatch repair deficiency. *Oncogene.* 22:9192–9196.
- Oliveira, C., S. Velho, C. Moutinho, A. Ferreira, A. Preto, E. Domingo, A.F. Capelinha, A. Duval, R. Hamelin, J.C. Machado, S.S. Jr, F. Carneiro, and R. Seruca. 2007. KRAS and BRAF oncogenic mutations in MSS colorectal carcinoma progression. *Oncogene.* 26:158–163.
- Omerovic, J., and I. a Prior. 2009. Compartmentalized signalling: Ras proteins and signalling nanoclusters. *FEBS J.* 276:1817–25.
- Palmqvist, R., J.N. Rutegård, B. Bozoky, G. Landberg, and R. Stenling. 2000. Human colorectal cancers with an intact p16/cyclin D1/pRb pathway have up-regulated p16 expression and decreased proliferation in small invasive tumor clusters. *Am. J. Pathol.* 157:1947–1953.
- Park, J.W., P.G. Voss, S. Grabski, J.L. Wang, and R.J. Patterson. 2001. Association of galectin-1 and galectin-3 with Gemin4 in complexes containing the SMN protein. *Nucleic Acids Res.* 27:3595–3602.
- Paron, I., A. Scaloni, A. Pines, A. Bachi, F.-T. Liu, C. Puppini, M. Pandolfi, L. Ledda, C. Di Loreto, G. Damante, and G. Tell. 2003. Nuclear localization of Galectin-3 in transformed thyroid cells: a role in transcriptional regulation. *Biochem. Biophys. Res. Commun.* 302:545–553.
- Paz, A., R. Haklai, G. Elad-Sfadia, E. Ballan, and Y. Kloog. 2001. Galectin-1 binds oncogenic H-Ras to mediate Ras membrane anchorage and cell transformation. *Oncogene.* 20:7486–7493.
- Plath, T., K. Detjen, M. Welzel, Z. Von Marschall, D. Murphy, M. Schirner, B. Wiedenmann, S. Rosewicz, M. Klinik, C. Virchow-klinikum, E. Onkologie, and A. The. 2000. A Novel Function for the Tumor Suppressor p16 INK4a : Induction of Anoikis via Upregulation of the α 5B1 Fibronectin Receptor. *J. Cell Biol.* 150:1467–1477.
- Plowman, S.J., N. Ariotti, A. Goodall, R.G. Parton, and J.F. Hancock. 2008. Electrostatic interactions positively regulate K-Ras nanocluster formation and function. *Mol. Cell. Biol.* 28:4377–4385.
- Povegliano, L.Z., C.T.F. Oshima, de O.L. Flávio, P.L.A. Scherholz, and N.M. Forones. 2011. Immunoeexpression of galectin-3 in colorectal cancer and its relationship with survival. *J. Gastrointest. Cancer.* 42:217–221.
- Prior, I.A., A. Harding, J. Yan, J. Sluimer, R.G. Parton, and J.F. Hancock. 2001. GTP-dependent segregation of H-ras from lipid rafts is required for biological activity. *Nat. Cell Biol.* 3:368–375.
- Prior, I.A., P.D. Lewis, and C. Mattos. 2012. A comprehensive survey of Ras mutations in cancer. *Cancer Res.* 72:2457–2467.
- Rabien, A., H. Sanchez-Ruderisch, P. Schulz, N. Otto, A. Wimmel, B. Wiedenmann, and K.M. Detjen. 2012. Tumor suppressor p16INK4a controls oncogenic K-Ras function in human pancreatic cancer cells. *Cancer Sci.* 103:169–175.
- Rabinovich, G.A., M.A. Toscano, S.S. Jackson, and G.R. Vasta. 2007. Functions of cell surface galectin-glycoprotein lattices. *Curr Opin Struct Biol.* 17:513–520.

- Radosavljevic, G., V. Volarevic, I. Jovanovic, M. Milovanovic, N. Pejnovic, N. Arsenijevic, D.K. Hsu, and M.L. Lukic. 2012. The roles of Galectin-3 in autoimmunity and tumor progression. *Immunol. Res.* 52:100–10.
- Rajagopalan, H., A. Bardelli, C. Lengauer, K.W. Kinzler, B. Vogelstein, and V.E. Velculescu. 2002. RAF/ RAS oncogenes and mismatch-repair status. *Nature.* 418:934.
- Rocco, J.W., and D. Sidransky. 2001. p16(MTS-1/CDKN2/INK4a) in cancer progression. *Exp. Cell Res.* 264:42–55.
- Sanchez-Ruderisch, H., C. Fischer, K.M. Detjen, M. Welzel, A. Wimmel, J.C. Manning, S. André, and H.-J. Gabius. 2010. Tumor suppressor p16 INK4a: Downregulation of galectin-3, an endogenous competitor of the pro-apoptosis effector galectin-1, in a pancreatic carcinoma model. *FEBS J.* 277:3552–3563.
- Sandouk, F., F. Al Jerf, and M.H.D.B. Al-Halabi. 2013. Precancerous lesions in colorectal cancer. *Gastroenterol. Res. Pract.* 2013:457901.
- Sanjuán, X., P.L. Fernández, A. Castells, V. Castronovo, F. Van Den Brule, F.U.T. Liu, A. Cardesa, and E. Campo. 1997. Differential Expression of Galectin 3 and Galectin 1 in Colorectal Cancer Progression. *Gastroenterology.* 113:1906–1915.
- Sano, H., D.K. Hsu, L. Yu, J.R. Apgar, I. Kuwabara, T. Yamanaka, M. Hirashima, and F.T. Liu. 2000. Human galectin-3 is a novel chemoattractant for monocytes and macrophages. *J. Immunol.* 165:2156–2164.
- Sarkisian, C.J., B. a Keister, D.B. Stairs, R.B. Boxer, S.E. Moody, and L. a Chodosh. 2007. Dose-dependent oncogene-induced senescence in vivo and its evasion during mammary tumorigenesis. *Nat. Cell Biol.* 9:493–505.
- Schoeppner, H.L., A. Raz, S.B. Ho, and R.S. Bresalier. 1995. Expression of an endogenous galactose-binding lectin correlates with neoplastic progression in the colon. *Cancer.* 75:2818–2826.
- Serrano, M., G.J. Hannon, and D. Beach. 1993. A new regulatory motif in cell-cycle control causing specific inhibition of cyclin D/CDK4. *Nature.* 366:704–707.
- Serrano, M., A.W. Lin, M.E. McCurrach, D. Beach, and S.W. Lowe. 1997. Oncogenic ras Provokes Premature Cell Senescence Associated with Accumulation of p53 and p16 INK4a. *Cell.* 88:593–602.
- Shalom-Feuerstein, R., T. Cooks, A. Raz, and Y. Kloog. 2005. Galectin-3 regulates a molecular switch from N-Ras to K-Ras usage in human breast carcinoma cells. *Cancer Res.* 65:7292–7300.
- Shalom-Feuerstein, R., S.J. Plowman, B. Rotblat, N. Ariotti, J.F. Hancock, and Y. Kloog. 2008. K-Ras Nanoclustering is Subverted by Over-expression of the Scaffold Protein Galectin-3. *Cancer Res.* 68:6608–6616.
- Shekhar, M.P.V., P. Nangia-Makker, L. Tait, F. Miller, and A. Raz. 2004. Alterations in Galectin-3 Expression and Distribution Correlate with Breast Cancer Progression. *Am. J. Pathol.* 165:1931–1941.
- Simons, K., and D. Toomre. 2000. Lipid rafts and signal transduction. *Nat. Rev. Mol. Cell Biol.* 1:31–39.
- Song, S., B. Ji, V. Ramachandran, H. Wang, M. Hafley, C. Logsdon, and R.S. Bresalier. 2012. Overexpressed galectin-3 in pancreatic cancer induces cell proliferation and invasion by binding Ras and activating Ras signaling. *PLoS One.* 7:e42699.
- De Stefano, A., and C. Carlomagno. 2014. Beyond KRAS: Predictive factors of the efficacy of anti-EGFR monoclonal antibodies in the treatment of metastatic colorectal cancer. *World J. Gastroenterol.* 20:9732–9743.
- Stillman, B.N., D.K. Hsu, M. Pang, C. Fred, P. Johnson, F. Liu, L.G. Baum, and C.F. Brewer. 2006. Galectin-3 and Galectin-1 Bind Distinct Cell Surface Glycoprotein Receptors to Induce T Cell Death 1. *J. Immunol.* 176:778–789.

- Straube, T., A.F. Elli, C. Greb, A. Hegele, H.-P. Elsässer, D. Delacour, and R. Jacob. 2011. Changes in the expression and subcellular distribution of galectin-3 in clear cell renal cell carcinoma. *J. Exp. Clin. cancer Res.* 30:89.
- Takenaka, Y., H. Inohara, T. Yoshii, K. Oshima, S. Nakahara, S. Akahani, Y. Honjo, Y. Yamamoto, A. Raz, and T. Kubo. 2003. Malignant transformation of thyroid follicular cells by galectin-3. *Cancer Lett.* 195:111–119.
- Théry, C., M. Boussac, P. Véron, G. Raposo, J. Garin, and S. Amigorena. 2001. Proteomic Analysis of Dendritic Cell-Derived Exosomes: A Secreted Subcellular Compartment Distinct from Apoptotic Vesicles. *J. Immunol.* 166:7309–7318.
- Tian, T., A. Harding, K. Inder, S. Plowman, R.G. Parton, and J.F. Hancock. 2007. Plasma membrane nanoswitches generate high-fidelity Ras signal transduction. *Nat. Cell Biol.* 9:905–914.
- Tominaga, O., M.E. Nita, H. Nagawa, S. Fujii, T. Tsuruo, and T. Muto. 1997. Expressions of Cell Cycle Regulators in Human Colorectal Cancer Cell Lines. *J. Cancer Res.* 88:885–860.
- Vandooren, J., N. Geurts, E. Martens, P.E. Van den Steen, and G. Opdenakker. 2013. Zymography methods for visualizing hydrolytic enzymes. *Nat. Methods.* 10:211–220.
- Vermeulen, K., D.R. Van Bockstaele, and Z.N. Berneman. 2003. The cell cycle: a review of regulation, deregulation and therapeutic targets in cancer. *Cell Prolif.* 36:131–149.
- Vögler, O., J.M. Barceló, C. Ribas, and P. V. Escribà. 2008. Membrane interactions of G proteins and other related proteins. *Biochim. Biophys. Acta.* 1778:1640–1652.
- WHO. 2014. World Health Organization. <http://www.who.int/topics/cancer/en/>, Accessed on 2nd Novembre 2014.
- Wu, K.-L., E.-Y. Huang, E.-W. Jhu, Y.-H. Huang, W.-H. Su, P.-C. Chuang, and K.D. Yang. 2013. Overexpression of galectin-3 enhances migration of colon cancer cells related to activation of the K-Ras-Raf-Erk1/2 pathway. *J. Gastroenterol.* 48:350–359.
- Yang, R., P.N. Hill, D.K. Hsu, and F. Liu. 1998. Role of the Carboxyl-Terminal Lectin Domain in Self-Association of Galectin-3. *Biochemistry.* 37:4086–4092.
- Yang, R., D.K. Hsu, and F. Liu. 1996. Expression of galectin-3 modulates T-cell growth and apoptosis. *Proc. Natl. Acad. Sci. United States Am. Immunol.* 93:6737–6742.
- Yang, R., G.A. Rabinovich, and F. Liu. 2008. Galectins : structure , function and therapeutic potential. *Expert Rev. Mol. Med.* 10:e17.
- Yi, J., Z. Wang, H. Cang, Y. Chen, R. Zhao, B. Yu, and X. Tang. 2001. p 16 gene methylation in colorectal cancers associated with Duke ' s staging. *World J. Gastroenterol.* 7:722–725.
- Yoshii, T., T. Fukumori, Y. Honjo, H. Inohara, H.-R.C. Kim, and A. Raz. 2002. Galectin-3 phosphorylation is required for its anti-apoptotic function and cell cycle arrest. *J. Biol. Chem.* 277:6852–6857.
- Yu, F., R.L. Finley, A. Raz, and H.-R.C. Kim. 2002. Galectin-3 translocates to the perinuclear membranes and inhibits cytochrome c release from the mitochondria. A role for synexin in galectin-3 translocation. *J. Biol. Chem.* 277:15819–15827.
- Zhang, D., Z. Chen, S. Liu, Z. Dong, M. Dalin, S. Bao, Y. Hu, and F. Wei. 2013. Galectin-3 gene silencing inhibits migration and invasion of human tongue cancer cells in vitro via downregulating β -catenin. *Acta Pharmacol. Sin.* 34:176–184.
- Zhang, H., X. Liang, C. Duan, C. Liu, and Z. Zhao. 2014. Galectin-3 as a marker and potential therapeutic target in breast cancer. *PLoS One.* 9:e103482.
- Zhao, Q., X. Guo, G.B. Nash, P.C. Stone, J. Hilken, R.M. Jonathan, and L.-G. Yu. 2009. Circulating galectin-3 promotes metastasis by modifying MUC1 localization on cancer cell surface. *Cancer Res.* 69:6799–6806.

VII.

SUPPLEMENTARY DATA



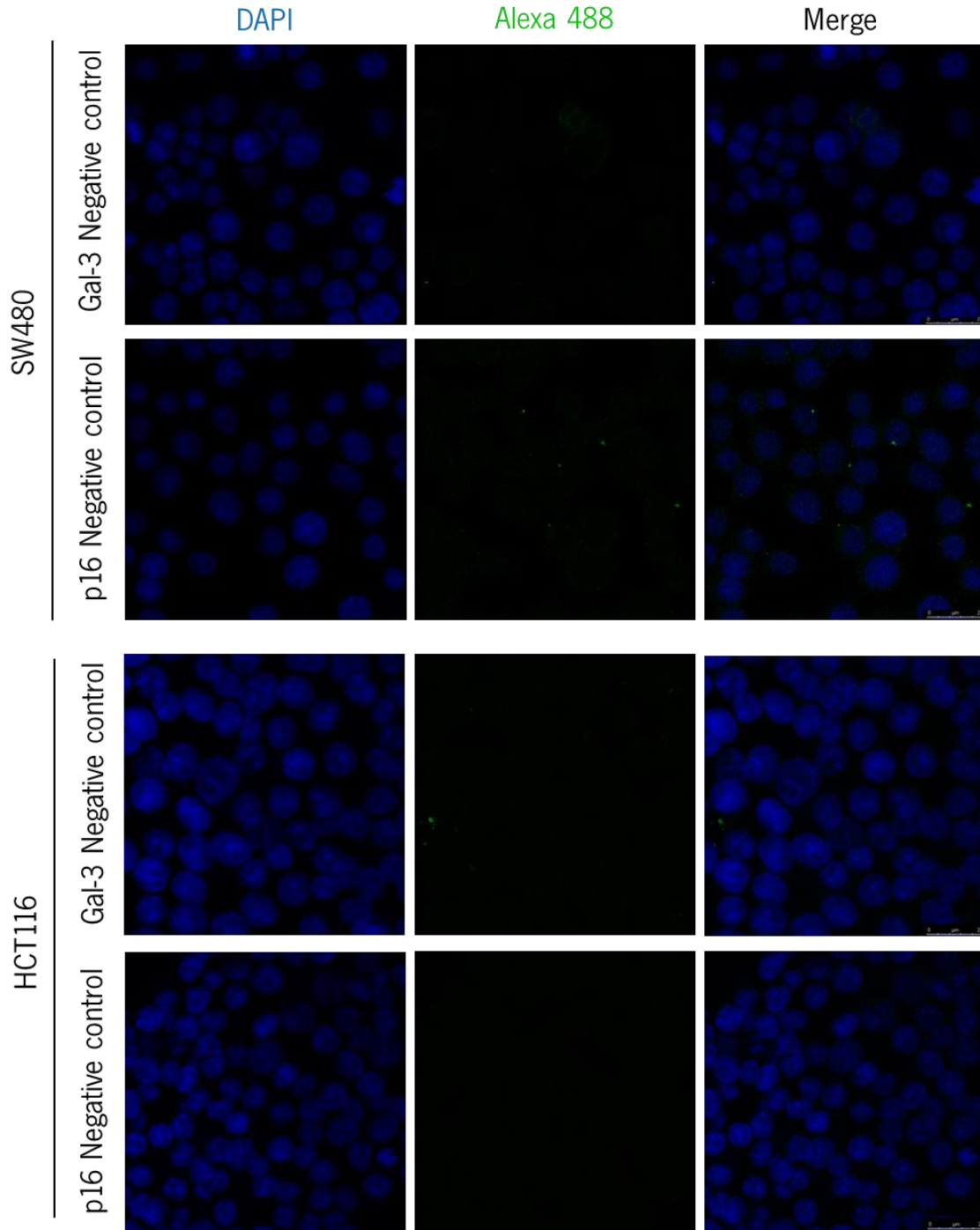


Fig. S1. Confocal fluorescence analysis of Gal-3 and p16 negative staining controls in high confluent SW480 and HCT116 cells. Coverslips were incubated only with Alexa-488 secondary antibody and nuclei are counterstained in blue with DAPI. Bottom right scale bars correspond to 25 μ m.

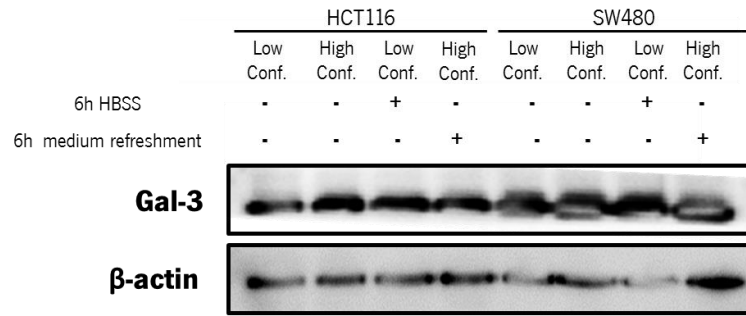


Fig.S2. Representative western blot showing similar Gal-3 expression independently of the cells confluence and nutritional availability.

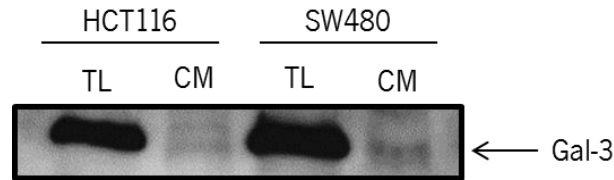


Fig.S3. Analysis of Gal-3 content in conditioned media (CM) from HCT116 and SW480 cells. Total lysates (TL) were used as positive controls and 50 μ g of protein were loaded in each lane.